

**THE GENERATION OF THE AMYLOID PRECURSOR  
PROTEIN INTRACELLULAR DOMAIN.**

A thesis submitted to the University of Manchester for the degree of  
Doctor of Philosophy in the Faculty of Science and Engineering.

2004

CLAIRE DUGGAN

Division of Biochemistry and Cell Biology  
School of Biological Sciences

## Table of contents

<b>LIST OF FIGURES.....</b>	<b>7</b>
<b>LIST OF TABLES .....</b>	<b>9</b>
<b>ABSTRACT.....</b>	<b>10</b>
<b>DECLARATION .....</b>	<b>11</b>
<b>ACKNOWLEDGEMENTS.....</b>	<b>12</b>
<b>ABBREVIATIONS.....</b>	<b>13</b>
<b>1 INTRODUCTION.....</b>	<b>16</b>
1.1 The secretory pathway .....	16
1.2 Targeting.....	17
1.3 Protein biogenesis at the ER.....	18
1.4 Sorting and vesicular traffic.....	19
1.5 Transmembrane proteins .....	20
1.6 Regulated intramembrane proteolysis.....	21
1.6.1 SREBP: A well-characterised example of RIP .....	21
1.6.2 Notch processing .....	22
1.7 Introduction to Alzheimer's disease.....	24
1.8 APP.....	25
1.9 APP processing.....	28
1.9.1 $\alpha$ -Secretase processing .....	28
1.9.2 $\beta$ -Secretase processing .....	30
1.10 $\gamma$ -Secretase processing .....	31
1.10.1 Evidence that presenilins are a core component of the $\gamma$ -secretase ...	31
1.10.2 Nicastrin and the $\gamma$ -secretase .....	35
1.10.3 Aph-1 and Pen-2.....	37
1.10.4 The $\gamma$ -secretase complex and its site of action.....	38
1.11 The assembly of the $\gamma$ -secretase subunits.....	40
1.12 The subcellular location of cleavage.....	41
1.13 The C-terminal fragment of APP .....	41

1.14	Epsilon cleavage of APP .....	42
1.15	Fe65.....	44
1.16	Insulin degrading enzyme (IDE).....	47
1.17	Aims of the project.....	48
<b>2</b>	<b>MATERIALS AND METHODS .....</b>	<b>50</b>
2.1	Materials .....	50
2.2	Generation of constructs .....	51
2.2.1	Generation of methionine mutants .....	53
2.2.2	Generation of tagged APP-derivatives .....	54
2.2.3	Transformation.....	54
2.3	Template production.....	55
2.3.1	Generation of DNA templates for transcription.....	55
2.3.2	Generation of truncated DNA templates missing the stop codon.....	56
2.4	In vitro transcription .....	56
2.5	Semi-intact cells.....	56
2.6	In vitro translation in rabbit reticulocyte lysate.....	57
2.7	In vitro translation in wheat germ extract .....	58
2.8	Isolation of microsomal membrane fractions.....	58
2.9	TCA precipitation .....	59
2.10	Endoglycosidase H treatment.....	59
2.11	Proteinase K treatment.....	59
2.12	Isolation of ribosome-associated nascent chains .....	59
2.13	Sodium carbonate extraction of the membrane-associated fraction ..	60
2.14	Polyethylene glycol treatment of semi-intact cells .....	60
2.15	BFA treatment .....	61
2.16	Preparation of a CHAPSO-solubilised crude membrane extract .....	61
2.17	RNase treatment.....	62
2.18	Immunoprecipitation.....	62
2.19	Immunodepletion .....	63
2.20	SDS-PAGE .....	63

2.21	Transient transfection .....	63
2.22	Western blotting.....	64
2.23	Immunofluorescence .....	64
<b>3</b>	<b>GENERATION AND FATE OF C-TERMINAL FRAGMENTS OF APP.....</b>	<b>67</b>
3.1	Membrane integration and orientation of CT72.....	68
3.2	Analysis of APP-derivatives for putative $\gamma$ -secretase processing .....	70
3.3	Origin of the CT57-like polypeptide observed during CT72 synthesis	72
3.4	In vitro degradation of CT49.....	75
3.5	In vitro degradation of <sup>Met</sup> CT57 .....	77
3.6	Stability of other AICD lengths .....	79
3.7	Synthesis CT49 and <sup>Met</sup> CT57 in wheat germ extract .....	80
3.8	Factors affecting AICD stability .....	83
3.9	Summary.....	86
3.10	Conclusion .....	87
<b>4</b>	<b>GENERATION OF N-TERMINAL FRAGMENTS OF APP.....</b>	<b>89</b>
4.1	Analysis of N-terminally tagged APP derivatives for $\gamma$ -secretase processing.....	89
4.2	Characterisation of ss- <sup>HA-Gly</sup> CT42-like product .....	92
4.3	Effect of inhibitors on generation of the ss- <sup>HA-Gly</sup> CT42-like product....	96
4.4	Summary.....	97
4.5	Conclusion .....	98
<b>5</b>	<b>INVESTIGATING THE <i>IN VITRO</i> PROCESSING OF APP ...</b>	<b>100</b>
5.1	APP-derived model substrates .....	100
5.2	Membrane-dependent processing in vitro .....	101
5.3	PEG-mediated membrane fusion.....	103
5.4	BFA-mediated compartment fusion .....	105
5.5	CHAPSO-solubilised crude membrane extract .....	109

5.6	Summary.....	112
5.7	Conclusion .....	113
6	<b>PRELIMINARY <i>IN VIVO</i> ANALYSIS OF APP-DERIVATIVES.....</b>	<b>115</b>
6.1	Analysis of HA-tagged derivatives .....	116
6.2	Use of opsin and flag tags at the N-terminus .....	117
6.3	Summary.....	122
6.4	Conclusion .....	122
7	<b>DISCUSSION.....</b>	<b>124</b>
7.1	Introduction .....	124
7.2	A CT72 APP-derivative is efficiently targeted to and integrated into the ER membrane .....	124
7.3	In vitro synthesised AICD fragments are rapidly degraded by a metalloproteinase activity, probably IDE .....	125
7.4	AICD-like products generated with a CT72 APP-derivative are due to alternative initiation .....	127
7.5	Factors present in human brain nuclear extract stabilise the AICD..	128
7.6	Only specific lengths of AICD are degraded in vitro.....	129
7.7	<sup>Met</sup> CT57 may be N-terminally processed in reticulocyte lysate to generate a CT49-like product.....	130
7.8	An A $\beta$ -like fragment generated with ss- <sup>HA-Gly</sup> CT99 is not a result of $\gamma$ -secretase cleavage .....	131
7.9	Fusion of different membrane compartments was unable to promote processing in vitro .....	132
7.10	Use of a solubilised membrane extract.....	134
7.11	In vivo analysis can be used to study APP processing in future .....	135
7.12	Conclusions.....	135
	<b>REFERENCES.....</b>	<b>136</b>
	<b>APPENDIX 1.1 .....</b>	<b>150</b>
	<b>APPENDIX 2.1 .....</b>	<b>152</b>

<b>APPENDIX 2.2 .....</b>	<b>153</b>
<b>APPENDIX 2.3 .....</b>	<b>154</b>
<b>APPENDIX 2.4 .....</b>	<b>155</b>
<b>APPENDIX 2.5 .....</b>	<b>156</b>
<b>APPENDIX 2.6 .....</b>	<b>157</b>
<b>APPENDIX 2.7 .....</b>	<b>158</b>
<b>APPENDIX 2.8 .....</b>	<b>159</b>
<b>APPENDIX 2.9 .....</b>	<b>160</b>

## List of Figures

<b>Figure 1.1</b>	Protein targeting and the secretory pathway	16
<b>Figure 1.2</b>	Model for the sterol-mediated proteolytic release of SREBPs from the membrane	22
<b>Figure 1.3</b>	Notch processing	23
<b>Figure 1.4</b>	Amyloid precursor protein (APP) processing	26
<b>Figure 1.5</b>	Schematic representation of the subunit organization of the $\gamma$ -secretase complex	40
<b>Figure 1.6</b>	APP cleavage sites	43
<b>Figure 3.1</b>	Transmembrane orientation of CT72 in the ER	69
<b>Figure 3.2</b>	Generation of C-terminal fragments of APP	71
<b>Figure 3.3</b>	Pulse chase analysis of CT72 products	72
<b>Figure 3.4</b>	Identification of CT72-derived lower molecular weight products	74
<b>Figure 3.5</b>	Effect of proteasome inhibition and temperature on CT49 stability	76
<b>Figure 3.6</b>	Effect of metal chelators on stability of CT49	77
<b>Figure 3.7</b>	Effect of PNT on <sup>Met</sup> CT57 stability	78
<b>Figure 3.8</b>	Effect of PNT on AICD stability	80
<b>Figure 3.9</b>	Relative mobilities of <sup>Met</sup> CT57 and CT49 in wheat germ and reticulocyte lysate	81
<b>Figure 3.10</b>	Stability of <sup>Met</sup> CT57 in wheat germ extract	81
<b>Figure 3.11</b>	Degradation of wheat germ-synthesised <sup>Met</sup> CT57 by factor(s) present in reticulocyte lysate	82
<b>Figure 3.12</b>	Factors in human brain nuclear extract stabilize <sup>Met</sup> CT57	83
<b>Figure 3.13</b>	Blot of reticulocyte lysate for insulin-degrading enzyme (IDE)	84
<b>Figure 3.14</b>	Effect of immunodepletion of IDE on <sup>Met</sup> CT57 stability	85
<b>Figure 4.1</b>	HA-tagged APP-derivatives used to investigate <i>in vitro</i> processing	90
<b>Figure 4.2</b>	Membrane integration of ss- <sup>HA-Gly</sup> CT99	91
<b>Figure 4.3</b>	Anti-sera epitopes	92

<b>Figure 4.4</b>	Characterisation of lower molecular weight products generated with ss- <sup>HA-Gly</sup> CT99	93
<b>Figure 4.5</b>	Characterisation of ss- <sup>HA-Gly</sup> CT42	94
<b>Figure 4.6</b>	Generation of a ss- <sup>HA-Gly</sup> CT42-like product from ss- <sup>HA-Gly</sup> CT99	95
<b>Figure 4.7</b>	Effect of inhibitors on the presence of the ss- <sup>HA-Gly</sup> CT42-like product generated with ss- <sup>HA-Gly</sup> CT99	97
<b>Figure 5.1</b>	APP-derivative constructs used to investigate <i>in vitro</i> processing	101
<b>Figure 5.2</b>	Processing of APP-derivatives using semi-intact cells	102
<b>Figure 5.3</b>	Effect of polyethylene glycol treatment of semi-intact cells on processing of APP-derivatives	104
<b>Figure 5.4</b>	Effect of polyethylene glycol treatment on N-linked glycans	105
<b>Figure 5.5</b>	Effect of brefeldin-A treatment of cells on processing of APP-derivatives	106
<b>Figure 5.6</b>	Immunofluorescence microscopy experiments of the BFA-induced redistribution of Golgi proteins	108
<b>Figure 5.7</b>	<i>In vitro</i> $\gamma$ -secretase assay	110
<b>Figure 5.8</b>	C-terminal fragments generated with <sup>Met</sup> C99 are not dependent on the presence of the solubilised membrane extract	111
<b>Figure 5.9</b>	Immunoblot of detergent solubilised membrane extract for presenilin	112
<b>Figure 6.1</b>	APP-derivative constructs used to investigate <i>in vivo</i> processing	115
<b>Figure 6.2</b>	Detection of HA-tagged ss-CT99 derivatives by Western blotting	117
<b>Figure 6.3</b>	Immunoprecipitation of opsin and flag-tagged ss-CT99 constructs	119
<b>Figure 6.4</b>	Detection of flag-tagged ss-CT99 derivatives by Western blotting	120
<b>Figure 6.5</b>	Detection of opsin-tagged ss-CT99 derivatives by immunoblotting	121

## List of Tables

<b>Table 1.1</b>	Evidence for PS as the catalytic component of the $\gamma$ -secretase	32
<b>Table 2.1</b>	Antisera	51
<b>Table 2.2</b>	PCR reaction	52
<b>Table 2.3</b>	Media composition	55
<b>Table 2.4</b>	Summary of APP-derivatives used in this study	57

## Abstract

Alzheimer's disease (AD) is the most common cause of a progressive decline of cognitive function in aged humans. It is thought to be a result of the formation of amyloid plaques in the brain that are largely composed of  $\beta$ -amyloid ( $A\beta$ ), which is one of the cleavage products of the amyloid precursor protein (APP). The amyloidogenic processing of APP to produce the  $A\beta$  peptides requires sequential proteolytic cleavages by the  $\beta$ - and  $\gamma$ -secretases. APP is first cleaved by the  $\beta$ -secretase to produce APP-C99, and this product is a substrate for further processing by the  $\gamma$ -secretase that cleaves within its transmembrane domain to produce N-terminal  $A\beta$  peptides and the C-terminal APP intracellular domain (AICD). On the basis of similarities to the Notch processing pathway, it has been postulated that the AICD may play a role in gene regulation following its release in response to some form of extracellular signal.

In order to better understand the production and fate of the AICD, I have investigated the potential for exploiting a cell-free system to study its generation and properties. Having generated a number of model APP-derived fragments and shown them to be efficiently membrane integrated *in vitro*, I went on to study AICD production. I discovered that AICD-like fragments are extremely labile when synthesised in a rabbit reticulocyte lysate system and are rapidly degraded via a metalloproteinase, most likely the insulin degrading enzyme (IDE). The *in vitro* stability of these model AICD-like fragments was dependent upon the precise chain length of the polypeptide and N-terminal processing may preface the activity of IDE *in vitro*. The rapid degradation of the AICD *in vitro* is in close agreement with previous *in vivo* studies, and taken together such data are consistent with a role for the AICD in a signalling pathway of some form.

A variety of approaches were also taken to try to generate the AICD by the  $\gamma$ -secretase mediated cleavage of the APP-C99 fragment, a biologically relevant substrate. In no case was any evidence of such cleavage observed *in vitro* and hence I conclude that the endoplasmic reticulum does not possess an active form of the  $\gamma$ -secretase. Preliminary *in vivo*-based studies did provide evidence for the  $\gamma$ -secretase cleavage of APP-C99 fragments, consistent with current models implying that such processing takes place at the cell surface and/or in endosomes and not at the endoplasmic reticulum.

## Declaration

No portion of the work referred to in this thesis has been submitted in support of an application for another degree or qualification of this or any other university or other institute of learning.

## Copyright Statement

1. Copyright in text of this thesis rests with the Author. Copies (by any process) either in full, or of extracts, may be made **only** in accordance with instructions given by the Author and lodged in the John Rylands University Library of Manchester. Details may be obtained from the Librarian. This page must form part of any such copies made. Further copies (by any process) of copies made in accordance with such instructions may not be made without the permission (in writing) of the Author.
2. The ownership of any intellectual property rights which may be described in this thesis is vested in the University of Manchester, subject to any prior agreement to the contrary, and may not be made available for use by third parties without the written permission of the University, which will prescribe the terms and conditions of any such agreement.
3. Further information on the conditions under which disclosures and exploitation may take place is available from the Head of the Division of Biochemistry and Cell Biology (School of Biological Sciences).

## Acknowledgements

Many thanks to everyone in the High, Woodman, Bishop and Lowe labs for their continued help and support throughout my PhD.

Extra-special thanks to Cornelia for helping me out even when she had a million and one other things to do.

Thanks also to my supervisor, Steve High, for all his advice and help, and without whom the project would not have been possible.

And finally, thanks to Ben for putting up with my moaning and, most of all, for asking me to marry him and hence providing the best reason in the world for me to get my thesis finished!

This project was supported by the Wellcome Trust.

## Abbreviations

A $\beta$	Amyloid-beta peptide
AD	Alzheimer's disease
ADAM	A disintegrin and metalloproteinase
ALLN	N-acetyl-leuciny-l-leuciny-l-norleucinal
ApoE	Apolipoprotein E
APLP	Amyloid precursor-like protein
APP	Amyloid precursor protein
APS	Ammonium persulphate
ATCA	Aurintricarboxylic acid
BACE	Beta-site APP-cleaving enzyme
BFA	Brefeldin-A
BiP	Heavy chain binding protein
CHAPSO	3-[(3-Cholamidopropyl)dimethylammonio]-2-hydroxy-1-propanesulfonate
COP	Coat protein
CRT	Calreticulin
CSL	CBF1/Suppressor of Hairless/Lag1
CTF	C-terminal fragment
DAPI	4',6-diamidino-2-phenylindole* 2HCl
DMSO	Dimethyl sulphoxide
DTT	Dithiothreitol
EDTA	Ethylenediaminetetraacetic acid
Endo H	Endoglycosidase H
ER	Endoplasmic reticulum
ERGIC	ER-Golgi intermediate compartment
FCS	Foetal calf serum
GFP	Green fluorescent protein
ICD	Intracellular domain
I-CLiP	Intramembrane-cleaving protease
IDE	Insulin-degrading enzyme
IP	Immunoprecipitation
MAP	Methionine aminopeptidase
NEM	N-ethyl maleimide

NICD	Notch intracellular domain
NTF	N-terminal fragment
OST	Oligosaccharyl transferase
PBS	Phosphate-buffered saline
PCR	Polymerase chain reaction
PEG	Polyethylene glycol
PMSF	Phenylmethylsulfonyl fluoride
PNT	1,10-phenanthroline
PPL	Preprolactin
PS	Presenilin
PTB	Phosphotyrosine-binding
RIP	Regulated intramembrane proteolysis
RNC	Ribosome/nascent chain complex
SBTI	Soy bean trypsin inhibitor
SDS-PAGE	Sodium dodecyl sulphate-polyacrylamide gel electrophoresis
SCAP	SREBP cleavage activating protein
SI-cells	Semi-intact cells
SNARE	Snap Receptor
SREBP	Sterol regulatory binding protein
SRP	Signal recognition particle
TACE	Tumour necrosis factor- $\alpha$ converting enzyme
TCA	Trichloroacetic acid
TM	Transmembrane
TRAM	Translocating chain-associated membrane protein
TRAP	Translocon-associated protein

# CHAPTER 1



## Introduction

# 1 Introduction

## 1.1 The secretory pathway

Eukaryotic cells are characterised by a variety of membrane-enclosed compartments called organelles, each of which has a specific protein composition that allows it to perform its function. In order to maintain distinct environments within these organelles, movement of both small molecules and proteins into and out of each organelle is normally regulated by a membrane barrier. The sub-cellular destination of a newly synthesised protein is initially determined by targeting elements, called “signal sequences” and these amino acid-based motifs function to direct the nascent chain from the cytosol to a particular cellular location (High, 1995).

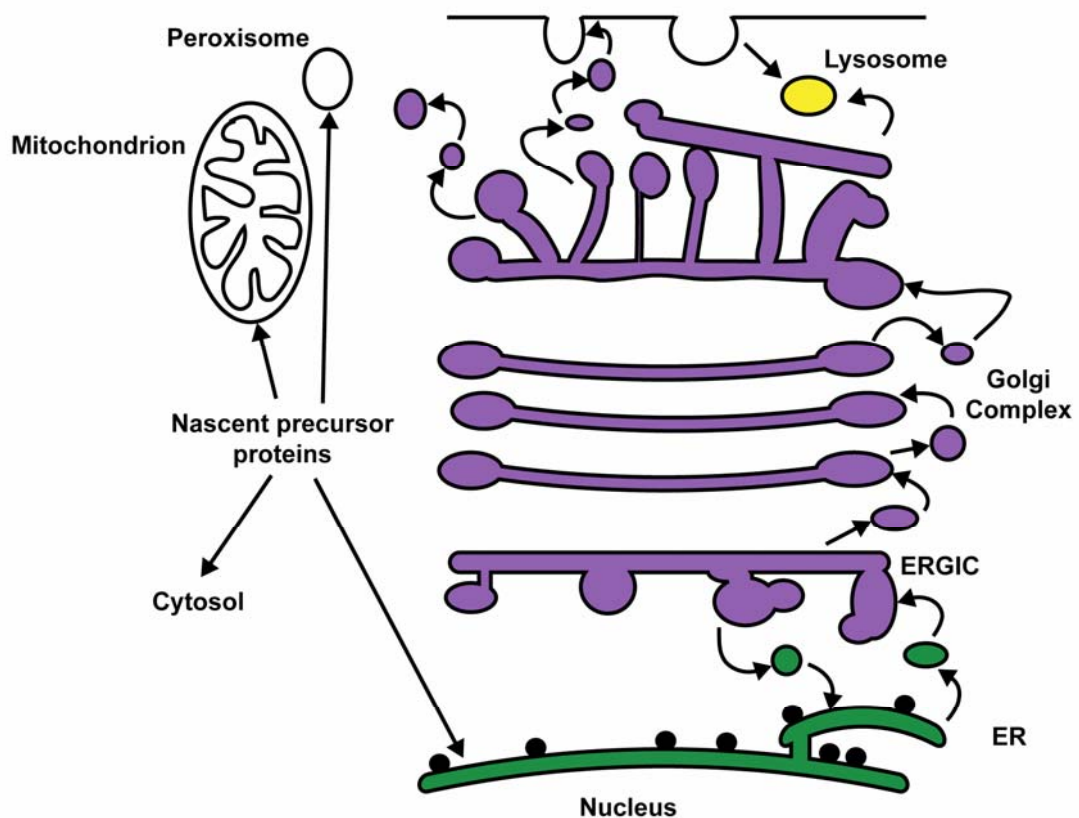


Fig 1.1. Protein targeting and the secretory pathway.

Newly made proteins may either remain in the cytosol or be targeted to organelles, such as mitochondria, peroxisomes, or the ER, which acts as the entry point for the secretory pathway. Once in the secretory pathway, proteins are transported through the ER-Golgi intermediate compartment (ERGIC) and the Golgi to the plasma membrane and lysosomes.

The endoplasmic reticulum (ER) is one example of a well-defined cellular organelle that plays an important role in the biogenesis and folding of membrane and secretory proteins that are destined for locations throughout the so called “secretory pathway” of eukaryotic cells (Palade, 1975). Most proteins that are destined for intracellular compartments along the secretory pathway, for example the ER-Golgi intermediate compartment (ERGIC), Golgi and lysosomes, must first enter the ER from the cytoplasm (Palade, 1975). Likewise, secretory proteins and integral membrane proteins of the plasma membrane are usually synthesised on membrane-bound ribosomes at the ER before being sorted to the cell surface.

## **1.2 Targeting**

In order to gain entry into the ER, proteins contain a hydrophobic targeting signal (Blobel and Dobberstein, 1975; von Heijne, 1995) that is recognised co-translationally by the Signal Recognition Particle (SRP) as it emerges from the ribosome (Keenan et al., 2001). SRP-binding causes a temporary “pause” in translation that is released when the ribosome-nascent chain complex interacts with the SRP-receptor (Keenan et al., 2001) at the ER membrane where it is associated with the ER translocation machinery (see section 1.3, and; Johnson and van Waes, 1999). The SRP-receptor acts to co-ordinate the release of SRP from the nascent chain such that the polypeptide is passed on to the translocon, thereby facilitating membrane insertion and/or integration (Meacock et al., 2000). It should be noted that there are some proteins that can be targeted to the ER membrane via a post-translational mechanism (Rapoport et al., 1999). Such proteins are translated and released from the ribosome before being directed to the ER translocon. Post-translational translocation is believed to utilise similar components to the co-translational pathway, although cytosolic chaperones may also contribute to maintaining the polypeptide in a translocation-competent state (Abell et al., 2004; Klappa et al., 1995).

Following SRP displacement and the insertion of the nascent chain into the translocation complex, signal sequences are often cleaved by signal peptidase and released into the ER membrane (Martoglio and Dobberstein, 1998), whilst the mature part of the protein is either translocated into the lumen of the ER or becomes integrated into the lipid bilayer of the ER membrane. Following removal

from the nascent chain, some signal peptides are further processed by signal peptide peptidase and the resulting fragments released into the cytosol or the ER lumen (Martoglio, 2003; Weihofen et al., 2002).

### **1.3 Protein biogenesis at the ER**

To enable transport of hydrophilic proteins across the hydrophobic lipid bilayer of the ER membrane, a protein-lined aqueous channel is present. In mammals, this channel is usually called the ER translocon and it is associated with additional membrane protein complexes (Gorlich and Rapoport, 1993; Johnson and van Waes, 1999). The mammalian translocon, or Sec61 complex, is comprised of three proteins, Sec61 $\alpha$ , Sec61 $\beta$  and Sec61 $\gamma$  (Gorlich and Rapoport, 1993; High, 1995). It was believed that oligomers of the Sec61 heterotrimeric complex were required to form an active translocation pore (Hanein et al., 1996). However, x-ray diffraction data from the *M. Jannaschii* SecY complex, which is analogous to the mammalian Sec61 complex, have suggested that whilst the heterotrimer is part of an oligomer, a single heterotrimer can serve as a functional translocation channel (Van den Berg et al., 2004). The same complex is also thought to play a role in signal sequence recognition and ribosome binding (Rapoport et al., 1996a; Rapoport et al., 1996b; Van den Berg et al., 2004).

Until recently, it was assumed that the permeability barrier of the ER membrane must be maintained during the process of polypeptide translocation and insertion, and that the translocon was gated in a regulated manner to ensure that an efficient seal was preserved. The translating ribosome had been postulated to form a barrier at the cytosolic face of the ER translocon (Crowley et al., 1994), whilst the gating of its luminal end was thought to be maintained by the ER chaperone, heavy chain binding protein (BiP) (Hamman et al., 1998) (Johnson, 2003). However, one recent study has suggested that the ER membrane may be permeable to small molecules, and it was postulated that this “leakiness” may ensure optimal conditions for protein folding (Le Gall et al., 2004). Hence the nature of the permeability barrier offered by the ER membrane *in vivo* remains open to question (Le Gall et al., 2004).

In addition to the Sec61 complex, other components, such as the translocating chain-associated membrane protein (TRAM) and the translocon-associated protein (TRAP) complex, are required for the translocation of many proteins (Hegde et al., 1998). The precise roles of these additional factors during translocation are unknown. Other ER proteins are also found in close proximity to the translocon, for example the signal peptidase complex (Wang and Dobberstein, 1999), that mediates signal-sequence processing (cf. section 1.2), and the oligosaccharyltransferase complex (OST) (Knauer and Lehle, 1999), that carries out *N*-glycosylation of nascent polypeptide chains. The OST is a multimeric complex that transfers a large precursor oligosaccharide (Glc<sub>3</sub>Man<sub>9</sub>GlcNAc<sub>2</sub>) from a dolichol lipid carrier to selected asparagine side chains (in an Asn-X-Ser/Thr consensus sequence) within nascent polypeptides during translocation (Knauer and Lehle, 1999). Whilst the nascent polypeptide is still in the ER, all three glucose residues and at least one mannose residue are enzymatically removed (Knauer and Lehle, 1999). Further modifications to the N-linked oligosaccharides occur within the Golgi apparatus, and result in the formation of various distinct “mature” glycoproteins (Knauer and Lehle, 1999).

#### **1.4 *Sorting and vesicular traffic***

Once proteins have been transported into the ER, they are often trafficked to specific cellular locations. Proteins can be transported from the ER in lipid-bound vesicles and elongated membrane tubules (Bonifacino and Glick, 2004; Gorelick and Shugrue, 2001). This is a complex process since hundreds of different proteins may move through the secretory pathway to distinct cellular compartments and this movement must be co-ordinated in response to the changing requirements of the cell.

Only correctly folded proteins are able to exit the ER, and this quality control process is regulated by chaperone proteins (Gorelick and Shugrue, 2001). Misfolded proteins are either retained in the ER and/or degraded (Gorelick and Shugrue, 2001). Some proteins are destined to function in the ER and will therefore not be trafficked to a downstream location. Thus, cargo proteins that are to be transported must be efficiently sorted from these resident ER proteins. Such resident proteins contain retention/retrieval signals that are recognised and allow

any proteins that do escape the ER to be transported back by a retrieval pathway (Gorelick and Shugrue, 2001). To ensure that nascent proteins can efficiently exit the ER and move to their cellular destinations, polypeptides destined for locations downstream of the ER are concentrated at ER exit sites, a process that is postulated to involve COPII coat proteins (Gorelick and Shugrue, 2001).

Following the selection of proteins to be transported from the ER, this cargo must be packaged into transport vesicles. This process involves the sequential action of coat complex II (COPII) and coat complex I (COPI) machinery (Gorelick and Shugrue, 2001). The formation of the multi-subunit COPII complex at the ER membrane involves the ordered recruitment of at least five cytosolic components in a process that acts to mediate both cargo selection and membrane deformation (Gorelick and Shugrue, 2001). The COPI complex is involved in the retrieval of proteins destined for recycling back to the ER (Gorelick and Shugrue, 2001).

### **1.5 *Transmembrane proteins***

Once proteins have been efficiently targeted to their particular sub-cellular compartment, they can begin to perform their specific functions, for example as enzymes, receptors, channels and transporters. One important function of membrane proteins is as cell surface receptor proteins that transduce extracellular signals to the inside of the cell. Classically, this signal transduction is achieved through the activation of G-proteins, the gating of ion channels, or by altering the activity of kinases. More recently, it has been suggested that proteolysis can act as an alternative method for enabling signal transduction (Brown et al., 2000). This mechanism relies upon the presence of pre-synthesised, inactive, transcription or signalling factors tethered to a membrane that retains the protein outside the nucleus (Rawson, 2002). Following receipt of a signal, these “dormant” proteins become activated and a fragment of the protein is released enabling it to transduce the signal (Rawson, 2002; Weihofen and Martoglio, 2003). Such proteolytic activation normally involves processing by two distinct enzymes. The first cleavage occurs upon delivery of the signal, and usually cleaves the protein within its hydrophilic ectodomain (Rawson, 2002). The second cleavage is dependent upon the primary processing event, and occurs within a transmembrane spanning region, releasing products into the cytosol or the

exoplasmic space (Rawson, 2002). Because the secondary cleavage cannot occur until after the ectodomain has been removed, this process has become known as “regulated intramembrane proteolysis” (RIP) (Ebinu and Yankner, 2002).

## **1.6 Regulated intramembrane proteolysis**

Regulated intramembrane proteolysis (RIP) involves the processing of a membrane-spanning protein within its “inaccessible” transmembrane domain (Ebinu and Yankner, 2002). RIP of transmembrane proteins is catalysed by intramembrane cleaving proteases (I-CLiPs), and it has been proposed that this cleavage promotes the controlled release of membrane-anchored proteins, such as transcription or signalling factors (Weihofen and Martoglio, 2003). The first I-CLiP to be identified was the site-2 protease (S2P), which is involved in the activation of the sterol regulatory element binding protein (SREBP).

### *1.6.1 SREBP: A well-characterised example of RIP*

RIP was discovered during studies of the transcriptional regulation of cholesterol metabolism. The sterol regulatory element binding proteins (SREBPs) have two membrane-spanning regions flanked by an N-terminal transcription factor domain and a C-terminal regulatory domain (Hua et al., 1995) (see Fig 1.2). SREBPs regulate multiple genes that are involved in the biosynthesis and uptake of cholesterol (Wang et al., 1994) and this regulation is achieved via the release of the N-terminal region of the SREBP from the membrane so that it is able to enter the nucleus and influence transcription (Brown and Goldstein, 1997). A two-step proteolytic cascade that is regulated by sterols mediates the release of the transcription factor domain (see Fig 1.2). SREBP site-1 protease (S1P) cleaves the protein on the luminal side of the first transmembrane spanning region in SREBP (Brown and Goldstein, 1997). This initial cleavage is regulated by SREBP cleavage activating protein (SCAP). SREBP is then cleaved within its transmembrane region by the SREBP site-2 protease (S2P) (Brown and Goldstein, 1997). Cleavage by S2P liberates the transcription factor domain, which is released into the cytosol from where it can enter the nucleus and activate gene transcription. Since the discovery of S2P, several other proteases have

been identified that are able to cleave proteins within their transmembrane domains. One well characterised example of a RIP-substrate is the Notch protein.

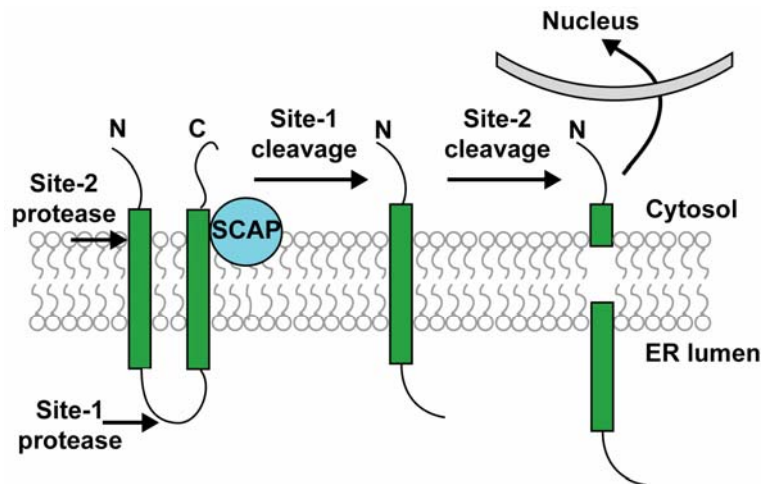


Fig 1.2. **Model for the sterol-mediated proteolytic release of SREBPs from the membrane.**

Release is initiated by site-1 protease, a sterol-regulated protease that recognises the SREBP/SCAP complex and cleaves SREBP in the luminal loop between the two transmembrane domains. SCAP allows site-1 cleavage to be activated when cells are depleted of sterols, and it inhibits this process when sterols are abundant. Once the two halves of SREBP are separated, a second protease, site-2 protease, cleaves the N-terminal domain of SREBP at a site located within the membrane-spanning region. After the second cleavage, the resulting N-terminal domain enters the nucleus where it activates target genes controlling lipid synthesis and uptake.

### 1.6.2 Notch processing

Notch is a single transmembrane spanning receptor that mediates many cell fate decisions (Schroeter et al., 1998). It is synthesised as a large precursor, which is cleaved at site-1 (S1) by a furin-like convertase in the Golgi during the trafficking of Notch to the cell surface. This processing event generates two fragments that remain associated as a heterodimeric complex at the cell surface (see Fig 1.3, and; De Strooper et al., 1999). Following the binding of one of several potential ligands to the Notch receptor, the C-terminal domain of Notch undergoes two further sequential processing events, the first at site-2 (S2) by an  $\alpha$ -secretase-like protease of the ADAM (a disintegrin and a metalloprotease)/TACE (tumor necrosis factor-alpha converting enzyme) family, and the second at site-3 (S3) by the  $\gamma$ -secretase complex (cf. section 1.9). These cleavages result in the release of the

Notch intracellular domain (NICD) from the membrane, which can then translocate to the nucleus. The final cleavage of the activated Notch receptor occurs via the  $\gamma$ -secretase and takes place after endocytosis (Gupta-Rossi et al., 2004). Once in the nucleus, the NICD interacts with, and is stabilized by, specific binding partners (CSL (CBF1, Suppressor of hairless, Lag-1) proteins) and the complex acts to regulate transcription and influence cell fate (Schroeter et al., 1998).

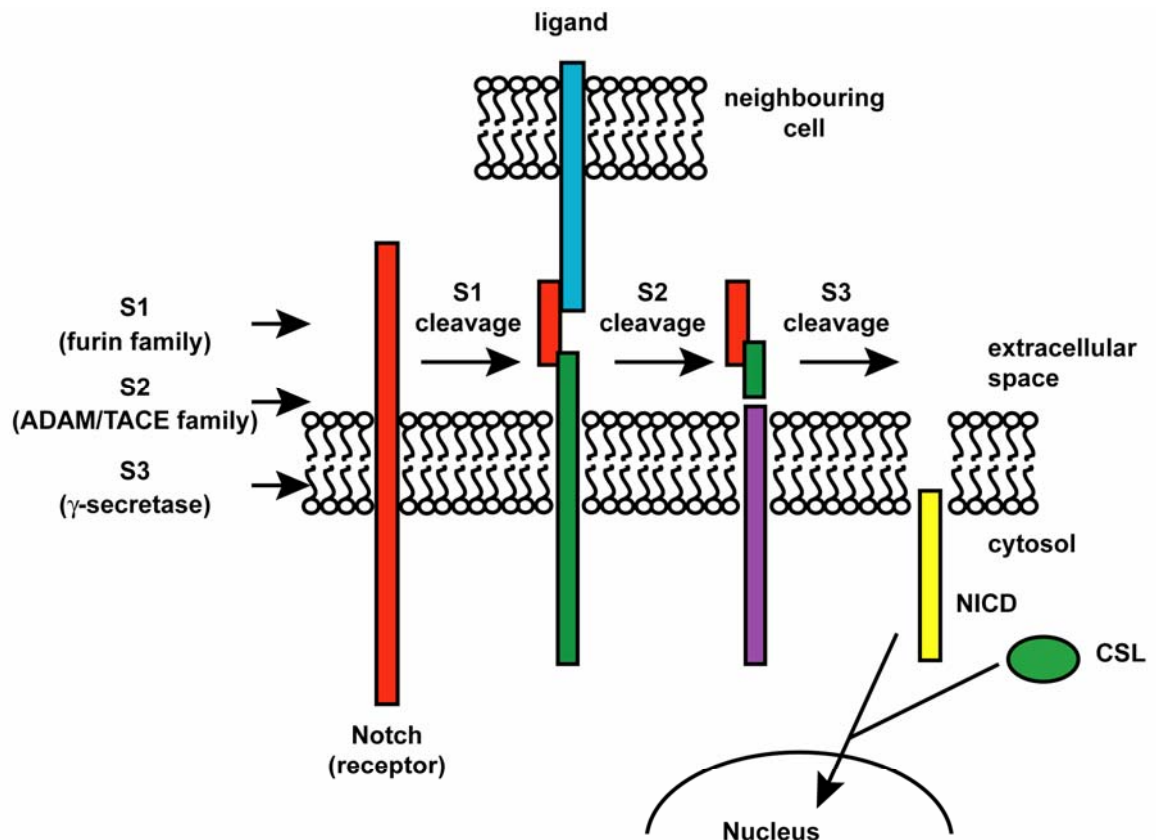


Fig 1.3. **Notch processing.**

Notch signalling depends on three proteolytic cleavages. Notch is first cleaved at S1 by a furin protease. The cleaved products remain associated before binding to Notch ligands (members of the Delta/Serrate/Lag-2 family) on the surface of a neighbouring cell. Cleavage at the S2 site by a TACE/ADAM family member generates a small membrane-bound fragment that can then be cleaved at S3. This S3 cleavage is similar to the  $\gamma$ -secretase cleavage of APP, and generates the Notch intracellular domain (NICD), which is then translocated to the nucleus where it regulates gene transcription.

It has been observed that the mechanism of RIP for Notch and the amyloid precursor protein (APP) is strikingly similar (Selkoe and Kopan, 2003). Moreover, the same proteases may be involved in cleaving both Notch and APP (Selkoe and Kopan, 2003). Intramembranous cleavage of APP was brought into the spotlight because one of the products of this cleavage, the amyloid- $\beta$  ( $A\beta$ ) peptide, forms the amyloid plaques that are associated with Alzheimer's disease (cf. section 1.6).

The discovery that both Notch and APP are processed by RIP generated substantial interest because of the possible implications for understanding fundamental mechanisms that underlie development and brain degeneration. In the remainder of this introduction, I will focus on APP and the proteolytic processing events that are involved its cleavage with particular reference to the A $\beta$  and AICD fragments generated during this process.

### **1.7 Introduction to Alzheimer's disease**

Alzheimer's disease (AD) is the most common cause of a progressive decline of cognitive function in aged humans (Fraser et al., 2000; Golde et al., 2000). The pathogenesis of the disease is multifaceted, and the common clinical and neuropathological characteristics can arise from a number of distinct heritable and sporadic causes that all lead to neuronal loss (Fraser et al., 2000).

The most prominent neuropathological signs of the disease are intracellular neurofibrillary tangles and extracellular neuritic plaques in the brain (Chapman et al., 2001; De Strooper et al., 1997). The former are mainly comprised from a highly polymerised form of the cytoskeletal protein tau, whereas the latter are composed largely of amyloid- $\beta$  (A $\beta$ ), which is one of the cleavage products of the amyloid precursor protein (APP) (for reviews see; Hardy, 1997; Mattson, 2004). On the basis of these observations, theories as to the cause of Alzheimer's disease have been based around the key features of cell loss, neurofibrillary tangle formation and the production, deposition and accumulation of A $\beta$ . Two main theories for the cause of AD have been proposed, and these can be defined as the amyloid hypothesis and the tau hypothesis (for review see; Chapman et al., 2001). Whilst there are mutations in tau that can cause polymerisation and formation of the paired-helical filaments that are found in the cytoplasm of affected neurons, these mutations are not solely associated with AD and are also found in other neurological diseases (Chapman et al., 2001; Selkoe, 1996). This suggests that the link between tau and AD is not absolute. Nevertheless, all of the tau mutations associated with familial AD lead to the eventual development of tau pathology. Conversely, inherited mutations linked to APP are associated with, and exclusive to, AD. Indeed, it was studies of A $\beta$ , the major component of amyloid

plaques that resulted in the identification of the first specific genetic cause of AD (Selkoe, 1996).

It is now clear that a small proportion of AD cases are transmitted as a pure autosomal dominant trait with age-dependence, but notably high penetrance (Fraser et al., 2000). Analysis of these pedigrees led to the identification of two Alzheimer's-related genes, that were found to encode the amyloid precursor protein (APP) and apolipoprotein E (ApoE) (for review see; Selkoe, 1996). ApoE is involved in cholesterol transport, metabolism and storage and can exist as one of three naturally-occurring isoforms,  $\epsilon 2$ ,  $\epsilon 3$  and  $\epsilon 4$  (for review see; Sorbi et al., 2001). Whilst the cause of the common, sporadic, form of Alzheimer's disease is not yet fully understood, there is an increased risk associated with the presence of the  $\epsilon 4$  allele of ApoE. It has been suggested that the ApoE  $\epsilon 4$  isoform may facilitate  $A\beta$  aggregation, as it has also been found to be associated with increased amyloid deposition (for review see; Selkoe, 1996). However, not all carriers of the  $\epsilon 4$  polymorphism get AD, and the allele is therefore considered to be a risk factor rather than causative for the disease (for reviews see; Selkoe, 1996; Sorbi et al., 2001).

Notwithstanding the role for ApoE outlined above, during the remainder of this introduction I will concentrate on describing APP, and how its intramembrane proteolysis is responsible for generating the peptide species believed to play a role in the pathology of Alzheimer's disease.

## **1.8 APP**

APP and related family members, amyloid precursor-like protein-1 and -2 (APLP-1 and APLP-2), are homologous type I integral membrane proteins with cleavable N-terminal signal sequences (see Fig 1.4). However, APP is the only member of the family that contains the amyloidogenic  $A\beta$  sequence and it is therefore the subject of particularly intense analysis. APP is expressed at high levels in neurons and glia, and contains a large extracellular region, a single transmembrane domain, and a short cytoplasmic tail (see Fig 1.4).

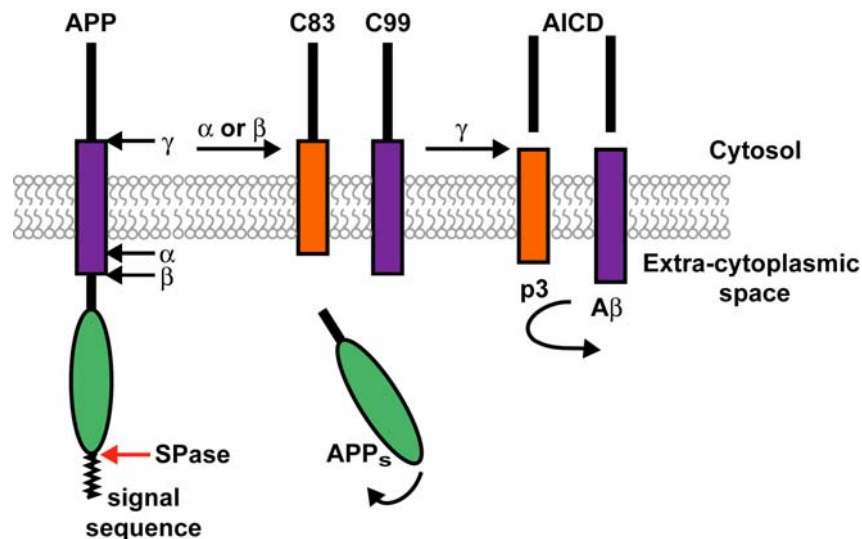


Fig 1.4. **Amyloid precursor protein (APP) processing.**

The red arrow indicates processing of the APP signal sequence by signal peptidase (SPase). The black arrows indicate the sites of constitutive proteolytic cleavages made by proteases designated  $\alpha$ -,  $\beta$ - and  $\gamma$ -secretase. Cleavage by  $\alpha$ -secretase enables secretion of the large, soluble ectodomain of APP (APP <sub>$\alpha$</sub> ) into the medium and retention of the 83-residue C-terminal fragment (C83) in the membrane. The C83 fragment can undergo cleavage by a protease called the  $\gamma$ -secretase at residue 711 or 713 to release the p3 peptides and the AICD. The alternative to  $\alpha$ -secretase cleavage is proteolytic cleavage after residue 671 by the  $\beta$ -secretase. This results in the production of a slightly truncated version of the APP ectodomain (APP <sub>$\beta$</sub> ) and the retention of a 99-residue C-terminal fragment (C99) in the membrane. The C99 fragment can undergo cleavage by the  $\gamma$ -secretase to release the A $\beta$  peptides and the AICD.

The main function of APP is unclear, although its distribution in neuronal synapses has been taken to suggest that it may have a role in signal transduction (Chapman et al., 2001), and several studies have suggested that the C-terminal fragment may play a role in gene regulation (cf. section 1.6 and; Baek et al., 2002; Cao and Sudhof, 2001; Cupers et al., 2001b; Kimberly et al., 2001). APP is synthesised in the ER, posttranslationally modified in the Golgi, including carbohydrate processing, phosphorylation and sulphonation, and transported to the cell surface via the secretory pathway (cf. sections 1.1-1.4). APP can be proteolytically processed to generate a number of different fragments, including the A $\beta$  peptides that are characteristic of amyloid plaques (Fig 1.4, and for reviews see; Fraser et al., 2000; Golde et al., 2000; Mattson, 2004; Selkoe, 1996).

Although numerous proteins are contained within the amyloid deposits generally found in AD, the main protein component is aggregates of the ~4 kDa polypeptide,

A $\beta$  (Golde et al., 2000; Mattson, 2004; Selkoe, 1996). The amyloidogenic processing of APP to produce the A $\beta$  peptides requires sequential proteolytic cleavages by the  $\beta$ - and  $\gamma$ -secretases at the N- and C- termini respectively (Fig 1.4, and for reviews see; Fraser et al., 2000; Golde et al., 2000; Selkoe, 1996)). Cleavage of APP by  $\beta$ -secretase generates an APP-C99 fragment, which is a substrate for further processing by the  $\gamma$ -secretase to produce A $\beta$ 40 and A $\beta$ 42/3. A third proteolytic activity, referred to as the  $\alpha$ -secretase, cleaves APP to produce an 83-amino acid C-terminal fragment, APP-C83. The  $\alpha$ -secretase processing occurs within the A $\beta$  sequence, thereby preventing A $\beta$  formation (Fig 1.4, and; Golde et al., 2000). APP-C83 can then be cleaved by the  $\gamma$ -secretase to generate the p3 peptide (Fig 1.4). Cleavage of both APP-C99 and APP-C83 by the  $\gamma$ -secretase also liberates the APP intracellular domain (AICD) (Fig 1.4), which has been postulated to translocate to the nucleus where it may regulate gene expression (Kimberly et al., 2001).

Detailed studies have shown that there are multiple forms of A $\beta$  (Sato et al., 2003), and alternative processing by the  $\gamma$ -secretase can generate both A $\beta$ 40 and A $\beta$ 42/3 peptides (for review see; Hardy, 1997). A major difference between these two species is their different rates of fibril formation, and although genetic evidence suggests a causal role for A $\beta$ 42 in AD pathogenesis, A $\beta$ 40 is deposited in significant amounts in the amyloid plaques present in typical late onset AD brain tissue (for review see; Hardy, 1997). In fact, in most studies A $\beta$ 40 appears to be the most abundant peptide found in the amyloid deposits present in blood vessels in the brain (Golde et al., 2000). It is likely that both A $\beta$ 40 and A $\beta$ 42 contribute to AD pathogenesis, but it has been suggested that A $\beta$ 40 deposition requires additional factors, such as the presence of ApoE  $\epsilon$ 4 (see section 1.7) or prior seeding by A $\beta$ 42 to promote its accumulation in amyloid plaques (Golde et al., 2000; Selkoe, 1996). It is also apparent that a large proportion of the mutations involved in familial AD lead to the production of A $\beta$ 42, whereas very few are associated with increased A $\beta$ 40 generation (Hardy, 1997). This also supports the idea that A $\beta$ 42 may be responsible for producing the “seed” that allows further amyloid deposition to occur (Lansbury, 1997).

Historically, a key question concerning the pathological mechanisms fundamental to AD has been whether modified processing of A $\beta$ , leading to its aggregation, triggers AD pathology or whether such modified processing is actually a by-product of that pathology. Inherited forms of AD have played a central role in resolving this issue; if A $\beta$  aggregation triggers the development of AD pathology then genetic alterations that produce AD should be related to A $\beta$  aggregation. This association was indeed established (for review see; Hardy, 1997), and this has provided the most compelling justification for studies of the factors that generate altered A $\beta$  metabolism and aggregation in AD (Golde et al., 2000).

Numerous studies have indicated that defects in the APP and ApoE  $\epsilon$ 4 genes alone cannot account for all of the cases of inherited AD, and a series of polymorphic markers on chromosomes 1 and 14 were found to be linked to a particularly severe form of early-onset familial AD. Investigation into these mutations led to the discovery of presenilin-1 (PS1) and presenilin-2 (PS2) (Alzheimer's Disease Collaborative Group, 1995). Like mutations in the APP gene, mutations in the genes encoding PS1 and PS2 that are linked to familial AD act to increase either total A $\beta$  production or the relative amount of the longer A $\beta$ 42-like peptides (Golde et al., 2000). The observation that mutations in PS1 and PS2 can result in alterations in the  $\gamma$ -secretase-dependent cleavage of APP clearly implicated these components in this process (cf. section 1.10.1), and taken together the observations outlined above suggest that the abnormal processing of APP may be a key cause of AD.

## **1.9 APP processing**

Normally, only a fraction of the total APP is cleaved, and all of the resulting fragments, including A $\beta$ , form a part of normal cellular physiology and are produced both *in vivo* and *in vitro* (Haass et al., 1992).

### **1.9.1 $\alpha$ -Secretase processing**

$\alpha$ -Secretase processing is the predominant cleavage that occurs in APP, and since it cleaves within the protein sequence that produces A $\beta$ , the  $\alpha$ -secretase

cleavage prevents A $\beta$  formation (De Strooper and Annaert, 2000). In cultured cells, it has been shown that the fraction of APP that is processed by  $\alpha$ -secretase can be increased by activating second messenger cascades, and specifically that the activation of protein kinase C causes the majority of APP to be cleaved via the so-called “regulated”  $\alpha$ -cleavage pathway (Gillespie et al., 1992).

Several  $\alpha$ -secretase candidates have been identified, and it appears that there may be several different proteases that are all capable of cleaving APP at the  $\alpha$ -secretase site. Tumour necrosis factor- $\alpha$  converting enzyme (TACE or ADAM17), a member of the ADAM (a disintegrin and metalloproteinase) family has been implicated in the “regulated”  $\alpha$ -secretase processing of APP (Buxbaum et al., 1998). This cleavage is thought to be a result of TACE itself acting on APP rather than via an intermediary since its catalytic domain was able to cleave a synthetic peptide at the  $\alpha$ -secretase site, demonstrating that TACE has the potential to cleave APP (Buxbaum et al., 1998). When TACE-deficient mouse fibroblasts were studied, they showed defects in APP secretion and processing (Buxbaum et al., 1998). However, TACE only appears to mediate protein kinase C-modulated cleavage, and constitutive  $\alpha$ -secretase processing of APP is still observed in TACE-knock out mice (Buxbaum et al., 1998).

This constitutive  $\alpha$ -secretase cleavage of APP is most probably mediated by another member of the ADAM family, ADAM10, and experiments using over-expression studies and synthetic substrates indicated that ADAM10 can mediate both constitutive and regulated  $\alpha$ -secretase processing (Lammich et al., 1999). *In vitro* both ADAM10 and TACE cleave APP at the site of  $\alpha$ -secretase cleavage defined *in vivo* in most cell types. Whilst ADAM10 has been shown to cleave APP when overexpressed *in vivo*, it has been pointed out that this could be an artefact resulting from over-expression (for review see; Schlondorff and Blobel, 1999). More compelling evidence comes from the observation that a dominant negative ADAM10 construct is able to inhibit the  $\alpha$ -secretase processing of APP (Lammich et al., 1999). However, studies using ADAM10 knock-out mice indicated that other proteases are able to compensate for an ADAM10 deficiency, as only a small proportion of mice lacking the enzyme showed defects in the  $\alpha$ -secretase processing of APP (Hartmann et al., 2002). A contribution by further members of

the ADAM family cannot be excluded, and over-expression of ADAM9 (MCD9) has also been shown to cause an increase in the cleavage of APP-derivatives at the  $\alpha$ -secretase site (Koike et al., 1999). However, similarly to the knock-out mice studies performed for ADAM10, ADAM9 deficient mice displayed comparable levels of  $\alpha$ -secretase cleavage products to wild-type mice (Weskamp et al., 2002). Taken together, these studies suggest that several proteases are capable of cleaving APP at the  $\alpha$ -secretase site (for review see; Allinson et al., 2003), and indeed two proteases have also been identified in the yeast *Saccharomyces cerevisiae* that are able to process APP at its authentic  $\alpha$ -secretase site (Komano et al., 1998). Whilst  $\alpha$ -secretase cleavage is a major processing pathway, this pathway does not exclusively process cellular APP and some is first cleaved by an alternative protease, the  $\beta$ -secretase, which competes with the  $\alpha$ -secretase for the APP substrate.

### 1.9.2 $\beta$ -Secretase processing

A $\beta$  generation involves the cleavage of APP first by the  $\beta$ -secretase, and then by the  $\gamma$ -secretase. Four independent studies all led to the identification of  $\beta$ -secretase as the membrane-bound aspartyl protease BACE (beta-site APP-cleaving enzyme) (Hussain et al., 1999; Sinha et al., 1999; Vassar et al., 1999; Yan et al., 1999). Studies of cultured mammalian cells defined the functional properties of the  $\beta$ -secretase early on, predicting it to be widely expressed, localised to the late Golgi and endosomes, and to have an acidic pH optimum (Vassar et al, 1999). In humans,  $\beta$ -secretase mRNA is highly expressed in the brain and is also found within a variety of human tissues (Vassar et al., 1999), which correlates with the observation that A $\beta$  is normally produced by many cell types (Haass et al., 1992). BACE has homology to the pepsin family of aspartyl proteases and is a type I integral membrane protein, which has two aspartate residues within the ectodomain that are responsible for its activity (Haniu et al., 2000).

Since BACE and the  $\gamma$ -secretase are responsible for the cleavage events that generate the amyloidogenic peptide A $\beta$ , these proteins are strong candidates for potential drug targets in the treatment of Alzheimer's disease. Studies using

BACE knock-out mice suggested that BACE may be an optimal drug target, since the mice were healthy and displayed no phenotype other than a reduction in cellular levels of A $\beta$  (Cai et al., 2001). One major concern in the development of drugs that inhibit the proteolytic cleavages of APP is the range of endogenous substrates that they may process. To date only two further BACE substrates in addition to APP have been identified (Kitazume et al., 2001; Lichtenthaler et al., 2003), however, it is possible that additional as yet unidentified substrates exist. Whilst the  $\beta$ -secretase is an essential part of the pathway, it is the  $\gamma$ -secretase cleavage that is responsible for the final event that generates A $\beta$  and the AICD.

### **1.10 $\gamma$ -Secretase processing**

It has been clear for some time that a proteolytic activity referred to as the  $\gamma$ -secretase is pivotal to the cellular production of the A $\beta$  peptides. The last decade has seen major advances in our understanding of the identity of the  $\gamma$ -secretase and the complexity of its function (Iwatsubo, 2004).

#### *1.10.1 Evidence that presenilins are a core component of the $\gamma$ -secretase*

The presenilins were the first sub-unit of the  $\gamma$ -secretase complex to be identified (De Strooper et al., 1998). Presenilins (PS) are polytopic integral membrane proteins that were initially discovered through genetic linkage analysis of families with autosomal dominant forms of Alzheimer's disease (cf. section 1.7). Mammalian PS consists of two homologous proteins, PS1 and PS2, which show strong sequence similarity, with 63% of amino acids conserved between the two proteins (De Strooper et al., 1997), and are ubiquitously expressed in the brain. PS have 10 hydrophobic domains that are postulated to represent 6-9 transmembrane (TM) spans together with additional hydrophobic regions. An 8 TM structure, with the N- and C-termini oriented towards the cytosol, is widely considered to be the most likely topology (see Fig 1.5 and; Doan et al., 1996; Li and Greenwald, 1998), although 7 and 9 TM models have also been proposed (Nakai et al., 1999). Newly synthesized full-length PS is endoproteolytically processed by an unknown enzyme, termed presenilinase, to generate N- and C-terminal fragments of ~30 kDa and ~20kDa respectively (Thinakaran et al., 1996).

These fragments remain associated as a heterodimeric complex (Thinakaran et al., 1998).

The role of presenilins in  $\gamma$ -secretase processing was first supported by studies of presenilin knock-out mice, in which a decrease in the production of A $\beta$  fragments was observed (De Strooper et al., 1998). Initially, because of their lack of homology to known proteases, presenilins were not considered likely candidates as an enzymatic component of the  $\gamma$ -secretase. However, there is now a plethora of evidence to suggest that this is the case, and for the sake of simplicity, these data are summarised in table 1.1.

**Table 1.1**

<b>Evidence For PS as the catalytic subunit of the <math>\gamma</math>-secretase</b>	<b>References</b>
Mutations in PS lead to altered APP processing	(Citron et al., 1997; Sherrington et al., 1995)
PS has an acidic optimum pH consistent with that observed for $\gamma$ -secretase	(Huse and Doms, 2001)
In the absence of PS, cleavage of APP by the $\gamma$ -secretase was prevented	(De Strooper et al., 1998)
PS mutations influence APP processing, causing elevation of the production of A $\beta$ 42	(Davis et al., 1998)
Two transmembrane aspartate residues in PS are required for presenilin endoproteolysis and for $\gamma$ -secretase activity	(Wolfe et al., 1999)
Transition-state analogue inhibitors of $\gamma$ -secretase bind to PS	(Li et al., 2000b)
Production of A $\beta$ 40 and A $\beta$ 42 was not detectable in cell lines lacking presenilin genes	(Zhang et al., 2000)
There is homology between the postulated active site of the $\gamma$ -secretase within PS and polytopic aspartyl proteases of bacterial origin	(Steiner et al., 2000)
Signal peptide peptidase is an aspartic protease that cleaves within hydrophobic signal peptides and closely resembles PS	(Weihofen et al., 2002)

Taken together, these studies strongly support the view that the presenilins act as aspartyl proteases with the active site located within the membrane (Fig 1.5). It has been suggested that aspartate residues in transmembrane domains 6 and 7 of PS form the active site of the  $\gamma$ -secretase enzyme (Fig 1.5), and this is supported by the observation that these aspartate residues appear to be highly conserved during evolution (Wolfe et al., 1999).

In contrast to the situation when the presenilins were first discovered, there are now several known multi-spanning transmembrane proteases including SREBP site-2 protease (cf. section 1.5.2, and; Brown and Goldstein, 1997) and the signal peptide peptidase (SPP) (Weihofen et al., 2002), both present in the ER. Whilst the site-2 protease is a distinct intramembrane protease, SPP is a member of the presenilin family and its conservation of structure and function has been seen as providing compelling evidence that the presenilins are also intramembrane proteases (Weihofen et al., 2002; Wolfe and Selkoe, 2002). In fact, the SPP is one of several potential presenilin homologues, suggesting that the presenilins represent one branch of a larger family of polytopic membrane-associated aspartyl proteases (Ponting et al., 2002).

It has been shown that PS regulates the processing of Notch in a similar way to APP, hence, a  $\gamma$ -secretase inhibitor that was designed on the basis of the primary amino acid sequence of the site of cleavage of  $\gamma$ -secretase in APP was found to prevent Notch-1 processing at concentrations similar to those that inhibited cleavage of APP (De Strooper et al., 1999). Such data are consistent with the hypothesis that the proteolytic activities responsible for the cleavage of Notch and APP are closely related (Selkoe and Kopan, 2003). It was also demonstrated that the transmembrane aspartyl residues in PS are involved in the proteolytic release of the NICD from Notch, and are required for PS activity in a Notch cleavage assay (Ray et al., 1999). However, there do appear to be subtle differences between the protease that cleaves Notch and that which cleaves APP, and some inhibitors have been found that can decrease APP processing, yet have no effect on Notch (Petit et al., 2001). Furthermore, *in vivo* studies have indicated that PS deficient mice are able to produce A $\beta$ , but are unable to generate NICD (Armogida et al., 2001).

Notwithstanding the evidence detailed above, since their first discovery several arguments have been put forward suggesting that the presenilins may not be an active component of the  $\gamma$ -secretase responsible for APP processing. Of these various counter-arguments, two of these are most relevant in the context of this thesis. In contrast to earlier work (cf. table 1.1), studies by Armogida and co-workers (Armogida et al., 2001) have suggested that presenilins are not the

catalytic sub-unit of the  $\gamma$ -secretase since A $\beta$  production can occur in the absence of both PS1 and PS2. These studies used embryonic fibroblasts derived from genotypically characterized PS1<sup>-/-</sup>PS2<sup>-/-</sup> double knockout mice and looked at the production of murine A $\beta$ 40 and A $\beta$ 42 from endogenous APP rather than from exogenous mutant APP (Armogida et al., 2001).

A second issue regarding the role of the presenilins in the  $\gamma$ -secretase has been the so-called “spatial paradox” (for review see; Huse and Doms, 2001). This was based on the observation that the  $\alpha$ - and  $\beta$ - secretases are located “downstream” of the bulk of the presenilins present in the secretory pathway. APP must first be cleaved by  $\alpha$ - or  $\beta$ - secretase before it can become a  $\gamma$ -secretase substrate, implying that  $\gamma$ -secretase activity must be present in a post-ER compartment. However, studies found that the majority of the presenilins are localised within the ER (De Strooper et al., 1997) whilst BACE ( $\beta$ -secretase) and  $\alpha$ -secretase are located in the late Golgi and in endosomal compartments. Given such distributions, it was unclear how APP would come into contact with the presenilins following cleavage by  $\alpha$ - or  $\beta$ -secretase. The spatial paradox argument began to crumble, however, when studies in which  $\gamma$ -secretase substrates were co-localized in the ER together with the bulk of the presenilins demonstrated that no processing occurred (Cupers et al., 2001a; Maltese et al., 2001).

It was concluded that additional factors that are located in compartments downstream of the ER are required for an active  $\gamma$ -secretase complex (Cupers et al., 2001a; Maltese et al., 2001). These observations led to the proposal that the ER pool of presenilins is required to regulate  $\gamma$ -secretase assembly, and possibly to allow the trafficking of other proteins (Herreman et al., 2003). Consistent with this hypothesis, complexes containing presenilins and APP-derivatives have been observed in endosomes and lysosomes (Pasternak et al., 2003a; Siman and Velji, 2003). These compartments are also associated with A $\beta$  production (Haass et al., 1992; Pasternak et al., 2003b; Sisodia and St George-Hyslop, 2002), and it has been demonstrated that lysosomal membranes are enriched in  $\gamma$ -secretase activity (Pasternak et al., 2003a). These studies provide a solution to the “spatial paradox”, suggesting that the active  $\gamma$ -secretase complex is present in a late

compartment of the secretory pathway and not in the ER, despite this being the major site of presenilin localization.

#### 1.10.2 Nicastrin and the $\gamma$ -secretase

That the presenilins existed as part of a protein complex was first suspected on the basis that the expression of PS1 and PS2 appeared to be tightly regulated by the limited abundance of another unknown component that formed a complex with these proteins (Thinakaran et al., 1997). Hence, if human PS1 is overexpressed in cultured murine cells, then the levels of accumulated murine PS1 and PS2 derivatives decreased, and this corresponded to an increase in the accumulation of human PS1 derivatives, despite the persistence of murine PS1 and PS2 mRNAs (Thinakaran et al., 1997). This phenomenon occurred not only in cultured cells, but was also observed to occur *in vivo* (Thinakaran et al., 1997). Such observations are consistent with a model in which PS1 and PS2 are stabilized and endoproteolytically processed by common, but limiting cellular factors, whereas overexpressed presenilin polypeptides are rapidly degraded.

This initial observation was followed by the discovery that the presenilins form detergent-sensitive, high molecular mass, complexes with the immature full-length PS1 found as part of ~180 kDa complex, whereas its mature N- and C-terminal endoproteolytic fragments form part of a ~250 kDa complex (Thinakaran et al., 1998). In order to find other components of such putative complexes, a large amount of solubilised presenilin was recovered from HEK293 cells by immunoprecipitation and proteins that co-purified were identified (Yu et al., 2000). Three proteins were discovered:  $\alpha$ - and  $\beta$ -catenin, which were already known to interact with presenilin, and a transmembrane protein of unknown function named nicastrin (Yu et al., 2000).

The nicastrin gene maps to a region of chromosome 1 that has genetic linkage to a very rare form of inherited Alzheimer's disease (Yu et al., 2000). The gene encodes a protein of 709 amino acids, with an N-terminal signal sequence; a long N-terminal hydrophilic domain containing glycosylation, N-myristoylation and phosphorylation motifs; a ~20-residue transmembrane domain; and a short hydrophilic carboxy terminus (cf. Fig 1.5). Immunoprecipitation studies using both

human brain tissue and HEK293 cells confirmed that the nicastrin-PS1 interaction was authentic and specific, and glycerol velocity gradient centrifugation showed that nicastrin co-fractionates with high molecular weight complexes of both PS1 and PS2 (Yu et al., 2000). Both nicastrin and PS1 show an overlapping sub-cellular distribution, being found primarily in the endoplasmic reticulum and Golgi (Yu et al., 2000). A role for nicastrin as a component of the  $\gamma$ -secretase is further underlined by the observation that it was co-immunoprecipitated with the product of  $\beta$ -secretase cleavage of APP, the C99 fragment (Yu et al., 2000).

A functional role for nicastrin as part of the  $\gamma$ -secretase complex is supported by the observation that deletion of a conserved domain leads to reduced A $\beta$  production (Yu et al., 2000). However, in this study no corresponding increase in the levels of C-terminal APP fragments generated by the  $\alpha$ - and  $\beta$ -secretases, which would be expected in the absence of  $\gamma$ -secretase activity, was observed. A more recent study utilising RNA-interference did result in an accumulation of both APP-C83 and APP-C99 in addition to a decrease in A $\beta$  production upon the loss of nicastrin (Edbauer et al., 2002b). This loss of  $\gamma$ -secretase activity was coupled with a decrease in the expression of PS1 and PS2 and a reduction in the levels of the high molecular weight complexes containing presenilins. Taken together, these data suggest that nicastrin exists as part of a complex with the presenilins, that this complex has  $\gamma$ -secretase activity, and that nicastrin plays a role in modulating the levels of presenilins present in the cell (Edbauer et al., 2002b; Yu et al., 2000).

It has also been demonstrated that nicastrin is required for the  $\gamma$ -secretase cleavage of Notch (Chung and Struhl, 2001; Hu et al., 2002; Lopez-Schier and St Johnston, 2002), supporting the data that was obtained during studies of APP processing. These studies also provide a potential solution to the spatial paradox (cf. section 1.10.1) since both nicastrin and PS1 have been shown to interact with Notch in the secretory pathway, invoking the possibility that a small proportion of the  $\gamma$ -secretase complex may be transported to the plasma membrane where it is active (Gupta-Rossi et al., 2004; Lopez-Schier and St Johnston, 2002).

Current models centre around the idea that nicastrin plays an important role as part of the  $\gamma$ -secretase complex, perhaps by regulating PS expression or stability (Hu et al., 2002; Lopez-Schier and St Johnston, 2002). However, the combination of presenilin and nicastrin alone proved insufficient to reconstitute  $\gamma$ -secretase activity (Kimberly et al., 2002), and this led to a search for other prospective subunits of the complex.

### 1.10.3 *Aph-1 and Pen-2*

Aph-1 was identified as an essential component of the Notch signalling pathway in *Caenorhabditis elegans* (Goutte et al., 2002). Following a genetic screen, two mutations were identified that mapped to a position on chromosome I that had not been previously associated with a component of the Notch signalling pathway (Goutte et al., 2002). When *APH-1* mutant embryos were analysed, they were found to have the anterior pharynx defective (Aph) phenotype, characteristic of mutations in the Notch signalling pathway (Goutte et al., 2002). Additionally, RNA interference of the *APH-1* gene product resulted in similar phenotypes to those observed with other components of the Notch pathway in *C. elegans*, such as presenilin (Goutte et al., 2002). The Aph-1 protein is conserved in higher eukaryotes, has 7 transmembrane domains (Fortna et al., 2004), and appears to function in facilitating the trafficking of nicastrin to the cell surface (Goutte et al., 2002).

Pen-2 was discovered by a different research group using a similar genetic screen of *Caenorhabditis elegans* to that used to identify Aph-1 (Francis et al., 2002). In order to favour the identification of components that act at the presenilin-dependent step in Notch signalling, *Caenorhabditis elegans* strains that were compromised for presenilin function were used. Several mutations were identified that caused presenilin-like Aph phenotypes, and three alleles mapped to a previously undescribed gene, *PEN-2* (Francis et al., 2002). *APH-1* was also identified in the same study (Francis et al., 2002), confirming the results of Goutte and co-workers (Goutte et al., 2002). *PEN-2* encodes a protein of 101 amino acids having two transmembrane-spanning segments with its N- and C-termini facing the extra-cytoplasmic face of the membrane (Crystal et al., 2003). Like

Aph-1, several orthologues of Pen-2 have been identified in humans, mice, zebrafish, *Drosophila* and *Arabidopsis* (Francis et al., 2002). Furthermore, the PEN-2 locus had previously been associated with late-onset Alzheimer's disease (Kehoe et al., 1999).

Studies in *Drosophila* S2 cells demonstrated that Aph-1 increases the stability of the so-called PS holoprotein present in the  $\gamma$ -secretase complex, and that Aph-1 is the least sensitive of the known  $\gamma$ -secretase subunits to changes in expression of other subunits (Takasugi et al., 2003). In addition, it was found that the depletion of Pen-2 by RNA interference prevented the formation of PS fragments and promoted stabilization of the holoprotein in both *Drosophila* and mammalian cells (Takasugi et al., 2003). Co-expression of *Drosophila* Pen-2 with Aph-1 and nicastrin was found to increase both the generation of presenilin fragments and  $\gamma$ -secretase activity (Takasugi et al., 2003). Thus, it was concluded that Aph-1 stabilizes the presenilin holoprotein in the  $\gamma$ -secretase complex, whilst Pen-2 is required for the endoproteolytic processing of PS and subsequent  $\gamma$ -secretase activity (Takasugi et al., 2003). However, further studies will be required to determine whether Pen-2 is actually the so-called presenilinase (cf. Fig 1.5) and if so, how it functions.

#### 1.10.4 The $\gamma$ -secretase complex and its site of action

That PS, nicastrin, Aph-1 and Pen-2 are all required for the  $\gamma$ -secretase processing of Notch and APP has been demonstrated by several different groups using RNA interference to downregulate each of the individual proteins in cultured cells (De Strooper et al., 1998; Edbauer et al., 2002b; Francis et al., 2002; Takasugi et al., 2003). Similarly, whilst the over-expression of any combination of one, two or three of these proteins does not increase  $\gamma$ -secretase activity, the over-expression of all four proteins in combination leads to a significant increase in  $\gamma$ -secretase processing (Edbauer et al., 2003; Kimberly et al., 2003; Takasugi et al., 2003).

Studies in which the four proteins were co-expressed in *Saccharomyces cerevisiae*, which contains no known homologues of any of the proposed  $\gamma$ -secretase subunits, nor detectable  $\gamma$ -secretase activity, showed that these four

proteins were sufficient to reconstitute  $\gamma$ -secretase processing in this heterologous system (Edbauer et al., 2003).  $\gamma$ -secretase activity was only observed when all four proteins were co-expressed, and was absent if an inactive mutant of PS was used in place of wild-type PS (Edbauer et al., 2003). Previous studies have suggested that  $\gamma$ -secretase activity is associated with the production of PS N- and C-terminal fragments generated by endoproteolysis (cf. section 1.10.1). Interestingly, when the four proteins were co-expressed in yeast, a significant proportion of the PS holoprotein was converted into fragments, a phenomenon that was not observed when the mutant PS was used (Edbauer et al., 2003). This is consistent with one or more of these four components acting as the presenilinase. PS, nicastrin, Pen-2 and Aph-1 were found to associate as a high molecular weight complex when expressed in yeast, and when this complex was immunoprecipitated it was found to have  $\gamma$ -secretase activity in an *in vitro* cleavage assay (Edbauer et al., 2003).

Significantly, Aph-1 has been found to have two mammalian homologues, Aph-1a and Aph-1b (Gu et al., 2003). Furthermore, Aph-1a can be alternatively spliced at its C-terminus to generate Aph-1a<sup>L</sup> and Aph-1a<sup>S</sup> (Gu et al., 2003). The presence of several distinct forms of Aph-1 in addition to the two PS isoforms (cf. section 1.10.1), means that several different  $\gamma$ -secretase complexes may exist, and these could theoretically be responsible for cleaving different substrates. There are indications that such complexity exists, and gene inactivation studies of PS1 and PS2 indicated that these proteins have overlapping, but different, functions (Herreman et al., 1999). Establishing whether alternative combinations of PS and Aph-1 isoforms are involved in regulating  $\gamma$ -secretase function could have important implications for the design of drugs to combat AD (De Strooper, 2003).

Whilst it appears that all of the components of the  $\gamma$ -secretase complex have now been identified, the roles of the individual subunits remain uncertain. Presenilin is widely assumed to contain the catalytic site, and there are several lines of evidence to suggest that this is the case (cf. section 1.10.1). However, how presenilin interacts with the other components of the enzyme is at present unclear.

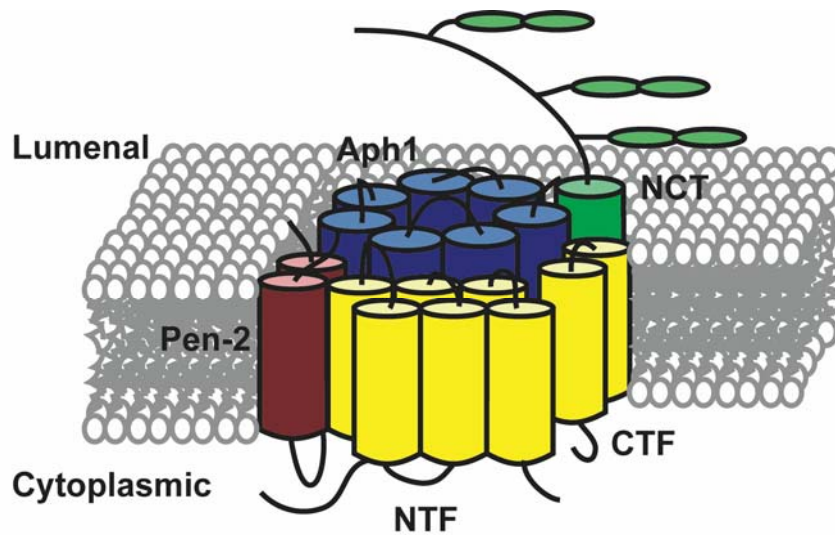


Fig 1.5. **Schematic representation of the subunit organisation of the  $\gamma$ -secretase complex.**

This model is based on the protein-protein interactions identified in the complexes generated by detergent-mediated dissociation of  $\gamma$ -secretase.

### **1.11 The assembly of the $\gamma$ -secretase subunits**

$\gamma$ -secretase activity requires the formation of a stable, high molecular weight complex containing endoproteolytic fragments of PS, nicastrin, Aph-1 and Pen-2. It has been demonstrated that Aph-1 forms a sub-complex with immature nicastrin as an intermediate in the pathway for the assembly of the complete  $\gamma$ -secretase enzyme (Hu and Fortini, 2003; LaVoie et al., 2003). PS and Pen-2 are thought to become incorporated into the complex later, since both proteins will only bind to “mature” nicastrin (LaVoie et al., 2003). Following the formation of the Aph1-nicastrin intermediate, a second sub-complex is formed that contains the PS holoprotein in addition to Aph-1 and nicastrin (LaVoie et al., 2003; Takasugi et al., 2003). Studies using the detergent dodecyl  $\beta$ -D-maltoside has allowed the  $\gamma$ -secretase to be inactivated and dissociated into smaller complexes (Fraering et al., 2004). Based on the complexes generated by this methodology, it was proposed that Pen-2 interacts with the N-terminal fragment of presenilin present within the active  $\gamma$ -secretase complex. It was also concluded that Aph-1 and nicastrin interact, and that they bind to the C-terminal fragment of presenilin (Fraering et al., 2004). Taken together, these data can be used to generate a

proposed model for  $\gamma$ -secretase assembly (see Fig 1.5, adapted from; Fraering et al., 2004).

### **1.12 The subcellular location of cleavage**

Like the role of the presenilins in APP processing, the cellular location of the active form of the  $\gamma$ -secretase has been a controversial and long-running area of debate (Huse and Doms, 2001). Subcellular fractionation of membrane vesicles and co-immunoprecipitation indicated that the  $\gamma$ -secretase subunits physically interact with one another within the Golgi/trans Golgi network compartments (Baulac et al., 2003). In addition to this, Aph-1, Pen-2 and presenilin were all found to interact with the  $\gamma$ -secretase substrates APP-C83/C89/C99 (Baulac et al., 2003). These data suggested that either Aph-1 and Pen-2 play a continuous role in the proteolysis step, or that they are involved in stabilizing presenilin. The absence of an observed interaction between nicastrin and any of the  $\gamma$ -secretase substrates in this study may be because it is not involved in the actual cleavage event, or it may be due to antibody interference (Baulac et al., 2003). The incubation of substrates with the Golgi-derived membrane vesicles allowed the generation of A $\beta$  and the AICD, suggesting that the  $\gamma$ -secretase is fully functional within these compartments (Baulac et al., 2003). Studies of Notch processing have suggested that  $\gamma$ -secretase cleavage of Notch requires both ubiquitination and endocytosis (Gupta-Rossi et al., 2004). However, analysis of APP processing has indicated that  $\gamma$ -secretase cleavage occurs post-Golgi, but pre-plasma membrane, suggesting that endocytosis is not a requirement for processing, and that the two pathways differ with regards to the location of  $\gamma$ -secretase cleavage (Khvotchev and Sudhof, 2004).

### **1.13 The C-terminal fragment of APP**

In the Notch signalling pathway, ligands bind to the Notch receptor and induce two sequential cleavage events, the second via the  $\gamma$ -secretase (De Strooper et al., 1999; Gupta-Rossi et al., 2004).  $\gamma$ -Secretase cleavage releases the Notch intracellular domain (NICD), which is then translocated to the nucleus where it is involved in transcriptional regulation (cf. Fig 1.3). APP is subject to similar cleavage events, and it is believed that the intracellular domain of APP (AICD) that

is generated as a result of the  $\gamma$ -secretase cleavage of the APP-C83, APP-C89 or APP-C99 fragments, is also involved in signalling (Cao and Sudhof, 2001; Kimberly et al., 2001) (cf. Fig 1.4). Recently it has been shown that the APP-like proteins APLP-1 and APLP-2 (see section 1.8) also generate small intracellular domains (ICDs) following cleavage by the  $\gamma$ -secretase, suggesting that these proteins may also have some role during signalling (Walsh et al., 2003). Furthermore, the structure of APP resembles that of receptors such as Notch, although only a small proportion of total cellular APP resides at the plasma membrane (Minopoli et al., 2001).

#### **1.14 Epsilon cleavage of APP**

The endogenous C-terminal fragment (CTF) of APP generated by  $\gamma$ -secretase processing is difficult to detect *in vivo* (Weidemann et al., 2002) and it was generally assumed that  $\gamma$ -secretase cleavage involves a single proteolytic event that generated the A $\beta$  fragment and a concomitant C-terminal fragment. The resulting C-terminal fragment should be 57-59 amino acids in length, depending on whether A $\beta$ 40 or 42 was generated by the  $\gamma$ -secretase. Similarly, the product of an  $\alpha$ -secretase followed by a  $\gamma$ -secretase cleavage would generate N-terminal p3 peptides (see Fig 1.4) and the same C-terminal fragments. However, when such C-terminal APP-fragments have been looked for *in vivo*, there has been no evidence that such peptides are generated (Weidemann et al., 2002). Fragments of APP have been observed that are of an approximate size to be the  $\gamma$ -secretase derived CTF (CTF- $\gamma$ ), but no N-terminal sequencing data was obtained to prove that this was indeed the case. In one study, APP CTFs were generated using a chimeric construct that allowed the C-terminal fragments to be stabilised through the addition of a tag encoding two z-domains from protein A (Weidemann et al., 2002). The <sup>35</sup>S-methionine labelled C-terminal fragment generated after  $\gamma$ -secretase cleavage was radio-sequenced, and rather than having the 57-59 amino acids that would be predicted from the generation of N-terminal A $\beta$  peptides, the predominant C-terminal product was found to be smaller, and apparently generated by proteolysis distal to the known  $\gamma$ -secretase cleavage site between Leu-49 and Val-50 at a point was termed the  $\epsilon$ -cleavage site (Weidemann et al., 2002).

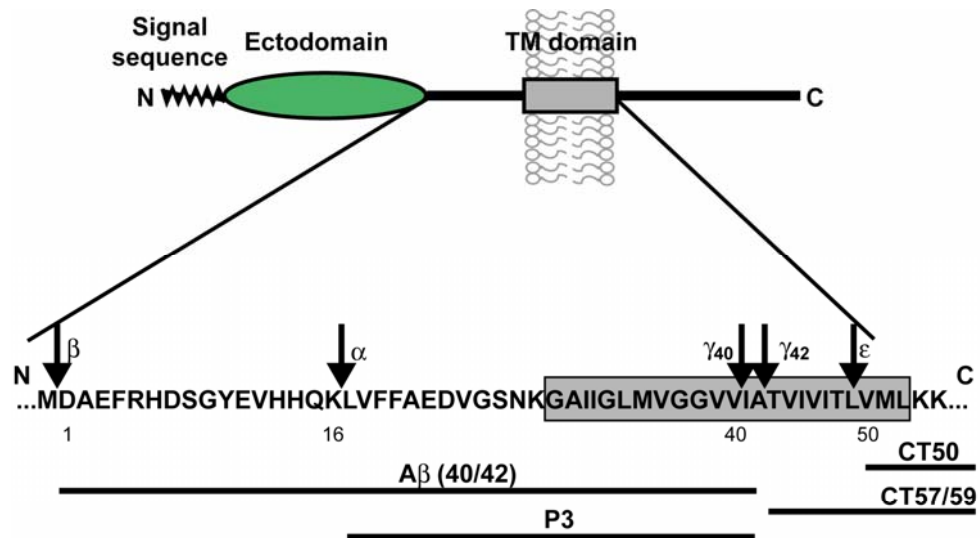


**Fig 1.6. APP cleavage sites.**

Schematic representation of APP. The transmembrane domain is indicated by a grey rectangle. The  $\alpha$ ,  $\beta$ ,  $\gamma$  and  $\epsilon$  sites are indicated by black arrows.

Like the S3-cleavage of Notch, the  $\epsilon$ -cleavage of APP occurs close to the cytoplasmic face of the membrane, whereas the  $\gamma$ -cleavage site is located more centrally within the transmembrane domain.  $\epsilon$ -Cleavage is also reminiscent of the cleavage of SREBP (cf. Fig 1.2), although in this case the two proteins have different membrane topologies. Similar results have been obtained by other groups, all of whom have been able to identify an  $\epsilon$ -CTF, but not the expected  $\gamma$ -CTF fragment (Gu et al., 2001; Sastre et al., 2001; Yu et al., 2001). Both  $\gamma$ - and  $\epsilon$ -cleavages are dependent on presenilins, occur late in the secretory pathway and can be inhibited by  $\gamma$ -secretase inhibitors, suggesting that they are both dependent on the same enzyme (Bergman et al., 2003; Sastre et al., 2001). It has been proposed that the two cleavage events are distinct, but the order of these events is uncertain. A longer  $\gamma$ -CTF has not been identified; this could be because APP is first processed at the  $\epsilon$ -cleavage site to generate  $\epsilon$ -CTF and longer A $\beta$  products that are then processed to A $\beta$ 40 and A $\beta$ 42. Some previous work has suggested that longer N-terminal fragments exist, but these peptides have not been found in all studies (Sato et al., 2003). It could also be the case that the two  $\gamma$ -secretase cleavages occur simultaneously to generate an additional small peptide that would

be difficult to detect (cf. Fig 1.6). Only by inhibiting the two separate cleavage events will this issue be resolved.

Despite these subtle differences the processing pathways of Notch and APP are very similar as they share dependence on presenilins and have a similar inhibition profile and membrane topology at the site of cleavage. These parallels have led to the hypothesis that APP, like Notch, is a cell surface receptor and that it may signal through the release and nuclear translocation of its C-terminal fragment, the APP intracellular domain (AICD) (Kimberly et al., 2001). In contrast to Notch, the C-terminal fragment generated by  $\gamma$ -secretase cleavage of APP is small and lacks either a nuclear localisation signal or any motifs commonly found in regulators of transcription. If the AICD is analogous to the NICD, then it would most likely associate with cellular factors prior to entering the nucleus. Several studies have suggested that the “adaptor” protein Fe65 might have a comparable role to the CSL proteins that bind the NICD, allowing the AICD fragment to be stabilised and transported to the nucleus (Cao and Sudhof, 2001; Walsh et al., 2003).

### **1.15 Fe65**

APP has a –GYENPTY- motif at the extreme C-terminus of the AICD, and since similar sequences are found in the transferrin and LDL receptors, it was hypothesised that this motif may play a role in the cellular trafficking of APP (Lai et al., 1995). However, the -GYENPTY- sequence is also implicated in protein binding, and a number of proteins have been identified that bind to the C-terminus of APP. The majority of these binding partners have several protein-protein interaction domains implying that they serve as “adaptor” proteins, linking APP to other cellular components (Minopoli et al., 2001). Three of these “adaptor” proteins are related, Fe65 and the Fe65-like proteins 1 and 2. Fe65 contains three known protein-protein interaction domains, a WW domain and two PTB domains, and it is capable of binding to the transcription factor CP2/LSF/LBP1 (Zambrano et al., 1998). It is thought that Fe65 might couple the C-terminus of APP to transcription factors through its multiple binding sites, and it is via one of its PTB domains that Fe65 binds to APP (Minopoli et al., 2001). APP can interact with other proteins via its second PTB domain and its WW motif (Ermekova et al., 1997). There is evidence to suggest that these other interacting partners are

suppressors and transcription factors. It is known that Fe65 can translocate to the nucleus (Minopoli et al., 2001) and experiments using GFP tagged versions of Fe65 indicated that the WW domain is responsible for its nuclear localisation (Minopoli et al., 2001).

However, whilst there is evidence that Fe65 can both bind APP and translocate to the nucleus, it is unclear whether Fe65 binding also enables the AICD fragment of APP to enter the nucleus. Several hypotheses have been advanced to explain the role of the interaction between APP and Fe65. Experiments by Minopoli and co-workers (Minopoli et al., 2001) suggest that APP binding to Fe65 prevents its nuclear import and acts as an extra-nuclear anchor for Fe65. These data would suggest that APP acts to prevent nuclear signalling rather than to promote it. In contrast, however, studies by Kimberly and colleagues in which a C-terminal fragment of APP was over-expressed have suggested that Fe65 enables the C-terminal portion of APP to enter the nucleus (Kimberly et al., 2001). Using both nuclear fractionation and immunofluorescence techniques, it was established that the majority of the AICD fragment was indeed localised in the nucleus, with the immunofluorescence signals for Fe65 and AICD merging to a large extent (Kimberly et al., 2001). However, it was also observed that the localisation of Fe65 was not dependent on the presence of the AICD as it was located in the nucleus whether cells were co-transfected with the AICD or not. Additionally, endogenous C-terminal fragments of APP could not be detected when cells were transfected with Fe65, therefore if Fe65 is indeed stabilising the AICD fragment, then the levels of the fragment present must be very low, and hence undetectable in the system used (Kimberly et al., 2001). In this regard, the AICD is similar to the Notch NICD fragment, and it is known that the NICD is difficult to detect unless stabilised by the CSL protein.

The hypothesis that C-terminal fragments of APP are transported to the nucleus where they have a role in transcriptional regulation is supported by experiments indicating that a C-terminal fragment of APP, CT59, is capable of down-regulating levels of a nuclear protein (Gao and Pimplikar, 2001). These studies also suggested that the different  $\gamma$ -secretase cleavage products generated by alternative cleavages may have different functions as CT59 had a greater effect on

the down-regulation of a nuclear protein than other lengths of AICD that were tested (Gao and Pimplikar, 2001).

Nuclear localisation of the AICD was also implied by a study by Cao and Sudhof that has suggested that the C-terminal fragment of APP may, as part of a complex with Fe65, be involved in transcriptional regulation (Cao and Sudhof, 2001). Experiments were performed in which fusion proteins of APP or AICD were generated with the DNA binding domains of Gal4 and LexA (Cao and Sudhof, 2001). It was discovered that whilst these constructs were unable to stimulate transcription alone, when co-transfected with Fe65 there was a >2000 fold increase in transcription from an exogenous reporter (Cao and Sudhof, 2001). This study also showed that AICD and Fe65 form a transcriptionally active complex with the histone acetyltransferase, Tip60, which is involved in the regulation of transcription (Cao and Sudhof, 2001). However, a more recent study suggests that Fe65 is not required for the formation of this complex and that Tip60 interacts with the AICD independently of Fe65 (Kinoshita et al., 2002). Furthermore, an additional investigation into the requirements for “transactivation” has suggested that whilst both  $\gamma$ -secretase processing of APP and nuclear localisation of Fe65 are necessary, the translocation of the AICD to the nucleus may in fact be superfluous (Cao and Sudhof, 2004). This resulted in the suggestion that Fe65 is normally in a closed conformation caused by an interaction between its WW and PTB domains (Cao and Sudhof, 2004) with the C-terminal tail of APP disrupting this interaction when it binds to Fe65, thereby allowing the WW domain to function as a transcriptional activator. Interestingly, this disruption appears to require the proximity of membranes since only when the AICD is placed in the context of a membrane is it capable of activating Fe65 (Cao and Sudhof, 2004). It may be that an additional, membrane-associated factor is required for transactivation in addition to AICD-binding.

Other studies of the stabilizing effect of Fe65 on the AICD fragments have suggested that, in addition to stabilising APP, it, and other Fe65 family members, can also stabilize the intracellular domain (ICD) fragments of APP-like proteins 1 and 2 (APLP-1 and APLP-2) (Walsh et al., 2003). The observation that three different Fe65 family members, Fe65 and the Fe65-like proteins 1 and 2, are able to bind to the ICDs liberated from APP, APLP-1 and APLP-2 suggests that Fe65

proteins may play a general role in regulating signalling pathways via proteolytically released intracellular domains.

In contrast to their predicted role in signal transduction, APP and Fe65 have also been shown to localise to focal complexes, suggesting that they may regulate cell motility (Sabo et al., 2001). Fe65 can simultaneously bind to APP, via a PTB domain, and to Mena, via its WW domain. Mena is required for normal neural development and regulates motility by binding to actin, and it therefore links Fe65 and APP to cytoskeletal dynamics and cellular motility and morphology (Ermeikova et al., 1997). More recently, Fe65 has been found to colocalize with APP in neuronal growth cones, nerve terminals and dendritic filopodia (Sabo et al., 2003). Using immunofluorescence, Fe65 and APP were observed to colocalize in growth cones, and the presence of both proteins was confirmed by immunoblotting of growth cones isolated from rat brains. Further investigation suggested that both proteins were concentrated in the so-called "P domain", which is the most motile structure within the growth cone, and that Mena was also in this region (Sabo et al., 2003).

If the AICD is indeed involved in nuclear signalling as some studies have suggested, then in addition to being stabilized and transported to the nucleus to promote signalling, it would also need to be removed to allow the down-regulation of such signalling pathways.

### **1.16 Insulin degrading enzyme (IDE)**

Insulin degrading enzyme (IDE) is an ~110kDa thiol zinc-metalloproteinase located in the cytosol, peroxisomes, endosomes and on the cell surface that cleaves small proteins of diverse sequence (Farris et al., 2003). Several studies have suggested that IDE plays a role in regulating levels of A $\beta$ , and recently it has been suggested that IDE is also involved in degrading the AICD (Edbauer et al., 2002a; Farris et al., 2003). If the AICD has a role in signal transduction, its activity may be controlled to allow down-regulation and prevent constitutive signalling. In the case of the Notch signalling pathway, the NICD, which is generated by  $\gamma$ -secretase processing, is degraded via an ubiquitin-dependent proteasomal mechanism. However, the AICD appears to be removed by a mechanism distinct

from the proteasome. Studies using cell cytosol fractions suggested that the AICD is degraded by a metalloproteinase, as the inclusion of EDTA or PNT, both of which chelate divalent metal ions, allowed accumulation of the AICD (Edbauer et al., 2002a). AICD degradation was also inhibited by the SH-alkylating agent NEM, suggesting that the enzyme responsible for the removal of the AICD was thiol-dependent (Edbauer et al., 2002a). These studies implicated IDE as the protease responsible. This was confirmed by experiments in which wild type and mutant IDE were over-expressed: cytosol fractions from cells expressing the wild-type protein had significantly more AICD-degrading activity than fractions from the cells expressing the mutant (Edbauer et al., 2002a). Furthermore, immunodepletion of the cytosol with an anti-IDE antibody caused a marked reduction in AICD degradation. These studies have been supported by work *in vivo* using IDE<sup>-/-</sup> mice (Farris et al., 2003). Levels of non-phosphorylated AICD were consistently increased in IDE<sup>-/-</sup> mice compared with IDE<sup>+/+</sup> mice, whilst levels of phosphorylated AICD remained unaffected. This suggested that IDE selectively regulates levels of unphosphorylated AICD *in vivo* (Farris et al., 2003).

Recently, it has been shown that the intracellular domain (ICD) fragments generated by  $\gamma$ -secretase cleavage of the APP-like proteins APLP-1 and APLP-2 are also highly labile (Walsh et al., 2003). Levels of these ICDs were found to be minimal in the absence of PNT and insulin, however, when these reagents were included much higher yields were obtained. These data suggest that IDE, or a very similar protease, is responsible for degrading APLP-1 and APLP-2 ICDs.

### **1.17 Aims of the project**

The principal aims of this project were: (1) to investigate the possibility of reconstituting the  $\gamma$ -secretase-dependent cleavage of APP in a cell-free system; (2) to follow the production and fate of the C-terminal fragment of APP resulting from the  $\gamma$ -secretase cleavage.

# **CHAPTER 2**



## **Materials and Methods**

## 2 Materials and methods

### 2.1 Materials

Epicurian Coli<sup>®</sup> supercompetent cells, the PCR-Script<sup>™</sup> Amp cloning kit, QuikChange<sup>™</sup> Site Directed Mutagenesis Kit and cloned *Pfu* DNA polymerase were purchased from Stratagene Ltd (Cambridge). The ABI Prism BigDye Terminator Cycle Sequencing Ready Reaction Kit for DNA sequencing was supplied by PE Applied Biosystems (Warrington). Restriction endonucleases and Endo-H were purchased from New England Biolabs (Hitchin). T7 RNA polymerase, transcription buffers, rNTPs, RNasin ribonuclease inhibitor, amino acids, wheat germ extract and the rabbit reticulocyte lysate were supplied by Promega (Southampton). Aurintricarboxylic acid (ATCA), cycloheximide, phenyl-methylsulphonyl fluoride (PMSF), 3-[(3-cholamidopropyl)dimethylammonio]-2-hydroxy-1-propanesulfonate (CHAPSO), protease inhibitor cocktail for mammalian cells (P8340), N-methylsuccinyl-ala-ala-pro-val-chloromethyl ketone and Triton X-100 were purchased from Sigma (Poole, Dorset). Polyethylene glycol (PEG) 400 was obtained from V.W.R. Scientific Products (West Chester, PA, USA). Easytag L-[<sup>35</sup>S]methionine was purchased from NEN Du Pont (Stevenage). All reagents for cell culture were obtained from Cambrex (Verviers, Belgium). Digitonin, porcine insulin, Brefeldin-A and  $\gamma$ -secretase inhibitors were supplied by Calbiochem (Nottingham). Lipofectamine-2000 was obtained from Invitrogen (Paisley). Human brain nuclear extract was purchased from Active Motif (Rixensart, Belgium). Fe65 was gifted by Dr. Frank Lee (University of Pennsylvania, USA). IDE (pProExH6-HA-wtIDE, pLIC-hIDE and hIDE E111Q pProExH6-HA-hIDE E111Q) was gifted by Dr. Wen Kuo (University of Chicago, USA) (Chesneau and Rosner, 2000). The Notch constructs used in the *in vivo* transfection experiments were gifted by Jon Barks (University of Manchester). Canine pancreatic microsomes were prepared essentially as described by Walter and Blobel (1983). All other chemicals were purchased from BDH/Merck (Poole, Dorset) and Sigma (Poole, Dorset).

**Table 2.1: Antisera**

Antisera	Epitope/peptide	Type	Company
$\alpha$ Flag	DYKDDDDKC (coupling cys)	Rabbit	ABR Affinity Bioreagents (Cambridge Bioscience, Cambridge)
Pan $\beta$ -amyloid	aa 15-30 of $\beta$ -amyloid peptide (1-40)	Rabbit polyclonal IgG	Calbiochem (Nottingham)
WO-2	N-terminal A $\beta$ peptide (2-16aa)	Mouse monoclonal	Gifted by Dr. Dirk Beher (Merck, Sharpe and Dohme, Essex)
$\alpha$ APP <sub>680-695</sub>	C-terminal 15 aa of APP	Rabbit	High Lab
$\alpha$ Opsin	N-terminal 2-32 residues of opsin	Mouse monoclonal	Gifted by Paul Hargrave (University of Florida, USA)
$\alpha$ TCP-1	aa 50-63 (coupled to sulpho SMCC KLH)	Rabbit polyclonal	High Lab
$\alpha$ ubiquitin	Ubiquitin purified from bovine RBCs conjugated to KLH	Rabbit polyclonal	Bioquote Ltd (York)
$\alpha$ PPLss	Preprolactin signal sequence	Rabbit polyclonal	Gifted by Dr. Bruno Martoglio (ETH, Zurich)
$\alpha$ rHA (H6908)	HA tag	Rabbit	Sigma
$\alpha$ HA	HA tag	Mouse	Sigma
$\alpha$ presenilin	N-terminal residues 1-70 of human PS1	Rabbit polyclonal IgG	Santa Cruz Biotechnology (Santa Cruz, CA, USA)
$\alpha$ IDE	hIDE	Rabbit polyclonal	Gifted by Dr. Ken Wuo (University of Chicago)
$\alpha$ CRT	Biotin-tagged recombinant hCRT	Sheep	High Lab
$\alpha$ GM130			Gifted by Dr. Martin Lowe (University of Manchester)

## 2.2 Generation of constructs

A plasmid encoding APP-CT99 with the preprolactin signal sequence at its N-terminus (ss-CT99) was kindly provided by Dr. Cornelia Wilson (University of Manchester). The ss-CT99 coding sequence was sub-cloned into pcDNA3.1(+); the ss-CT99 sequence including the flanking HindIII and EcoRV flanking sites was produced via PCR (for reaction conditions, see table 2.1) using using the “pSputK HindIII for” and “pSputK ECoRV rev” primers (see Appendix 1.1).

**Table 2.2: PCR reaction**

50pmol	5' and 3' primer each
5 $\mu$ l	10x PWO buffer
25ng	plasmid DNA template
0.2mM	deoxyribonucleotide triphosphates (A, T, G and C)
10U	PWO polymerase
To a final vol of 50 $\mu$ l	H <sub>2</sub> O

The PCR reaction was carried out using the following protocol:

95°C	1 min	} 30x
95°C	45 sec	
55°C	45 sec	
72°C	30 sec	
72°C	10 min	

The pcDNA3.1(+) vector and the *HindIII*-ss-CT99-*EcoRV* PCR products were digested with *HindIII* and *EcoRV* restriction endonucleases at 37°C for 2 hours. The digested products were purified using a QIAGEN PCR purification kit and eluted in 30 $\mu$ l dH<sub>2</sub>O. DNA concentrations were estimated from an agarose gel, and these concentrations were used to estimate ratios of PCR product and insert for use in ligation reactions. The ss-CT99 PCR product was ligated into the pcDNA3.1(+) vector and the sequence was verified by DNA sequencing using the ABI Prism BigDye Terminator Cycle Sequencing Ready Reaction Kit for DNA sequencing (see table 2.3 and Appendix 2.1).

CT72 was produced from ss-CT99 via PCR using the “CT72 for” and “C99 rev” primers (see table 2.3, Appendix 1.1 and Appendix 2.2). The PCR products were digested for 2 hours at 37°C with 20 units of *DpnI* to remove parental DNA, and purified using the QIAGEN PCR purification kit according to the manufacturer’s instructions before analysis on a 1% agarose gel. The purified PCR products were ligated directly into the PCR-Script Amp SK(+) vector as described in the manufacturer’s instructions. The resulting product was then transformed into competent cells as described in section 2.3.

### 2.2.1 Generation of methionine mutants

The methionine mutants of CT72, CT72-1 and CT72-2, were generated using the QuikChange Site-Directed Mutagenesis Kit according to the manufacturer's protocol. After amplification, samples were digested with *DpnI* to remove any methylated parental DNA template, leaving PCR amplified plasmid containing the desired mutation.

Complementary CT72 M8I primers were designed to mutate the methionine residue at codon 8 to an isoleucine (see table 2.3 and Appendix 1.1), resulting in CT72-1 (see Appendix 2.2). This product was purified using a QIAgen PCR Purification Kit and used as a template for a second round of mutagenesis using the CT72 M24I primers (see table 2.3 and Appendix 1.1) to generate double mutants with isoleucine substitutions at positions 8 and 24, denoted CT72-2 (see Appendix 2.2). Several short C-terminal fragments of APP: CT49, <sup>Met</sup>CT56, <sup>Met</sup>CT57, <sup>Met</sup>CT58, <sup>Met</sup>CT59, <sup>Met</sup>CT60, and CT65 were also generated using the QuikChange Site-Directed Mutagenesis Kit. In this case, complementary primers were used to remove the CT72 start codon (see table 2.3 and Appendix 1.1) following the manufacturer's recommendations. Naturally occurring in-frame methionine codons were used to generate CT49 (CT72-1 mutant with the initiator methionine removed) and CT65 (CT72-2 with the initiator methionine removed) (see Appendix 2.2), or alternative start codons were introduced at codon 57 (<sup>Met</sup>CT56), 58 (<sup>Met</sup>CT57), 59 (<sup>Met</sup>CT58), 60 (<sup>Met</sup>CT59) or 61 (<sup>Met</sup>CT60) (see table 2.3, Appendix 1.1, Appendix 2.3 and Appendix 2.4).

In the case of CT72-Gly, complementary primers were used to mutate a proline residue at position 62 of CT72 to a glutamine to generate a *N*-glycosylation consensus sequence (see table 2.3, Appendix 1.1 and Appendix 2.2). In each case, the purified PCR products were transformed into competent cells after *DpnI* treatment as described in section 2.3.

### 2.2.2 Generation of tagged APP-derivatives

N-terminally HA-tagged, Flag-tagged and Opsin-tagged APP-derivatives and a C-terminally HA-tagged construct were all generated using the QuikChange™ Site-Directed Mutagenesis Kit according to the manufacturer's protocol, as indicated in the previous section. Complementary primers were designed to mutate ss-CT99 in pcDNA3.1(+) to contain an HA epitope tag (+ glycosylation site) at the N-terminus, just distal to the preprolactin signal sequence, or at the C-terminus (-glycosylation site), just prior to the stop codon (see table 2.3, Appendix 1.1, Appendix 2.5 and Appendix 2.7). In addition, the resulting ss-<sup>HA-Gly</sup>CT99 derivative was itself mutated to generate flag and opsin-tagged derivatives (see table 2.3, Appendix 1.1, and Appendix 2.9). For the flag tagged constructs a one-step mutagenesis was performed, but the larger size of the opsin tag required a two-step approach. Internal reference standards to aid the identification of products resulting from the  $\gamma$ -secretase cleavage of N-terminally-tagged constructs were generated by introducing a stop codon at the site of  $\gamma$ -secretase processing (see table 2.3, Appendix 1.1 and Appendix 2.6). Complementary primers were used to mutate the initiator methionine of ss-<sup>HA-Gly</sup>CT99 to isoleucine to generate <sup>Met</sup>CT99 (see table 2.3, Appendix 1.1 and Appendix 2.7). The mutated plasmids were transformed into competent cells as described below.

### 2.2.3 Transformation

PCR-generated products were transformed into Epicurian Coli® XL1-Blue supercompetent cells. Bacterial cells were thawed on ice, 50 $\mu$ l cells per transformation were transferred to pre-chilled Falcon 2059 tubes, and 2 $\mu$ l  $\beta$ -mercaptoethanol was added to each tube. After incubating for 10 minutes on ice, the desired DNA was added and gently mixed. The transformation mixture was left on ice for 30 minutes before heat-shocking the cells for 45 seconds at 42°C, followed by a 2-minute incubation on ice. The cells were then spread onto Luria Broth (LB, 1% w/v tryptone, 0.5% w/v yeast extract, 1% w/v NaCl) bactoagar plates (1.5% w/v agar) containing 100 $\mu$ g/ml ampicillin and grown overnight at 37°C. Single colonies were picked and grown in 3ml LB containing 100 $\mu$ g/ml

ampicillin overnight and the plasmid DNA was purified using the QIAgen Miniprep Kit, according to the manufacturer's instructions.

**Table 2.3: Summary of APP-derivatives used in this study**

APP-derivative	Signal	Mutation and primer set(s)	Amino acids*	Epitope tag
CT72	"SA"		72	-
CT72-1	"SA"	CT72 M8I	72	-
CT72-2	"SA"	CT72 M8I M24I	72	-
CT72-Gly	"SA"	CT72 P62Q	72	
<sup>Met</sup> CT56	"SA"	CT72 M1I T16M	57	-
<sup>Met</sup> CT57	"SA"	CT72 M1I A15M	58	-
<sup>Met</sup> CT58	"SA"	CT72 M1I I14M	59	-
<sup>Met</sup> CT59	"SA"	CT72 M1I V13M	60	-
<sup>Met</sup> CT60	"SA"	CT72 M1I V12M	61	-
<sup>Met</sup> CT99	"SA"	ss- <sup>HA-Gly</sup> CT99 M1I	100	-
CT49	"SA"	CT72 M1I M8I	49	-
CT65	"SA"	CT72 M1I	65	-
ss- <sup>HA-Gly</sup> CT99	PPL	ss-CT99 + HA-Gly	144 (114)	HA
ss- <sup>HA-Gly</sup> CT42	PPL	ss- <sup>HA-Gly</sup> CT99 T88STOP	87 (57)	HA
ss- <sup>opsin-HA-Gly</sup> CT99	PPL	ss- <sup>HA-Gly</sup> CT99 + opsin	160 (130)	HA, Opsin
ss- <sup>opsin-HA-Gly</sup> CT42	PPL	ss- <sup>opsin-HA-Gly</sup> CT99 T104STOP	160 (130)	HA, Opsin
ss- <sup>flag-HA-Gly</sup> CT99	PPL	ss- <sup>HA-Gly</sup> CT99 + flag	152 (122)	HA, Flag
ss- <sup>flag-HA-Gly</sup> CT99	PPL	ss- <sup>flag-HA-Gly</sup> CT99 T96STOP	152 (122)	HA, Flag
ss-CT99 <sup>HA</sup>	PPL	ss-CT99 + HA	141 (111)	HA

\* number in brackets indicates the amino acid length following signal sequence cleavage

## 2.3 Template production

### 2.3.1 Generation of DNA templates for transcription

DNA templates for *in vitro* transcription of mRNA were generated by PCR. Upstream primers annealing ~150 bases upstream of the promoter region (-150 T7 PCRscript or -150 T7 pcDNA3.1(+)) and a reverse primer (C99 rev for most constructs, C99 CT-HA rev for the C-terminally HA-tagged construct, and C99  $\gamma$ -sec NT rev for the N-terminally tagged markers of  $\gamma$ -secretase processing) were used to generate DNA templates for transcription (see Appendix 1.1).

### 2.3.2 Generation of truncated DNA templates missing the stop codon

In some experiments stable ribosome-nascent chain complexes were required and mRNA lacking a stop codon was generated. To produce DNA templates lacking a stop codon from the APP-derivatives, the standard 5' primer (-150 T7 PCRscript or -150 T7 pcDNA3.1(+); see Appendix 1.1) and a 3' primer annealing directly upstream of the stop codon (see Appendix 1.1) were used for PCR reactions as described above.

### 2.4 *In vitro* transcription

~2.5µg of PCR product was used for *in vitro* transcription. The DNA template was transcribed in a final volume of 100µl containing 40mM Tris.HCl pH7.5, 6mM MgCl<sub>2</sub>, 2mM spermidine, 2mM NaCl, 10mM DTT, 1mM rNTPs, 100 units of RNasin and 80 units of T7 RNA polymerase. All reagents were mixed at room temperature, and the reaction was incubated at 37°C for 2 hours. RNA was purified using the QIAgen RNeasy Mini Kit (as per manufacturer's instructions), eluted with 50µl H<sub>2</sub>O, and stored at -80°C. The amount and purity of the RNA obtained was assessed on a 1% agarose gel stained with ethidium bromide prior to use in an *in vitro* translation reaction.

### 2.5 *Semi-intact cells*

Semi intact HEK293, COS7 or HT1080 cells (SI cells) were prepared using a method adapted from Wilson *et al.* (1995). Cells were grown to ~90% confluence in 75cm<sup>2</sup> flasks (for media composition, see Table 2.4 below), washed twice with phosphate-buffered saline (PBS) and detached from the flask by incubation with 2ml trypsin-EDTA (0.5g/litre Trypsin, 0.2g/litre EDTA) for 5 minutes. Further proteolysis by trypsin was prevented by the addition of 4ml KHM buffer (110mM potassium acetate, 2mM magnesium acetate, 20mM HEPES.KOH pH 7.2) containing 100µg/ml Soybean Trypsin Inhibitor, and the cells were transferred to a polypropylene tube for collection by centrifugation at ~250 x g for 3 minutes at 4°C. The pellet was resuspended in 4ml KHM buffer and the cells permeabilised for 5 minutes on ice by addition of 20mg/ml digitonin (dissolved in DMSO) to a final

concentration of 40µg/ml. Any excess digitonin was diluted by addition of 10ml ice-cold KHM buffer, and the cells pelleted immediately by centrifugation at ~250 x g for 3 minutes at 4°C. Following resuspension in 5ml of HEPES buffer (50mM potassium acetate, 90mM HEPES.KOH pH 7.2), the cells were incubated on ice for 10 minutes. After centrifugation at ~250 x g for 3 minutes at 4°C, cells were resuspended in 100µl KHM, transferred to a microfuge tube and spun for 10 seconds in a benchtop microcentrifuge at ~16,000 x g. The cell pellet was resuspended in 100µl KHM buffer, CaCl<sub>2</sub> was added to 1mM and 1µl calcium-dependent micrococcal nuclease (100-300U/ml) was added to degrade endogenous RNA. After incubation at room temperature for 12 minutes, the nuclease was inactivated with 4mM EGTA. Cells were isolated by spinning for 10 seconds in a microcentrifuge, and finally resuspended in 50µl KHM buffer to give approximately 0.5x10<sup>5</sup> cells/ml. Typically, 3µl of cells were used in an *in vitro* translation reaction.

**Table 2.4: Media composition**

<b>Cell Type</b>	<b>Media composition</b>
HEK293	Minimum essential medium (MEM) (+ Earle's salts, + L-glutamine), 1% MEM non-essential amino acids, 10% heat-inactivated foetal bovine serum, 1% penicillin/streptomycin.
HT1080	MEM2 (+ Earle's salts, + L-glutamine), 10% heat-inactivated foetal bovine serum, 1.4% MEM vitamins, 1% glutamine, 1% sodium pyruvate, 1% MEM non-essential amino acids.
COS7	DMEM, 1% glutamine, 1% MEM non-essential amino acids, 10% heat-inactivated foetal bovine serum.

## **2.6 *In vitro* translation in rabbit reticulocyte lysate**

RNA was translated in nuclease-treated rabbit reticulocyte lysate, in some cases supplemented with either canine pancreatic microsomes or semi permeabilised mammalian cells as an ER membrane source. In general, 17.5µl of the rabbit reticulocyte lysate was mixed on ice with all amino acids except methionine added to a final concentration of 20µM, 20µCi [<sup>35</sup>S]-methionine (specific activity 1175 Ci/mMol), 1.5µl microsomes (~45 OD<sub>280</sub>/ml) or 3.0µl SI cells and 2µl RNA were added. Where membranes were not required, 1.5µl of microsome resuspension buffer (instead of microsomes) or 3.0µl KHM buffer (instead of SI cells) was added

instead to maintain uniform salt concentrations. The volume was adjusted to 25 $\mu$ l with H<sub>2</sub>O and incubated at 30°C for 1 hour, unless otherwise stated. Aurintricarboxylic acid (ATCA) was then added to 0.1mM and samples were incubated for a further 10 minutes at 30°C followed by 5 minutes on ice. ATCA blocks initiation of translation without inhibiting elongation, and following the 10-minute incubation with ATCA, all nascent chains should be completed. Samples were processed as described in the following sections, or analysed directly by SDS-PAGE (see section 2.20).

### ***2.7 In vitro translation in wheat germ extract***

RNA was translated in the absence of membranes in wheat germ extract. 25 $\mu$ l of the wheat germ extract was mixed on ice with all the amino acids except methionine to a final concentration of 20 $\mu$ M each, 40 $\mu$ Ci [<sup>35</sup>S]-methionine (specific activity 1175 Ci/mMol) and 2 $\mu$ l RNA were added. The volume was adjusted to 50 $\mu$ l with H<sub>2</sub>O and incubated at 26°C for 15 minutes, unless otherwise stated. Aurintricarboxylic acid (ATCA) was then added to 0.1mM and samples were incubated for a further 10 minutes at 26°C followed by 5 minutes on ice. Samples were processed as described in the following sections, or analysed directly by SDS-PAGE (see section 2.20).

### ***2.8 Isolation of microsomal membrane fractions***

Following translation reactions, microsomal membranes were isolated by ultra-centrifugation through a high-salt sucrose cushion (HSC: 250mM sucrose, 500mM potassium acetate, 5mM magnesium acetate, 50mM Hepes.KOH, pH 7.9) at 130,000 x g for 10 minutes at 4°C in a Beckman ultra-centrifuge. The supernatant was discarded and the membrane pellet was resuspended in 25 $\mu$ l KHM (110mM potassium acetate, 2mM magnesium acetate, 20mM HEPES.KOH pH 7.2), prior to further manipulation or analysis by SDS-PAGE (see section 2.20).

## **2.9 TCA precipitation**

Proteins were precipitated by the addition of an equal volume of 20% Trichloroacetic acid (TCA)/50% acetone (final volume) and incubation for 10 minutes on ice. The samples were then centrifuged at ~16,000 x *g* for 10 minutes in a microcentrifuge, and the resulting pellet washed with 500µl of cold acetone before drying and solubilising in sample buffer for analysis by SDS-PAGE (section 2.20).

## **2.10 Endoglycosidase H treatment**

Endoglycosidase H (EndoH) treatment was carried out according to the manufacturer's instructions. Denaturing buffer (5% SDS, 10% β-mercaptoethanol) was added to samples at 1:10 dilution, and samples were incubated at 37°C for 30 minutes. Following the incubation, G5 buffer (0.5M sodium citrate, pH 5.5) was added at 1:10 dilution and PMSF was added to a final concentration of 2mM. Finally, ~2,000U of EndoH was included in the reaction mixture, and samples were incubated at 37°C for 2 hours prior to analysis by SDS-PAGE (section 2.20).

## **2.11 Proteinase K treatment**

Membrane-associated translation products were isolated as in section 2.8 and resuspended in low salt/sucrose buffer (LSB: 250mM sucrose, 100mM potassium acetate, 5mM magnesium acetate, 50mM Hepes.KOH, pH 7.9). Proteinase K was added to a final concentration of 0.25 mg/ml, and samples were incubated on ice for 30 minutes. Samples were then TCA precipitated (section 2.9) and analysed by SDS-PAGE (section 2.20).

## **2.12 Isolation of ribosome-associated nascent chains**

Ribosome-associated nascent chains were generated by synthesising APP-derivatives from mRNAs that lacked a stop codon. Their purification was achieved by layering the sample over 500µl of a high salt/high sucrose cushion (HSHSC: 0.5M sucrose, 500mM potassium acetate, 5mM magnesium acetate, 50mM HEPES.KOH pH 7.9 with cycloheximide added to 2mM immediately prior to use)

and centrifugation at 70,000 x *g* for 20 minutes at 4°C. The supernatant was removed with care to avoid disturbance of the pellet, the pelleted material resuspended in HSC and the ribosomes re-isolated through a high salt/high sucrose cushion as described above. The supernatant was carefully removed, the pelleted material resuspended in LSB and nascent chains released by treatment with 2mM puromycin at 30°C for 10 minutes prior to further analysis.

### ***2.13 Sodium carbonate extraction of the membrane-associated fraction***

In order to confirm membrane integration, membrane-associated products were isolated as described in section 2.8 and the membrane pellet was extracted with 0.1M Na<sub>2</sub>CO<sub>3</sub>, pH ~11.3. Membranes were resuspended in 200µl of the 0.1M Na<sub>2</sub>CO<sub>3</sub> and incubated for 10 minutes on ice. Membranes were re-isolated by ultracentrifugation through a cushion containing 1/3 extracting agent and 2/3 low salt sucrose cushion (v/v). The resulting pellet was resuspended in sample buffer for analysis by SDS-PAGE. Proteins were recovered from the supernatant by TCA precipitation (section 2.9) and resuspended in sample buffer for analysis by SDS-PAGE (section 2.20).

### ***2.14 Polyethylene glycol treatment of semi-intact cells***

Semi-intact cells were prepared as described in section 2.5, and following the synthesis of APP-derivatives, the membrane fraction was isolated by centrifugation in a microcentrifuge at ~16,000 x *g*. The resulting pellet was washed twice with KHM and resuspended in PEG buffer (10mM Hepes, 0.1 M potassium acetate, 5mM magnesium acetate, pH 7.2), 15% (w/v) PEG-4000 (in PEG buffer) or 30% (w/v) PEG-4000 (in PEG buffer) and incubated at 30°C for 5-15 minutes. The membranes were re-isolated by centrifugation at ~100,000 x *g* and resuspended in KHM buffer before being used for further experiments or analysed by SDS-PAGE (section 2.20).

### **2.15 BFA treatment**

COS7 cells were grown to ~90% confluency in either 75cm<sup>3</sup> flasks (to prepare SI cells) or on coverslips (for immunofluorescence). The media was removed, cells washed twice with PBS and 10ml of fresh media was added to the cells. Brefeldin A (BFA) was added to 10 µg/ml final concentration, from a 10mg/ml stock in methanol, or an equivalent volume of methanol was added as a control and cells were incubated at 37°C for 2 hours. Semi-intact cells were prepared from the BFA-treated cells (section 2.5) and coverslips were processed for immunofluorescence microscopy (section 2.22).

### **2.16 Preparation of a CHAPSO-solubilised crude membrane extract**

A CHAPSO-solubilised crude membrane extract previously reported to show  $\gamma$ -secretase activity was prepared essentially as described by Li et al. (2000). A 6 litre culture of HeLa S3 cells was grown in suspension using DMEM containing 10% heat inactivated foetal bovine serum, 2 mM glutamine, and 100 µg/ml each of penicillin and streptomycin. Cells were recovered by centrifugation at ~250 x g for 5 minutes and washed twice with PBS, and the cell pellets snap-frozen in liquid nitrogen and stored at -80°C. Frozen HeLa cell pellets were resuspended in a total of 20ml of buffer A (50 mM Mes, pH 6.0, 5 mM MgCl<sub>2</sub>, 5 mM CaCl<sub>2</sub>, 150 mM KCl) containing 200µl Sigma protease inhibitor cocktail (Ref. P8340). The cells were lysed by a single-pass through a French Press, and lysis was verified by microscopy. Cell debris and nuclei were removed by centrifugation at 800 x g for 10 minutes and the resulting supernatant centrifuged at 100,000 x g for 60 minutes. The membrane pellet was resuspended in 9ml of buffer A without protease inhibitors and centrifugation was repeated as above. The final membrane pellet was resuspended in 2ml of buffer A to yield a protein concentration of ~4 mg/ml. All procedures were performed at 4°C and the final membrane preparation was stored at -80°C. The crude HeLa cell membrane fraction was solubilised with 1% 3-[(3-cholamidopropyl)dimethylammonio]-2-hydroxy-1-propanesulfonate (CHAPSO) in buffer A for 60 minutes on ice, insoluble material removed by centrifugation at 100,000 x g for 60 minutes, and the

resulting supernatant solution is defined as CHAPSO-solubilised crude membrane extract.

### **2.17 RNase treatment**

In order to remove t-RNA that remained attached to nascent polypeptides, all samples were treated with ~0.5U Ribonuclease A per translation reaction and incubated at 37°C for 5 minutes prior to the addition of SDS sample buffer or IP buffer.

### **2.18 Immunoprecipitation**

Samples were denatured by adding SDS to 1% (w/v) and heating for 30 minutes at 37°C. After heating, four volumes of Triton X-100 immunoprecipitation (IP) buffer (10mM Tris-HCL. pH 7.6, 140mM NaCl, 1mM EDTA, 1% Triton X-100) were added and samples were incubated on ice for 15 minutes with intermittent vortexing. Once “solubilisation” was complete, the sample was spun in a microcentrifuge for 2 minutes ~16,000 x g to remove any debris, and the resulting supernatant was removed. To reduce any background from unincorporated [<sup>35</sup>S]-methionine, 1mM methionine was added to the samples and the protease inhibitor phenylmethylsulphonyl fluoride (PMSF) was also included at a final concentration of 1mM. The supernatant was pre-cleared by incubating with 15µl *Staphylococcus aureus* cells per translation reaction for 1 hour at 4°C on a roller. The samples were then centrifuged as above and the supernatant transferred to a clean tube. Supernatant aliquots of 100µl or 200µl were mixed with the appropriate antisera, and the samples were mixed overnight at 4°C. The following day, 15µl of a Protein A Sepharose bead slurry was added to each aliquot and the samples were incubated for a further 2 hours. The Protein A Sepharose beads had been pre-incubated with 20% bovine serum albumin and washed 5 times with IP buffer. Following the 2 hour incubation, the Protein A Sepharose beads were pelleted by centrifugation in a microcentrifuge and the beads were washed five times using 1ml aliquots of cold Triton X-100 IP buffer. Residual IP buffer was removed using a Hamilton syringe and the beads were resuspended in SDS-PAGE sample buffer.

### **2.19 Immunodepletion**

Depleted reticulocyte lysate preparations were generated by immunoprecipitation using excess amounts of  $\alpha$ IDE or preimmune serum as a control. 10 $\mu$ l antisera aliquots were mixed with the 50 $\mu$ l of a Protein A Sepharose bead slurry (see section 2.18), that had been washed 5 times with dH<sub>2</sub>O and once with 20mM HEPES (pH 7.2) to remove any Triton X-100, and the samples were incubated for 4 hours at 4°C. Following the 4 hour incubation, 150 $\mu$ l of rabbit reticulocyte lysate was added to the beads and the samples were incubated overnight at 4°C. The beads were then pelleted by centrifugation in a microcentrifuge and the reticulocyte lysate was carefully removed. The resulting immunodepleted lysate was then re-centrifuged twice to remove any residual beads.

### **2.20 SDS-PAGE**

Before resolving on SDS polyacrylamide gels, samples were denatured and solubilised in SDS sample buffer by incubation at 95°C for 5 minutes, followed by a 1-minute spin at 16,000 x *g* to remove insoluble material. The protein samples were resolved on glycine or tricine-based acrylamide gels ranging from 10-19% acrylamide as required. After running, gels were fixed for a minimum of 10 minutes (20% methanol, 10% acetic acid) and dried on a Bio Rad Model 583 Gel Dryer. The gels were then exposed to Fuji bioimaging plates, which were analysed using a Fuji BAS-2000 Bioimaging system. Quantification of the phosphorimages was then carried out using the AIDA software supplied by Raytek.

### **2.21 Transient transfection**

COS7 cells were grown on sterile 13mm diameter coverslips until ~90% confluent (for media, see table 2.4). The media was then removed from the cells and, after washing twice with PBS, replaced with media that lacked serum and antibiotics. Cells were then transfected with the appropriate plasmid DNA using Lipofectamine-2000 according to the manufacturer's instructions. Cells were

grown for 24-48 hours before the coverslips were processed for immunofluorescence.

## **2.22 Western blotting**

Cells were washed twice with phosphate-buffered saline (PBS) and Triton X-100 immunoprecipitation buffer was added to solubilise the cells. Cells were resuspended in 20 $\mu$ l SDS-PAGE sample buffer and heated to 95°C for 5 minutes, before loading on a 14-19% Tris-Tricine gel. Following SDS-PAGE separation, the gel was soaked in transfer buffer (20mM Tris.HCl pH7.5, 150mM glycine, 20% v/v methanol) for 10 minutes. Transfer onto a nitrocellulose membrane was performed using a semi-dry blotting apparatus at 20V for 30 minutes. Efficient transfer was determined by visualising the proteins on the membrane with Ponceau S. The membrane was then washed with water and blocked overnight at 4°C in 25ml blocking solution (TBST (50mM Tris.HCl, 150mM NaCl, 0.05% Tween 20, pH 8.0) supplemented with either 5% w/v low fat milk powder or 3% w/v BSA). Following the blocking step, the blocking solution was removed, and 2ml of fresh blocking solution containing the appropriate dilution of primary antibody was added and the membrane incubated for 1 hour at room temperature with gentle agitation. The membrane was then washed 5 times with TBST and an appropriate secondary antibody coupled to alkaline horse-radish peroxidase was added at 1:5000 dilution in blocking solution. Following an hour incubation at room temperature with gentle agitation, the membrane was washed 5 times with TBST and once with PBS. The bound secondary antibody was detected by enhanced chemiluminescence (Pierce). Blots were incubated in the ECL solutions for 1 minute before exposure to BioMax MR film for between 10 seconds-20 minutes.

## **2.23 Immunofluorescence**

Coverslips generated by transient transfection (section 2.20) were washed with PBS, drained and fixed by placing in methanol and storing at -20°C for 10 minutes. After rehydrating by incubation in PBS for 5 minutes, the coverslips were incubated, cell-side down, with 30 $\mu$ l of the appropriate dilution of primary antibody(s) for 20 minutes at room temperature. Coverslips were washed 3 times

for 5 minutes in PBS, before being transferred to a 30 $\mu$ l aliquot of the appropriate secondary antisera (1:100 dilution). Following a 20 minute incubation at room temperature, coverslips were washed as before and incubated in 30 $\mu$ l of 4',6-diamidino-2-phenylindole\*2HCl (DAPI) (1:10,000 dilution) for 20 minutes at room temperature. Coverslips were washed as described previously, rinsed once with deionised H<sub>2</sub>O and mounted on 6 $\mu$ l of freshly made Mowiol mountant (Longin et al., 1993) (6g glycerol, 2.4g Mowiol, 12ml dH<sub>2</sub>O, 12ml 0.2M Tris (pH 8.5)) containing 25mg/ml antifade (1,4-diazobicyclo[2,2,2]-octane (DABCO)). After leaving to dry, the cells were visualised using a Leica DMRXA microscope fitted with a Photometrics CH250 CCD camera (+2.25mm).

## **CHAPTER 3**

---

### **Results:**

#### **Generation and fate of C-terminal fragments of APP**

### 3 Generation and fate of C-terminal fragments of APP

The production of the C-terminal APP intracellular domain (AICD) from APP by  $\gamma$ -secretase cleavage and its subsequent function are relatively poorly characterised to date. Whilst current evidence strongly implicates the N-terminal A $\beta$  fragment in amyloid plaque formation (Selkoe, 1999), less is known about the fate of the C-terminal fragment. Recent studies, consistent with earlier proposals based on apparent similarities to the Notch pathway, have suggested that the AICD might play a role in signalling (Cao and Sudhof, 2001). To date, the majority of studies of APP processing and AICD generation have been performed *in vivo* (see Introduction), although two studies have suggested that  $\gamma$ -secretase cleavage can be recapitulated using an *in vitro* system (De Strooper et al., 1999; Weihofen et al., 2003).

The aim of this study was to investigate the reconstitution of  $\gamma$ -secretase cleavage *in vitro* with particular focus on the generation and fate of the resulting C-terminal fragments. In order to simplify the analysis of any processing products, I first attempted to reduce the APP-derived  $\gamma$ -secretase substrate to the absolute minimum sequence predicted to be efficiently targeted to the ER membrane but would still be capable of undergoing  $\gamma$ -secretase cleavage. The AICD (CT57) together with the complete transmembrane domain of APP seemed the smallest element that would achieve this end, and relied upon the transmembrane domain serving as a “signal anchor” sequence (High and Dobberstein, 1992) to allow the protein’s targeting and integration at the ER membrane. I therefore generated two constructs: CT72, which represents the AICD plus the full transmembrane domain, and <sup>Met</sup>CT57, to serve as a marker to aid the identification of AICD-like products that may result from  $\gamma$ -secretase processing (cf. Fig 3.4A).

### 3.1 Membrane integration and orientation of CT72

To establish whether the CT72 construct was efficiently integrated into ER membranes following its synthesis in the presence of microsomal membranes, translation products were assessed for membrane insertion using three different assays (Fig 3.1). In the first instance, microsomal membranes were isolated by centrifugation through a high salt/sucrose cushion and the resulting membrane pellet extracted with alkaline sodium carbonate solution prior to the re-isolation of the membrane fraction. This procedure efficiently removes the majority of peripherally bound proteins and the soluble content of the ER lumen, leaving a pellet that is highly enriched in integral membrane proteins (Fujiki et al., 1982). The majority of the CT72 product is found in the membrane pellet following treatment with alkaline sodium carbonate solution (Fig 3.1A, cf. lanes 3 and 4), a pattern that closely resembles that seen with a known integral membrane protein, the invariant chain (Fig 3.1A, cf. lanes 1 and 2). I therefore concluded that CT72 was efficiently targeted to, and inserted into, the ER membrane *in vitro*.

Although these data indicate that CT72 is membrane inserted, they provide no information regarding its orientation within the membrane. In order to achieve authentic  $\gamma$ -secretase processing, the polypeptide should be in the same type I orientation as for full-length APP (see Fig 3.1B), with the C-terminus oriented in the cytoplasm (De Strooper and Annaert, 2000). Two alternative methods were used to assess the orientation of CT72; *N*-glycosylation and treatment with proteinase K.

*N*-glycosylation occurs in the ER lumen, and therefore a region of polypeptide can only be *N*-glycosylated if it has been translocated into the ER lumen. CT72 is not normally *N*-glycosylated, and so an Asn-X-Ser/Thr consensus sequence for *N*-glycosylation was inserted into the C-terminal portion of CT72 at residues 61-63 by site-directed mutagenesis. The resulting protein, CT72-Gly, can only be *N*-glycosylated if it assumes an incorrect, type II, orientation (see Fig 3.1B). To test this possibility, CT72-Gly, CT72 and the invariant chain were synthesised in the presence of microsomal membranes and their *N*-glycosylation status established by treatment with Endoglycosidase H. The invariant chain carries two *N*-linked glycans and, upon EndoH treatment, a clear reduction in the precursor's apparent

size was observed, consistent with the removal of the glycans (Fig 3.1C, cf. lanes 5 and 6). In contrast, neither the CT72-Gly nor the CT72 polypeptides showed an alteration in migration upon EndoH treatment (Fig 3.1C, cf. lanes 1-4).

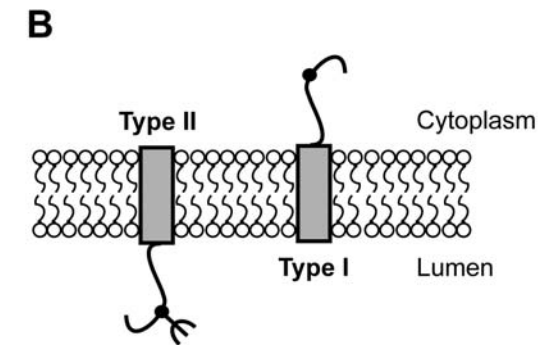
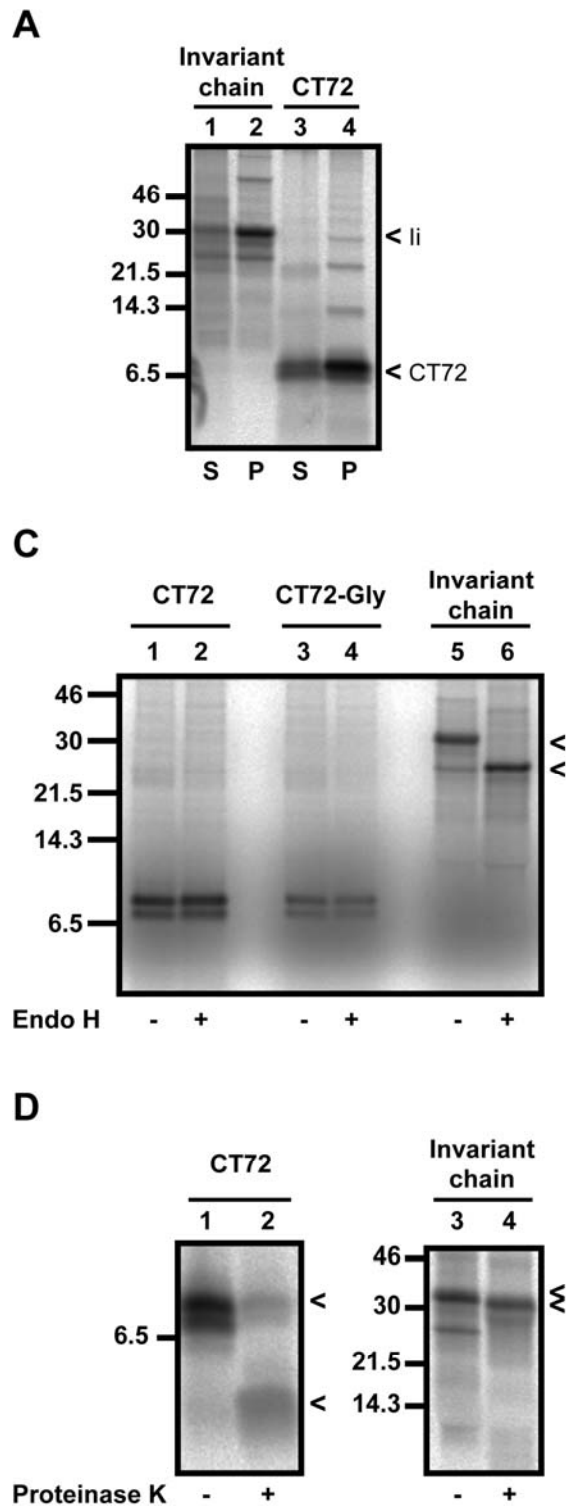


Fig 3.1. **Transmembrane orientation of CT72 in the ER.**

**(A)** CT72 and invariant chain (li) transcripts were translated in a rabbit reticulocyte lysate system for 1 hour at 30°C in the presence of canine pancreatic microsomes. Samples were treated with ATCA prior to isolating the membranes. Membranes were resuspended in 0.1M Na<sub>2</sub>CO<sub>3</sub> and incubated on ice for 15 minutes. The membrane fraction was re-isolated and solubilised in sample buffer (pellet, represented by "P"). Any proteins remaining in the supernatant from this step were precipitated with TCA and resuspended in sample buffer (supernatant, represented by "S"). The products were separated by SDS-PAGE.

**(B)** Possible topologies. The position of the potential glycosylation site that was added to CT72-Gly by site-directed mutagenesis is indicated by a black circle.

**(C)** CT72, CT72-Gly and invariant chain transcripts were translated as for (A), but for 30 minutes. Samples were incubated with ATCA before adding either sample buffer (lanes 1, 3 and 5) or treating with Endo H (lanes 2, 4 and 6). Products were then separated by SDS-PAGE.

**(D)** CT72 and invariant chain transcripts were translated as in (A). Membranes were resuspended in either low salt buffer (lanes 1 and 3) or low salt buffer + 0.25mg/ml proteinase K (lanes 2 and 4). Samples were incubated on ice for 30 minutes and products were TCA precipitated. The pellet were resuspended in sample buffer and separated by SDS-PAGE.

I therefore concluded that CT72-Gly is not *N*-glycosylated and is most likely in the “correct” type I orientation with its C-terminus on the cytoplasmic side of the membrane (Fig 3.1B). The alternative interpretation of the behaviour of CT72-Gly is that it assumes a type II topology, but the novel *N*-glycosylation site introduced as a reporter cannot be utilised. For this reason, the transmembrane orientation of CT72 in the ER membrane was confirmed by a protease-protection study (Fig 3.1D). As indicated in Fig 3.1D, when CT72 is subjected to treatment with proteinase K the majority of the polypeptide is digested, consistent with a significant proportion of the polypeptide being exposed on the cytosolic face of the membrane and therefore accessible to protease-mediated degradation (Fig 3.1D, cf. lanes 1 and 2, indicated by arrowheads). This supports the idea that CT72 assumes a type I transmembrane orientation with the bulk of the polypeptide on the cytosolic face of the membrane. Conversely, the majority of the invariant chain polypeptide is ER luminal and hence inaccessible to proteinase K digestion, resulting in only a small decrease in molecular weight from the loss of its short cytoplasmic tail (Fig 3.1D, lanes 3 and 4, arrowheads). Thus, taken together, these data all suggest that CT72 is efficiently targeted to the ER membrane and inserted in an orientation compatible with  $\gamma$ -secretase cleavage.

### **3.2 Analysis of APP-derivatives for putative $\gamma$ -secretase processing**

Having verified that CT72 is correctly integrated at the ER membrane, I synthesised CT72 in the presence and absence of microsomal membranes to assess the production of lower molecular weight products that might result from  $\gamma$ -secretase processing. To aid the detection of any C-terminal fragments derived from CT72 the putative product of its  $\gamma$ -secretase cleavage, CT57 together with an initiating methionine (<sup>Met</sup>CT57), was run alongside the CT72 samples to provide an internal reference. Of particular interest were any small peptides that were seen only in the presence of membranes. Whilst a lower molecular weight product with a mobility similar to that of the putative <sup>Met</sup>CT57 product was observed, this fragment was seen in both the presence and absence of added membranes (Fig 3.2A, cf. lanes 3 and 4 indicated by arrows).

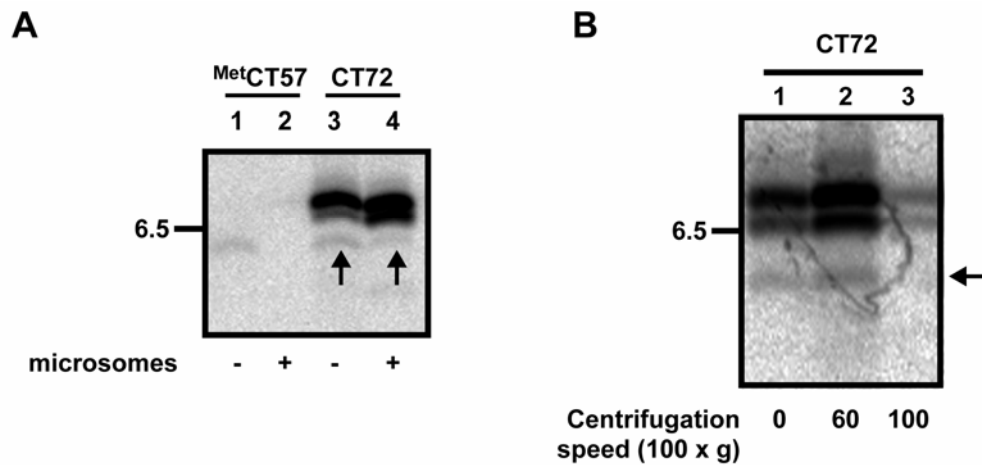


Fig 3.2. **Generation of C-terminal fragments of APP.**

**(A)** MetCT57 and CT72 transcripts were translated in a rabbit reticulocyte lysate system for 30 minutes at 30°C in the presence or absence of canine pancreatic microsomes. Samples were treated with ATCA prior to isolating the membranes (+ microsome samples). Both + and - microsome samples were immunoprecipitated with  $\alpha\text{APP}_{680-695}$  and the products were analysed by SDS-PAGE. CT57-like products are indicated by black arrows.

**(B)** Prior to setting up translation reactions, rabbit reticulocyte lysate was left untreated (lane 1) or centrifuged at 60,000 x g (lane 2) or 100,000 x g (lane 3) for 10 minutes. CT72 transcripts were then translated as in (A). Samples were treated with ATCA and immunoprecipitated with  $\alpha\text{APP}_{680-695}$  and resolved by SDS-PAGE.

Given that authentic  $\gamma$ -secretase cleavage would be a membrane-dependent process, I investigated whether there were any residual membranes present in the lysate that might result in CT72 processing. To this end, the analysis of CT72 was repeated using reticulocyte lysate that had first been centrifuged at 60,000 or 100,000 x g, and the products were assessed for the presence of a CT57-like fragment in the absence of any exogenously added membranes. Centrifugation at 60,000 x g had no obvious effect on the products synthesised by the lysate and a CT57-like product was still observed (Fig 3.2B, cf. lane 2, position indicated by arrow). Increasing the centrifugation to 100,000 x g dramatically reduced the translation efficiency, presumably due to the loss of ribosomes (Fig 3.2B, cf. lane 3). I concluded that this CT57-like product was not due to membrane contamination of the rabbit reticulocyte lysate translation system.

### **3.3 Origin of the CT57-like polypeptide observed during CT72 synthesis**

Given the unexpected appearance of a CT57-like product during CT72 synthesis in the absence of ER-derived membranes, I further investigated the production of this fragment. If the CT57-like product were generated as the result of a proteolytic cleavage event, then one would expect the product to accumulate with increasing time as more processing of the precursor occurs. Similarly, the levels of a precursor would be expected to decrease over time as it is converted to its products. For this reason, I set up a “pulse-chase” experiment to look at levels of the CT57-like product with time. CT72 was synthesised in rabbit reticulocyte lysate, translation was inhibited, and samples were removed at increasing time points (Fig 3.3A). Unexpectedly, rather than the levels of the CT57-like product increasing over the time course, the levels actually decreased (Fig 3.3A, cf. black arrow; Fig 3.3B, red line). In contrast, the levels of the CT72 precursor remained relatively constant (Fig 3.3B, cf. blue line). Whilst the graph shown in Fig 3.3B was constructed from the results of a single experiment, the same profile was consistently observed. This behaviour was not consistent with the CT57-like product resulting from CT72 processing.

Having established that the CT57-like product did not exhibit the characteristics of a product of proteolytic cleavage, I explored the possibility that it was in fact the result of alternative initiation from a downstream methionine residue in the CT72 coding region. CT72 contains several methionine residues in addition to the initiator methionine (Fig 3.4A and appendix 2.1), but only those at positions 8 and 24 seemed likely to generate products of a size akin to <sup>Met</sup>CT57. To assess whether initiation from one of these methionine residues was responsible for the CT57-like product, CT72 derivatives that lacked Met-8 (CT72-1) or both Met-8 and Met-24 (CT72-2) were generated by site-directed mutagenesis.

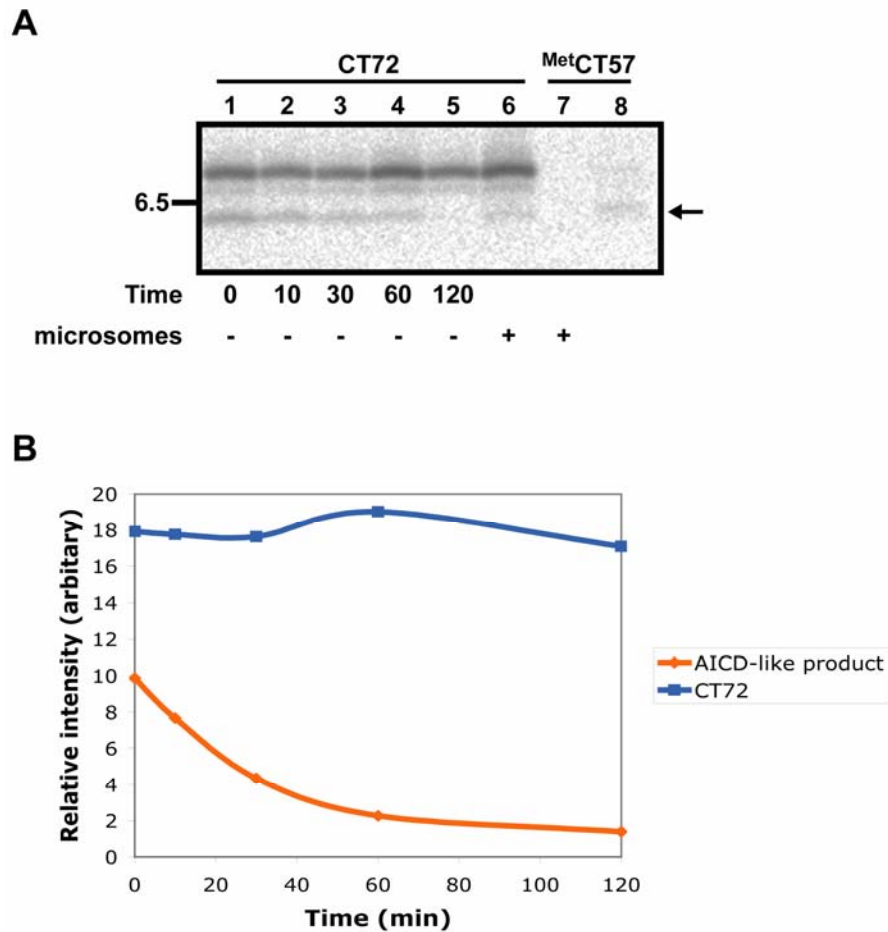


Fig 3.3. **Pulse-chase analysis of CT72 products.**

**(A)** CT72 transcripts were translated in a rabbit reticulocyte lysate system for 15 minutes at 30°C. Initiation of translation was inhibited by addition of ATCA and puromycin. Samples were incubated at 30°C and aliquots were removed at the times indicated. Samples were immunoprecipitated with  $\alpha$ APP<sub>680-695</sub> before analysis by SDS-PAGE. The position of the CT57-like product is indicated by a black arrow.

**(B)** Graphical representation of the levels of CT72 and CT57-like product across a 120 minute time course.

Further derivatives were that were initiated at Met-8 (CT65) or Met-24 (CT49) were also created (Fig 3.4A). The removal of Met-8 from CT72 led to the loss of the lower band of the doublet habitually seen in all cell-free translation reactions (Fig 3.4, cf. lanes 1 and 2, black square), whilst the removal of both Met-8 and Met-24 resulted in the loss of the lower part of the doublet and the CT57-like product (Fig 3.4, cf. lanes 1 and 3, black square and black diamond).

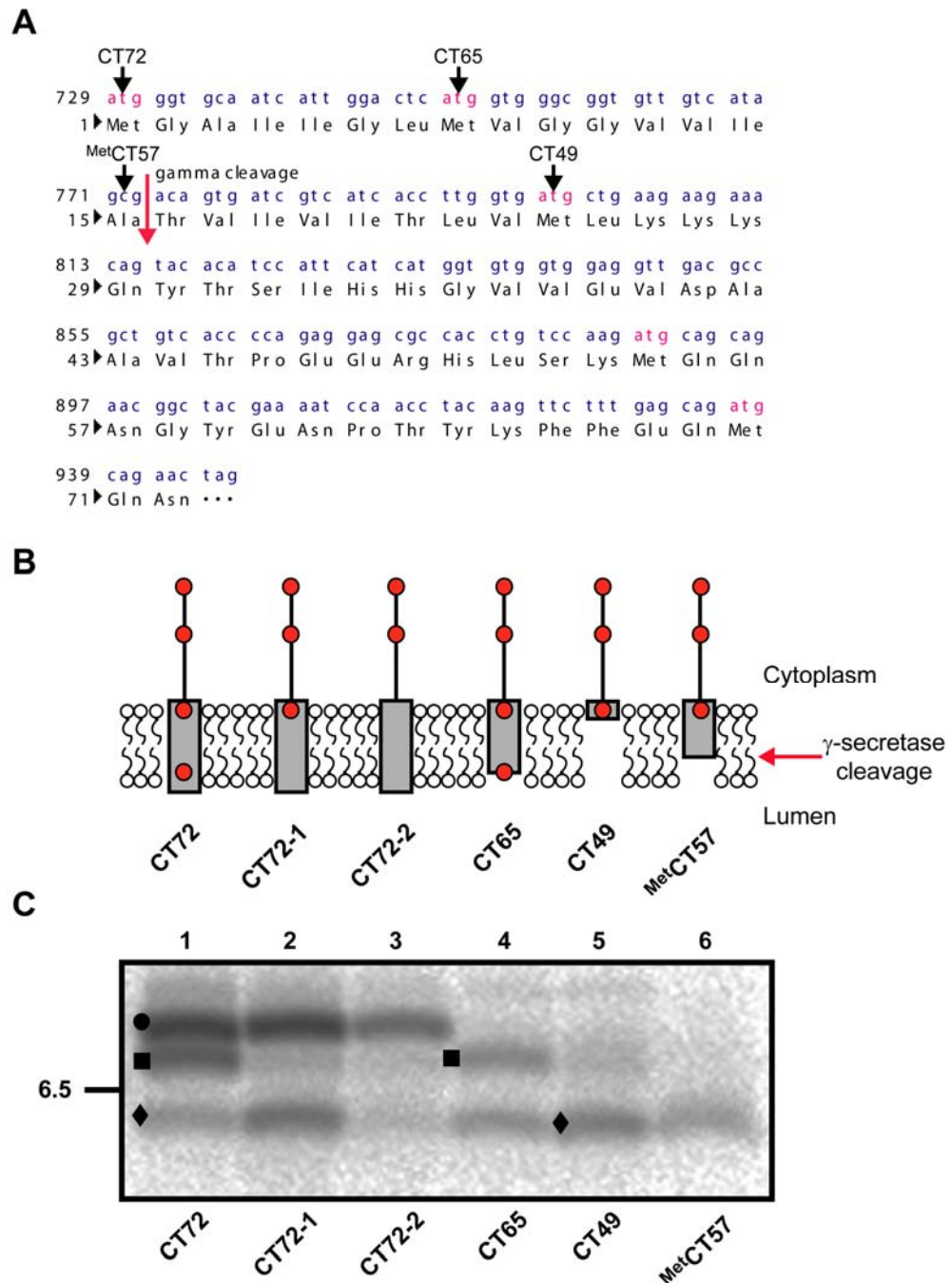


Fig 3.4. Identification of CT72-derived lower molecular weight products

(A) Sequence of CT72. Methionine codons are highlighted in pink.

(B) Versions of the CT72 coding region lacking specific ATG codons were generated by site-directed mutagenesis to enable the identification of lower molecular weight products. Transmembrane regions of the resulting polypeptides are highlighted in grey. Methionine residues are shown by red circles. The  $\gamma$ -secretase cleavage site is indicated by a red arrow.

(C) The CT72 derivatives shown in (B) were synthesised in the presence of  $^{35}\text{S}$  methionine at  $30^\circ\text{C}$  for 15 minutes. Further initiation of translation was inhibited by adding ATCA and puromycin. Products were immunoprecipitated with  $\alpha\text{APP}_{680-695}$  and analysed by SDS-PAGE. The product indicated by ■ was found to be a result of alternative initiation from the methionine at position 8, producing the CT65 polypeptide. Similarly, the product indicated by ◆ was found to be due to alternative initiation from the methionine at position 24, producing the CT49 polypeptide. The "shadows" of alternative products in lanes 3 and 5 are most likely due to spill-over from adjacent lanes.

When initiation occurred at residue 8, only the lower part of the doublet together with the CT57-like product were seen, whilst initiation from residue 24 generated only the CT57-like product (Fig 3.4, cf. lanes 1, 4, 5 and 6). Taken together, these data show that the CT57-like product present in CT72 translation reactions results from alternative initiation at residue 24 of the coding region, and that the resulting product, CT49, has a similar mobility to the <sup>Met</sup>CT57 marker on the tricine gel system used for this study (Fig 3.4, cf. lanes 5 and 6). In contrast, the difference in mobility between CT72 and CT65 is readily apparent (Fig 3.4, cf. lanes 3 and 4).

### **3.4 *In vitro* degradation of CT49**

The rapid and specific degradation of the CT57-like product (now referred to as CT49) after synthesis in rabbit reticulocyte lysate (Fig 3.3) was unusual and unexpected. Given that this region of APP may have one or more biological functions upon its release into the cytosol, I determined to investigate this process further, taking advantage of the *in vitro* system that I had established. One obvious candidate for the removal of the CT49 product from the crude translation system was proteasomal degradation. I therefore investigated whether the proteasome was responsible for the lability of CT49 observed using my *in vitro* system. To this end, a similar experiment to that described in Figure 3.3 was performed, with the exception that the proteasome inhibitor ALLN was to the translation reaction and CT49 stability was tested over 120 minutes (Fig 3.5A). The inclusion of ALLN had no effect on the stability of CT49 (Fig 3.5A, compare top and bottom panels), with levels of the polypeptide being minimal after 10 minutes, and becoming virtually undetectable by 120 minutes. These data suggest that the degradation of CT49 observed in reticulocyte lysate is not due to removal by the proteasome. However, these studies were performed using haemin-treated reticulocyte lysate, which would not be expected to contain functional proteasomes. In addition, no control substrate was utilised that would normally be degraded by the proteasome. Therefore, ideally these experiments should be repeated using haemin-free reticulocyte lysate both with and without the ALLN inhibitor and a control substrate should be included that is degraded by the proteasome.

To further characterise the degradation of CT49, a similar time course was performed in which samples were incubated at 0°C and 30°C for 120 minutes (Fig 3.5B, compare products across time courses at the two temperatures). The stability of CT49 at 0°C suggests that CT49 is being degraded by a protease activity.

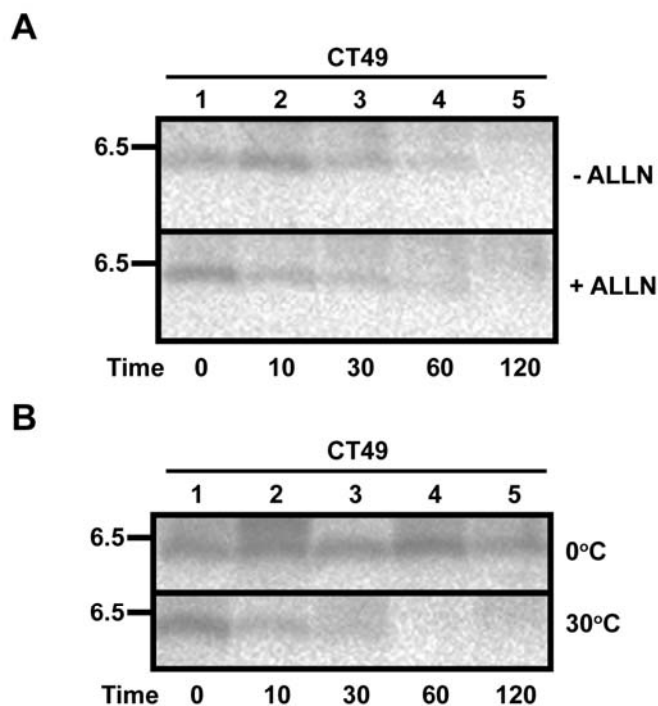


**Fig 3.5. Effect of proteasome inhibition and temperature on CT49 stability.**

**(A)** [<sup>35</sup>S]-labelled CT49 was synthesised in a rabbit reticulocyte lysate system at 30°C for 15 minutes. 5mM ALLN was added to the translation reactions where indicated. Translation was inhibited by addition of ATCA and puromycin. Samples were incubated at 30°C for the times shown before aliquots were removed and immunoprecipitated with  $\alpha$ APP<sub>680-695</sub>. Products were resolved by SDS-PAGE.

**(B)** [<sup>35</sup>S]-labelled CT49 was synthesised as in (A). Samples were incubated at 0°C or 30°C as indicated and aliquots were removed at the times shown. Products were immunoprecipitated with  $\alpha$ APP<sub>680-695</sub> before analysis by SDS-PAGE.

In some studies it had been shown that AICD-like polypeptides similar to CT49 can be stabilised by the presence of the metal-chelators EDTA and PNT that are assumed to inhibit metalloproteinases (Edbauer et al., 2002a). To establish whether this was also the case in my system, I synthesised CT72 and then added EDTA or PNT at the beginning of the time course (Fig 3.6). In the absence of these reagents, levels of CT49 observed were generally low and following a 120 minute incubation were virtually undetectable (Figs 3.6A and 3C, cf. lane 5).

However, in the presence of EDTA or PNT, CT49 was stabilised (Figs 3.6B and D, cf. lanes 1-5), consistent with the degradation of CT49 by a metalloproteinase.

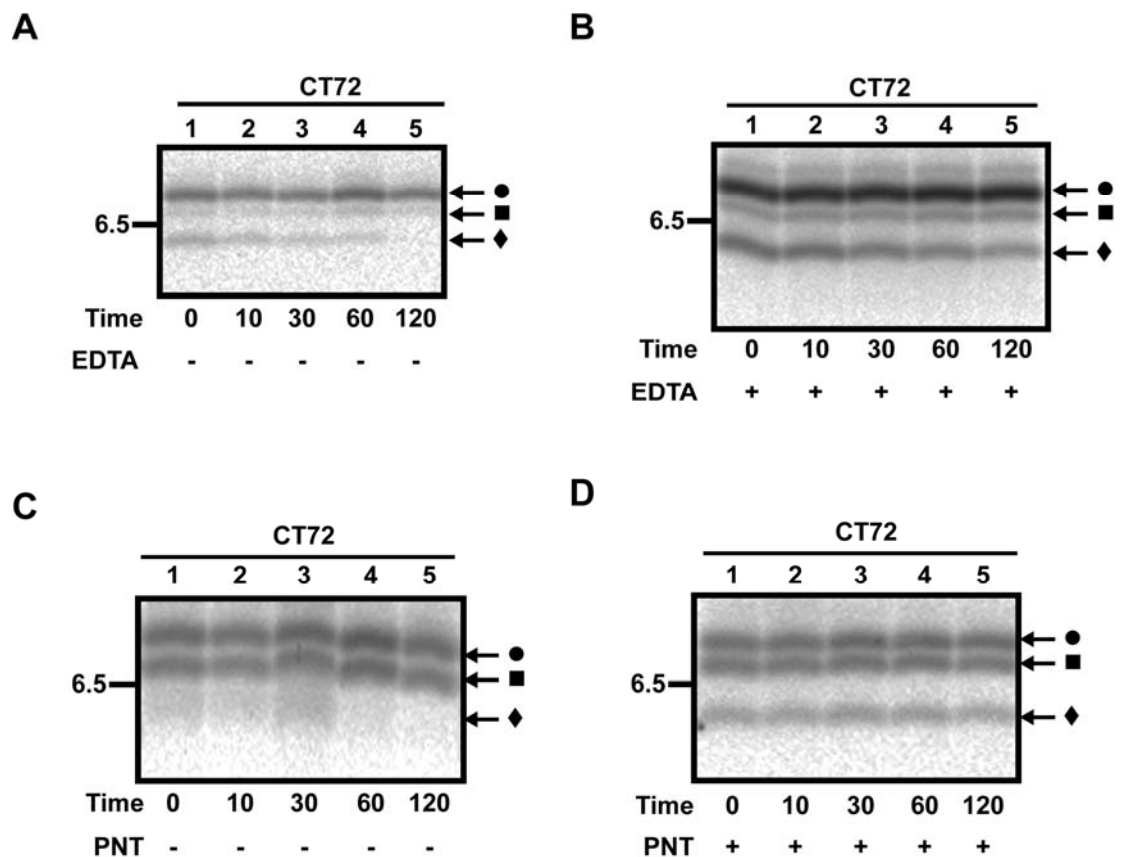


Fig 3.6. Effect of metal-chelators on stability of CT49.

CT72 was synthesised as described in the legend to Figure 3.3 and samples then left untreated (A and C), treated with 5mM EDTA (B). In the case of panel (D), 5mM PNT was included in the translation reaction, and CT72 was synthesised as described previously (Fig 3.3). Immunoprecipitation and sample analysis was also as previously described (Fig 3.3).

### 3.5 *In vitro* degradation of <sup>Met</sup>CT57

The CT49 product is 8 residues shorter than the authentic AICD fragment of APP predicted to result from  $\gamma$ -secretase cleavage (see also Introduction). In order to further investigate the *in vitro* degradation observed in reticulocyte lysate, I carried out similar time course studies using the <sup>Met</sup>CT57 polypeptide, which more closely mimics the putative AICD.

<sup>Met</sup>CT57 was synthesised in rabbit reticulocyte lysate, translation was inhibited, and samples were removed at increasing time points in a comparable study to that described in Figure 3.3 (Fig 3.7A). Similarly to the results obtained with CT49,

levels of <sup>Met</sup>CT57 decreased over the time course (Fig 3.7A, compare lanes 1-5). These data suggested that like CT49, <sup>Met</sup>CT57 is also degraded in reticulocyte lysate.

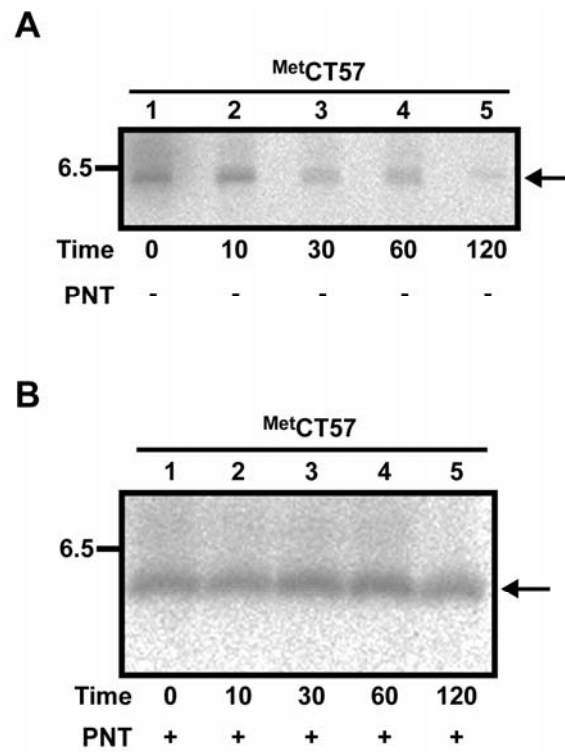


Fig 3.7. Effect of PNT on <sup>Met</sup>CT57 stability.

**(A)** <sup>Met</sup>CT57 transcripts were synthesised in rabbit reticulocyte lysate at 30°C for 30 minutes. Further initiation of translation was stopped by addition of ATCA and puromycin. Samples were incubated at 30°C and aliquots were removed at the times indicated. Products were immunoprecipitated by  $\alpha$ APP<sub>680-695</sub> prior to analysis by SDS-PAGE.

**(B)** A similar experiment was performed to that in panel A, with the exception that synthesis was performed for only 15 minutes in the presence of 5mM PNT.

Since I have shown that CT49 can be stabilised by the inclusion of metalloproteinase inhibitors, I investigated whether this was also the case for the <sup>Met</sup>CT57 polypeptide. An analogous experiment to that described in Figure 3.6 (panels C and D) was performed using <sup>Met</sup>CT57, and its stability in the presence of PNT was analysed over 120 minutes (Fig 3.7B). In the absence of PNT, levels of <sup>Met</sup>CT57 observed were very low, and were virtually undetectable at any time point (Fig 3.7A). However, in the presence of PNT, <sup>Met</sup>CT57 was significantly stabilised,

with readily detectable levels apparent even after 120 minutes (Fig 3.7B), consistent with <sup>Met</sup>CT57, like CT49, being degraded by a metalloproteinase.

### **3.6 Stability of other AICD lengths**

The  $\gamma$ -secretase dependent cleavage of APP generates a number of distinct fragments since there can be subtle variations in the precise location of the proteolytic cleavage that should result in AICDs of predominantly 57-59 residues in length (Weidemann et al., 2002). Whilst the  $\gamma$ -secretase cleavage of the APP  $\beta$ -secretase product to produce A $\beta$ <sub>42</sub> and AICD<sub>57</sub> is most relevant to Alzheimer's disease, the cleavage producing A $\beta$ <sub>40</sub> and AICD<sub>59</sub> is probably the predominant pathway under normal circumstances *in vivo*. I therefore further studied the relationship between the precise length of the AICD fragment and its behaviour in my cell-free system. AICDs of 57 (<sup>Met</sup>CT56), 59 (<sup>Met</sup>CT58), 60 (<sup>Met</sup>CT59) and 61 (<sup>Met</sup>CT60) residues were all generated by incorporating an in-frame methionine residue in front of the relevant coding region. Surprisingly, in contrast to the CT49 and <sup>Met</sup>CT57 fragments, all of these AICD derivatives were stable when synthesised in a rabbit reticulocyte lysate system and were unaffected by the inclusion of PNT into the reaction (Fig 3.8, cf. lanes 1-24). In contrast, low levels of the CT49 fragment were only seen in the presence of PNT (Fig 3.8, cf. lanes 4-6, 11-12, 16-18 and 22-24, filled circle) confirming that degradation could occur in these lysates. It should be noted that only the CT49 fragment represents a peptide that could occur *in vivo*, and all of the other AICD-derived fragments required a non-natural methionine residue at their N-termini to enable synthesis. It is possible that the presence of this methionine residue might influence the subsequent fate of the polypeptide, although in the case of <sup>Met</sup>CT57 rapid degradation was observed (see Discussion). I therefore conclude that CT49 and <sup>Met</sup>CT57 are specifically degraded in the cell-free system used in this study.

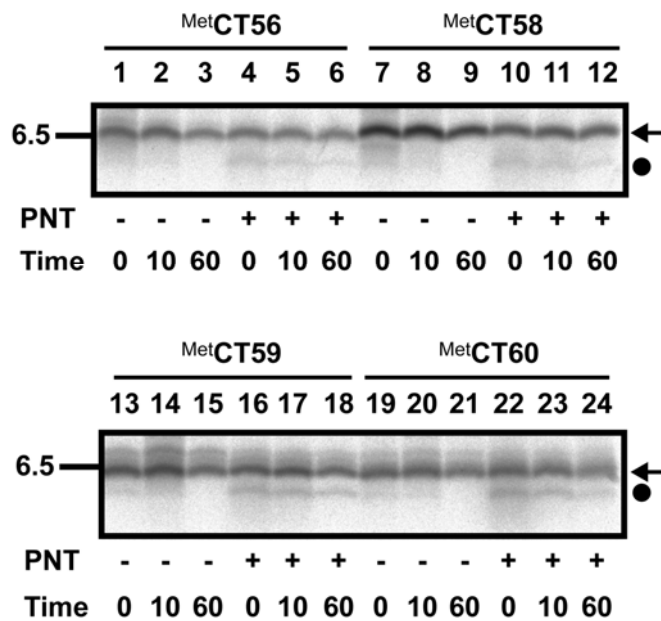


Fig 3.8. Effect of PNT on AICD stability.

MetCT56, MetCT58, MetCT59 and MetCT60 transcripts were synthesised in rabbit reticulocyte lysate at 30°C for 15 minutes in the presence or absence of 5mM PNT as indicated. Further initiation of translation was stopped by addition of ATCA and puromycin. Samples were incubated at 30°C and aliquots were removed at the times shown. Products were immunoprecipitated by  $\alpha$ APP<sub>680-695</sub> prior to analysis by SDS-PAGE. The location of the complete precursor (arrow) and CT49 resulting from alternative initiation (filled circle) are shown.

### 3.7 Synthesis CT49 and <sup>Met</sup>CT57 in wheat germ extract

Given that during previous experiments using reticulocyte lysate the mobilities of <sup>Met</sup>CT57 and CT49 upon SDS-PAGE were very similar (cf. Figs 3.2 and 3.4), I investigated whether this was also the case when the polypeptides were synthesised in a wheat germ extract. To this end, <sup>Met</sup>CT57 and CT49 were synthesised in both reticulocyte lysate and wheat germ translation reactions and the products were run alongside each other on a gel (cf. Fig 3.9). Whilst <sup>Met</sup>CT57 and CT49 have almost indistinguishable apparent molecular weights when synthesised in reticulocyte lysate (Fig 3.9, cf. lanes 1 and 2), when the same polypeptides were generated in a wheat germ system the resulting products visibly differed in size (Fig 3.9, cf. lanes 3 and 4) with the <sup>Met</sup>CT57 product appearing larger than that produced in reticulocyte lysate (Fig 3.9, compare lanes 1 and 3, products indicated by filled circles). One possible explanation for the contrasting

mobilities of <sup>Met</sup>CT57 between the two systems is that the <sup>Met</sup>CT57 that is produced in reticulocyte lysate is N-terminally processed to a shorter CT49-like peptide and that the protease responsible for such processing is not active in the wheat germ extract (see Discussion).

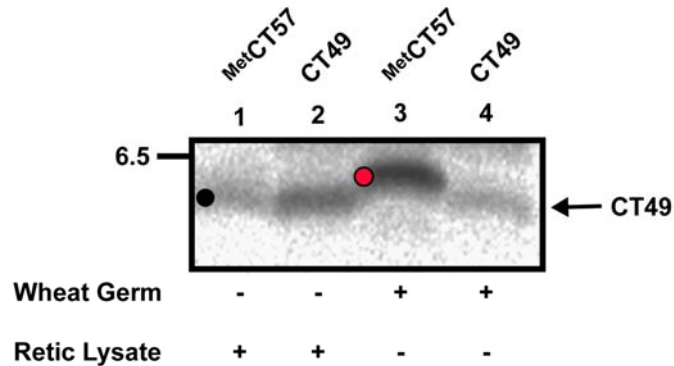


Figure 3.9. Relative mobilities of <sup>Met</sup>CT57 and CT49 in wheat germ and reticulocyte lysate.

[<sup>35</sup>S]-labelled <sup>Met</sup>CT57 and CT49 were synthesised at 30°C (reticulocyte lysate) or 26°C (wheat germ extract) for 15 minutes. Further initiation of translation was inhibited by addition of ATCA and puromycin prior to analysis by SDS-PAGE. The position of CT49 is indicated by an arrow. The position of <sup>Met</sup>CT57 is shown by a black circle (retic) or a red circle (wheat germ).

The rapid degradation of CT49 and <sup>Met</sup>CT57 when synthesised in reticulocyte lysate complicated the study of this process, and I therefore investigated whether such polypeptides were also degraded in a wheat germ system.

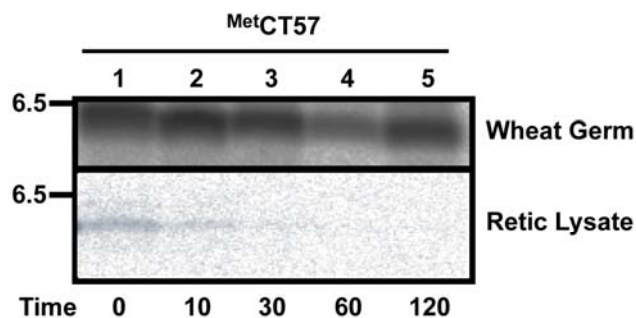
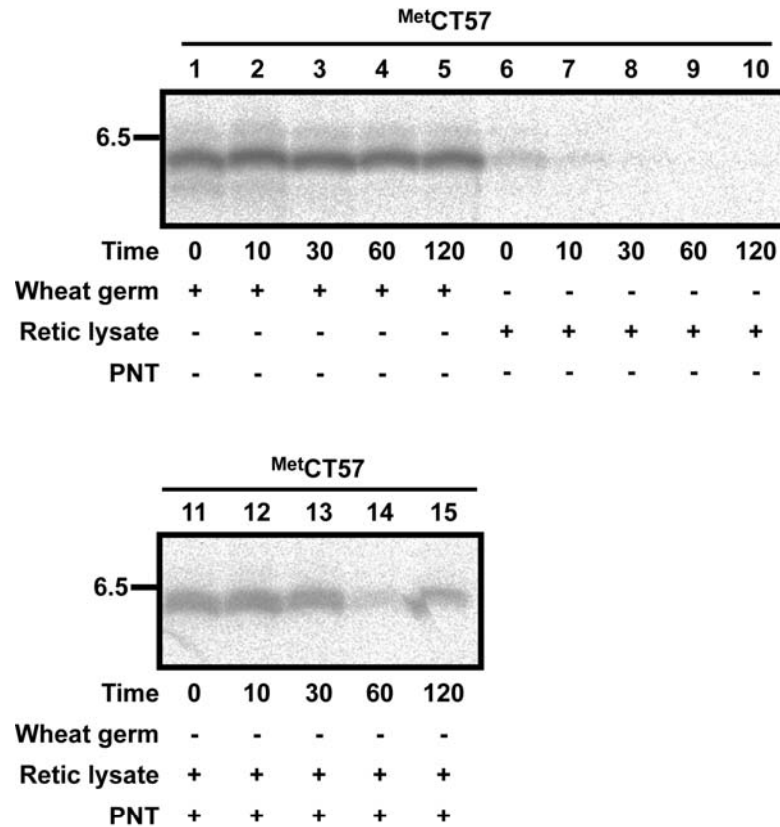


Figure 3.10. Stability of <sup>Met</sup>CT57 in wheat germ extract.

[<sup>35</sup>S]-labelled <sup>Met</sup>CT57 was synthesised at 30°C (reticulocyte lysate) or 26°C (wheat germ extract) for 15 minutes. Further initiation of translation was inhibited by addition of ATCA and puromycin and samples were incubated at 30°C. Aliquots were removed at the times indicated and products were immunoprecipitated by  $\alpha$ APP<sub>680-695</sub> prior to analysis by SDS-PAGE.

In contrast to the rabbit reticulocyte lysate system, the <sup>Met</sup>CT57 polypeptide was found to be relatively stable across a 2-hour incubation, even in the absence of PNT (Fig 3.10, compare upper and lower panels).



**Fig 3.11. Degradation of wheat germ-synthesised <sup>Met</sup>CT57 by factor(s) present in reticulocyte lysate.**

<sup>Met</sup>CT57 transcripts lacking a stop codon were synthesised in wheat germ extract at 26°C for 7 minutes. Ribosome-nascent chain complexes were isolated by ultra-centrifugation through a high salt high sucrose cushion for 2 x 20 minutes at 70,000 x *g*. Ribosome-nascent chain complexes were resuspended in low salt/sucrose buffer and nascent chains were released from the ribosome by addition of puromycin. Polypeptide chains were then resuspended in either wheat germ extract (lanes 1-5), rabbit reticulocyte lysate (lanes 6-10) or PNT-treated lysate (lanes 11-15) and incubated at 30°C. Aliquots were removed at the times indicated and products were immunoprecipitated by  $\alpha$ APP<sub>680-695</sub> prior to analysis by SDS-PAGE.

The CT49 fragment showed a similar behaviour and was also more stable in wheat germ than reticulocyte lysate (data not shown). On the basis of this observation, I was able to exploit the wheat germ system to synthesise stable <sup>Met</sup>CT57 and then reconstitute its degradation by factors present in reticulocyte lysate. Thus mRNA encoding <sup>Met</sup>CT57, but lacking a stop-codon, was translated

using a wheat germ system so as to produce stable ribosome/nascent chain complexes (RNCs). These RNCs were purified by centrifugation and the nascent chains were released from the ribosome by puromycin treatment before being subjected to a variety of treatments. In the first instance, it was found that these “wheat germ-made polypeptides” were a substrate for degradation upon the addition of reticulocyte lysate, but not wheat germ extract (Fig 3.11, cf. lanes 1-5 and 6-10). The degradation observed upon reticulocyte lysate addition was inhibited if PNT was also present (Fig 3.11, cf. lanes 6-10 and 11-15).

### 3.8 Factors affecting AICD stability

*In vivo* studies of AICD fragments have suggested that these polypeptides can be stabilised by the binding of specific proteins, such as the adaptor protein Fe65 that is present at high levels in neuronal tissue (Kesavapany et al., 2002). I therefore investigated whether such components might stabilise the AICD-like <sup>Met</sup>CT57 that I had found to be rapidly degraded *in vitro* by constituents of a rabbit reticulocyte lysate translation system.

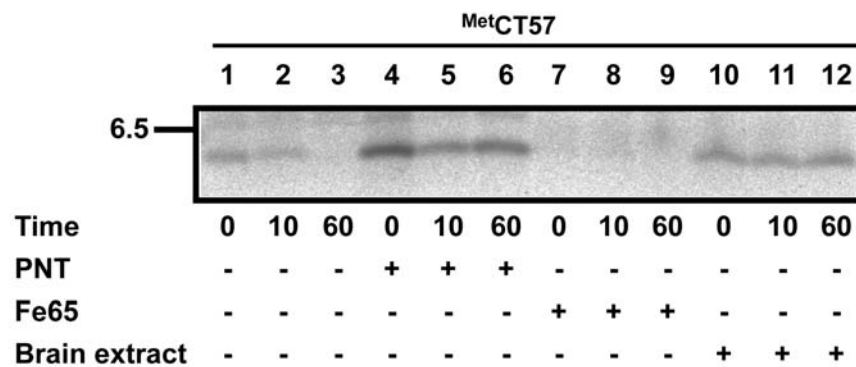


Fig 3.12. Factors in human brain nuclear extract stabilise <sup>Met</sup>CT57.

<sup>Met</sup>CT57 RNCs were synthesised and isolated as previously described (see Figure 3.11). Ribosome-nascent chain complexes were resuspended in low salt/sucrose buffer and nascent chains were released from the ribosome by addition of puromycin. Polypeptide chains were then resuspended in either rabbit reticulocyte lysate (lanes 1-3), PNT-treated lysate (lanes 4-6), lysate pre-treated with Fe65 (lanes 7-9) or lysate pre-treated with human brain extract (lanes 10-12). Samples were incubated at 30°C and aliquots were removed at the times indicated. Products were immunoprecipitated by  $\alpha$ APP<sub>680-695</sub> prior to analysis by SDS-PAGE.

To this end, a similar experiment to that described in Figure 3.11 was performed with the exception that, after synthesis in a wheat germ system, semi-purified <sup>Met</sup>CT57 was mixed with reticulocyte lysate that had been pre-incubated with human brain nuclear extract or recombinant Fe65 (see Fig 3.12).

As previously seen, <sup>Met</sup>CT57 was rapidly degraded in the presence of reticulocyte lysate, and was stabilised when PNT was included in the reaction (Fig 3.12, cf. lanes 1-6). Likewise, the addition of human brain nuclear extract also resulted in the stabilisation of <sup>Met</sup>CT57, although perhaps to a lesser degree than PNT (Fig 3.12, cf. lanes 4-6 and 10-12). In contrast, the recombinant Fe65 did not stabilise the <sup>Met</sup>CT57 product, and in fact if anything resulted in a more rapid degradation (Fig 3.12, cf. lanes 1-3 and 7-9). Taken together, these data are consistent with factors present in human brain nuclear extract stabilising the AICD, although a specific role for Fe65 in this process could not be defined.

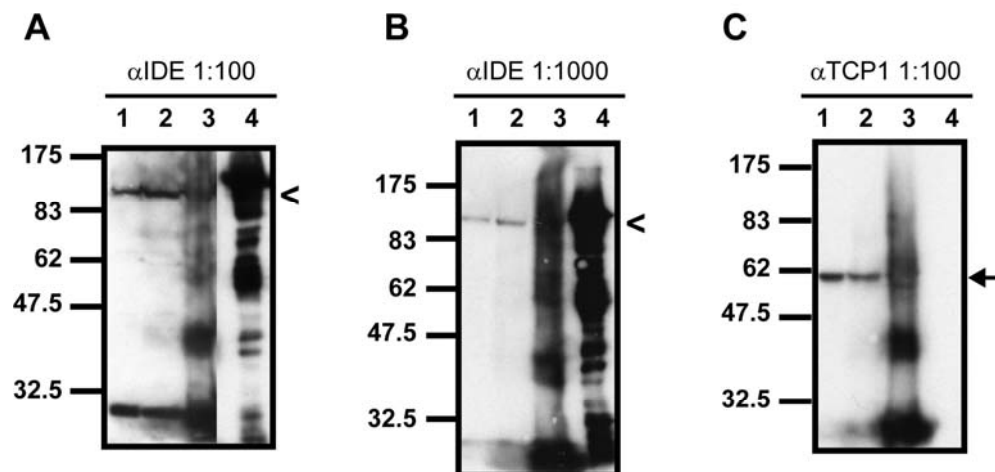


Fig 3.13. **Blot of reticulocyte lysate for insulin-degrading enzyme (IDE).**

(A, B and C) 2 $\mu$ l (lane 1), 5 $\mu$ l (lane 2) and 10 $\mu$ l (lane 3) samples of rabbit reticulocyte lysate were loaded on a 10% tris-glycine gel alongside 0.5 $\mu$ g of purified recombinant IDE as a control (lane 4). Proteins were transferred to nitrocellulose membrane and probed with primary anti-sera specific for either IDE (panels A and B) or TCP1 (panel C) using the dilutions indicated. The positions of IDE and TCP1, which acted as a positive control, are indicated by a black arrowhead and a black arrow respectively.

A prime candidate for the specific degradation of AICD-like fragments is the cytosolic protease, insulin-degrading enzyme or IDE (Edbauer et al., 2002a). I therefore investigated whether IDE was present in the reticulocyte lysate I had been using during the course of this study. Western blot analysis confirmed the

presence of a ~100 kDa product in reticulocyte lysate (Figs 3.13A and B, cf. lanes 1-3). This was slightly smaller than the control recombinant IDE run as a standard on the same blots, since the recombinant protein included a short His-tag to facilitate its purification (Figs 3.13A and B, cf. lane 4). Thus, the presence of detectable IDE in the reticulocyte lysate combined with the inhibition of <sup>Met</sup>CT57 degradation by the metal chelators PNT and EDTA are both consistent with a model where IDE present in the reticulocyte lysate degrades <sup>Met</sup>CT57 shortly after its synthesis.

To further investigate the role of IDE in the degradation of AICD-like fragments in my *in vitro* system, I attempted to immunodeplete the rabbit reticulocyte lysate of IDE by incubation with an immobilised  $\alpha$ IDE antiserum prior to its addition to wheat germ synthesised <sup>Met</sup>CT57. A similar experiment to that described in Fig 3.12 was performed, with the exception that semi-purified <sup>Met</sup>CT57 was mixed with reticulocyte lysate that had been preincubated with either  $\alpha$ IDE serum or a preimmune serum (Fig 3.14).

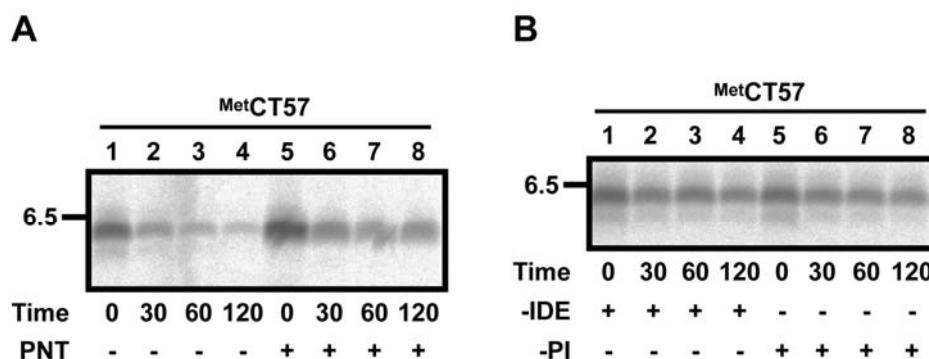


Fig 3.14. Effect of immunodepletion of IDE on <sup>Met</sup>CT57 stability.

<sup>Met</sup>CT57 RNCs were synthesised and isolated as previously described (see Figure 3.11). The isolated ribosome-nascent chain complexes were resuspended in low salt/sucrose buffer and the nascent chains were released from the ribosome by addition of puromycin.

**(A)** Polypeptide chains were resuspended in rabbit reticulocyte lysate that was left untreated (lanes 1-4) or treated with 5mM PNT (lanes 5-8) and incubated at 30°C. Aliquots were removed at the times indicated and products were immunoprecipitated by  $\alpha$ APP<sub>680-695</sub> prior to analysis by SDS-PAGE.

**(B)** Polypeptide chains were resuspended in rabbit reticulocyte lysate that had been incubated with either immobilised  $\alpha$ IDE antisera (-IDE, lanes 1-4) or a pre-immune serum (-PI, lanes 5-8) and incubated at 30°C. Aliquots were removed at the times indicated and products were immunoprecipitated by  $\alpha$ APP<sub>680-695</sub> prior to analysis by SDS-PAGE.

As previously seen, <sup>Met</sup>CT57 was rapidly degraded in the presence of reticulocyte lysate, and was partly stabilised when PNT was included in the reaction (Fig 3.14A, compare lanes 1-4 with lanes 5-8). <sup>Met</sup>CT57 degradation was also markedly reduced when reticulocyte lysate was immunodepleted of IDE (Fig 3.14B, cf. lanes 1-4). However, a similar reduction in <sup>Met</sup>CT57 degradation was also observed when a preimmune serum was used in place of  $\alpha$ IDE as a control (Fig 3.14B, cf. lanes 5-8), suggesting that the AICD-degrading activity is non-specifically removed from the reticulocyte lysate during immunodepletion. Taken together, these data fail to unequivocally confirm the role of IDE in AICD degradation and show that further supplementary analysis will be required.

### 3.9 Summary

The objective of the work presented in this chapter was to establish whether  $\gamma$ -secretase cleavage could be efficiently reconstituted using a minimal APP-derived substrate, CT72. Having first determined that CT72 was efficiently membrane targeted and inserted in the correct orientation, I went on to look for evidence of  $\gamma$ -secretase processing of the polypeptide using an *in vitro* system supplemented with canine pancreatic microsomes. No evidence of such cleavage was detected, and two smaller CT72-derived products were found to be the result of alternative initiation from downstream methionine codons. During the analysis of these lower molecular weight products, I found that both CT49 (generated by alternative initiation) and <sup>Met</sup>CT57 (a putative product of the  $\gamma$ -secretase processing of APP with an artificial initiator methionine) were highly labile in my *in vitro* system. This instability was not due to proteasome-mediated degradation, but was prevented by the inclusion of the metalloproteinase inhibitors EDTA and PNT. I found that <sup>Met</sup>CT57 could be stabilised by a factor present in a nuclear extract prepared from human brain, consistent with the *in vitro* degradation observed reflecting an *in vivo* pathway for the regulated removal of the AICD, most likely via its IDE-mediated proteolysis.

### **3.10 Conclusion**

The results presented in this chapter show that when AICD-like fragments of APP are generated in a rabbit reticulocyte translation system they can be rapidly degraded. For this reason, my subsequent analysis of *in vitro*  $\gamma$ -secretase activity focussed on the N-terminal A $\beta$ -like products, which should be released into the ER lumen and therefore protected from degradation by cytosolic factors such as IDE. Where appropriate, I also incorporated the use of the metalloproteinase inhibitor PNT in my cell-free system in order to try and stabilise any AICD-like fragments that were produced.

## **CHAPTER 4**

.....

### **Results:**

#### **Generation of N-terminal fragments of APP**

## 4 Generation of N-terminal fragments of APP

In the previous chapter, the potential for the  $\gamma$ -secretase-like processing of a minimal  $\gamma$ -secretase substrate, CT72, was explored using an *in vitro* system supplemented with canine pancreatic microsomes. However, I found no evidence for  $\gamma$ -secretase cleavage of this construct using this system.

There are several potential explanations for the lack of processing observed with this *in vitro* system. One possibility is that the rapid degradation of any AICD-like fragments prevented their detection. I therefore investigated whether it was possible to detect the potentially more stable, N-terminal fragments of APP-C99 resulting from  $\gamma$ -secretase processing.

### 4.1 Analysis of N-terminally tagged APP derivatives for $\gamma$ -secretase processing

Since the data presented in chapter 3 showed that the C-terminal fragments likely to be generated as a result of  $\gamma$ -secretase processing are potentially unstable even *in vitro*, APP-C99 derivatives were generated with an N-terminal HA-epitope tag, ss-<sup>HA-Gly</sup>CT99, to facilitate the identification of any N-terminal cleavage products. Whilst the cleavage of full-length APP by either the  $\alpha$ - or  $\beta$ -secretase is a prerequisite for  $\gamma$ -secretase processing (see Introduction, section 1.8), the derivatives used here are based upon the product of the  $\beta$ -secretase cleavage and should therefore be direct substrates for the  $\gamma$ -secretase. Thus, ss-<sup>HA-Gly</sup>CT99 has the 30 residue cleavable signal sequence from preprolactin to allow efficient targeting (Kraft, 2001) followed by an HA epitope tag, a consensus N-glycosylation site and the complete APP-C99 sequence (Fig 4.1A). This precursor is 144 residues in length, but should generate a mature protein of 114 residues after authentic integration at the ER membrane and the cleavage of the N-terminal signal sequence. In order to facilitate the detection of any  $\gamma$ -secretase cleavage events, the putative N-terminal product of ss-<sup>HA-Gly</sup>CT99 processing, ss-<sup>HA-Gly</sup>CT42, was also generated to act as an internal reference for SDS-PAGE detection (Fig 4.1B).

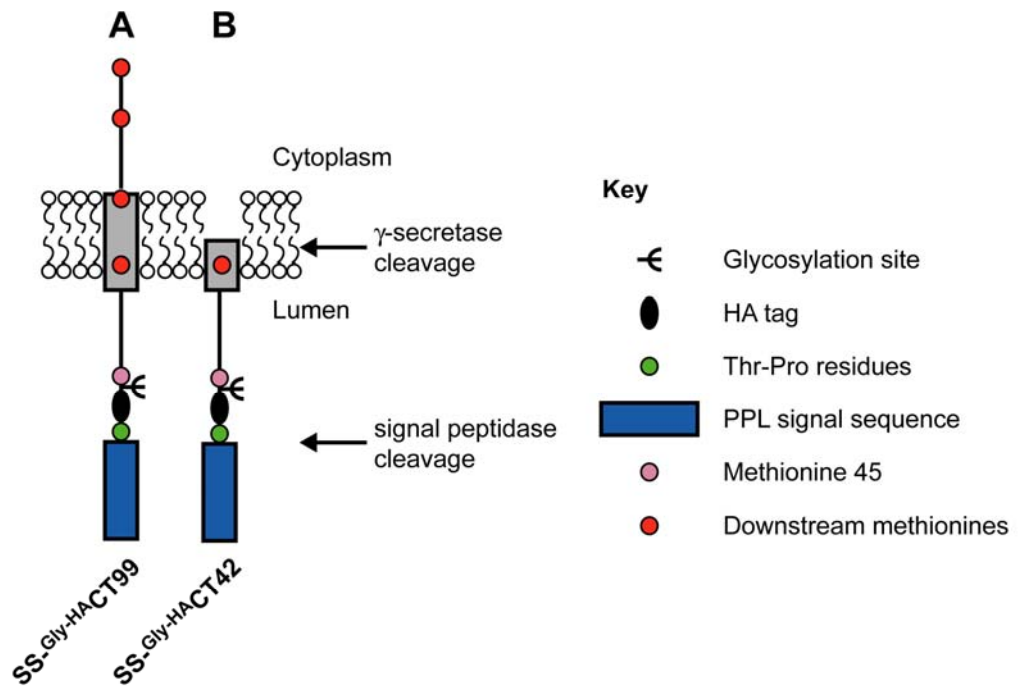


Fig 4.1. HA-tagged APP-derivatives used to investigate *in vitro* processing.

Pre-prolactin signal sequences shown as blue rectangles, additional Thr-Pro residues from mature prolactin are shown as green circles, potential *N*-glycosylation sites are shown as Ψ, transmembrane domains are shown as grey rectangles, approximate positions of downstream methionine residues are indicated by red circles or a pink circle (Met-45), additional APP-derived sequence are shown as black lines,  $\gamma$ -secretase and signal peptidase cleavage sites are indicated by black arrows.

Authentic  $\gamma$ -secretase cleavage is a membrane-dependent process, and requires that the substrate be correctly targeted to, and inserted into, the ER membrane. To establish whether this was the case for the ss<sup>HA-Gly</sup>CT99 derivative, translation products were assessed for membrane insertion by looking at their *N*-glycosylation status. *N*-glycosylation occurs in the ER lumen, and therefore proteins can only be *N*-glycosylated if they have been integrated into the ER membrane. The ss<sup>HA-Gly</sup>CT99 was translated in the presence and absence of microsomes, and translation products were immunoprecipitated with antisera specific for either the C-terminus of APP or the N-terminal HA-epitope tag (Fig 4.2).

In the presence of membranes, a clear increase in a significant fraction of the precursor's apparent size was observed, consistent with the acquisition of *N*-linked glycans (Fig 4.2, compare lanes 1 and 2 with lanes 3 and 4, products indicated by arrowheads). In addition to the full-length ss<sup>HA-Gly</sup>CT99 and *N*-glycosylated forms, there were also a number of lower molecular weight products observed (cf. Fig 4.2). The largest of these products (Fig 4.2, cf. black triangle) has a molecular

weight too large to be a result of  $\gamma$ -secretase processing and is probably due to alternative initiation from the methionine at 45 residues downstream of the start-codon (cf. Fig 4.1C). Any N-terminal products generated by  $\gamma$ -secretase processing of ss-<sup>HA-Gly</sup>CT99 should be membrane-dependent and recognised by the HA-specific antisera, but would not contain the  $\alpha$ APP<sub>680-695</sub> epitope, since this would have been removed following cleavage. Therefore, of particular interest is the membrane-dependent product observed after immunoprecipitation with the HA-specific antisera, but not the antisera that recognises the C-terminus of APP (Fig 4.2, compare lanes 3 and 4, see asterisk). The product observed in lane 4 that appears to interact with the  $\alpha$ HA antisera cannot be due to alternative initiation from Met-45, since such a product would not contain the HA epitope tag. Rather, this product is believed to be caused by the presence of cold light chain.

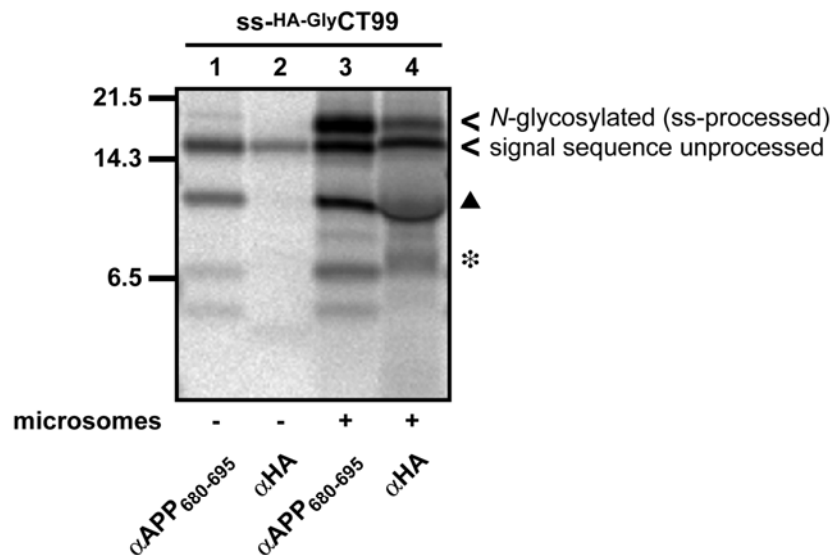


Fig 4.2. **Membrane integration of ss-HA-GlyCT99.**

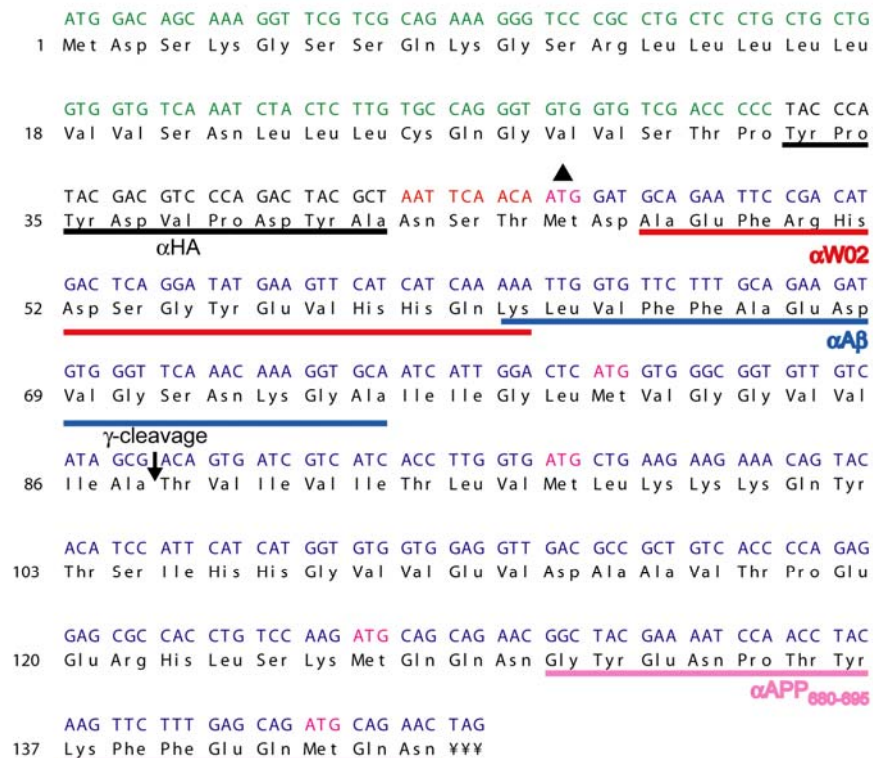
ss-HA-GlyCT99 was translated in rabbit reticulocyte lysate in the presence or absence of canine pancreatic microsomes (where indicated) for 30 minutes at 30°C. Translation initiation was then inhibited by the addition of ATCA. Products were immunoprecipitated with antisera specific for either the C-terminus of APP ( $\alpha$ APP<sub>680-695</sub>) or the HA epitope ( $\alpha$ HA) prior to analysis by SDS-PAGE. A product proposed to be the result of alternative initiation from Met-45 is shown by a filled triangle. A potential N-terminal product of  $\gamma$ -secretase processing is indicated by an asterisk. The product observed in lane 4 that has a similar mobility to the product indicated by a filled triangle is most likely the result of cold light chain affecting the background signal.

## 4.2 Characterisation of ss<sup>HA-Gly</sup>CT42-like product

To further characterise the lower molecular weight products generated with ss<sup>HA-Gly</sup>CT99, ss<sup>HA-Gly</sup>CT99 was translated next to the putative product of its  $\gamma$ -secretase cleavage, ss<sup>HA-Gly</sup>CT42, using a rabbit reticulocyte lysate system supplemented with membranes (cf. Fig 4.4A) and products were immunoprecipitated with a variety of different antisera (for epitopes, see Fig 4.3). A new derivative, ss<sup>HA-Gly</sup>CT99 M45C, was also generated, in which the methionine at residue 45 was altered to a cysteine by site-directed mutagenesis in order to prevent any alternative initiation from this point. Transcripts of ss<sup>HA-Gly</sup>CT99 M45C were also translated in reticulocyte lysate in the presence of membranes (Fig 4.4B).

Fig 4.3. Anti-sera epitopes.

Diagrammatic representation of ss<sup>HA-Gly</sup>CT99 indicating the epitopes (underlined regions) recognised by various anti-sera used throughout this chapter. Methionine codons are shown in pink (Met-45 is indicated by a filled triangle), the pre-prolactin signal sequence is shown in green, the HA-epitope tag sequence is shown in black, an *N*-glycosylation consensus sequence is shown in red, the APP-derived sequence is shown in blue.



Three major products were observed with the ss<sup>HA-Gly</sup>CT42 derivative (Fig 4.4A, cf. lanes 1-6), one of which had a similar mobility to one of the lower molecular weight products seen with ss<sup>HA-Gly</sup>CT99 (Fig 4.4A, products indicated by asterisks). Interestingly, this product is also immunoprecipitated with the  $\alpha$ A $\beta$  and  $\alpha$ WO2 antisera, which recognise epitopes within the N-terminal region of the APP-C99 fragment (see Fig 4.3). The upper band observed with ss<sup>HA-Gly</sup>CT42 (Fig 4.4A, lanes 1-4, indicated by an open square) is believed to be the glycosylated product due to its diffuse nature, whereas the major ss<sup>HA-Gly</sup>CT42 product (indicated by an asterisk in Fig 4.4A, lanes 1-4) is thought to be signal sequence unprocessed ss<sup>HA-Gly</sup>CT42, which was later confirmed (cf. Fig 4.5).

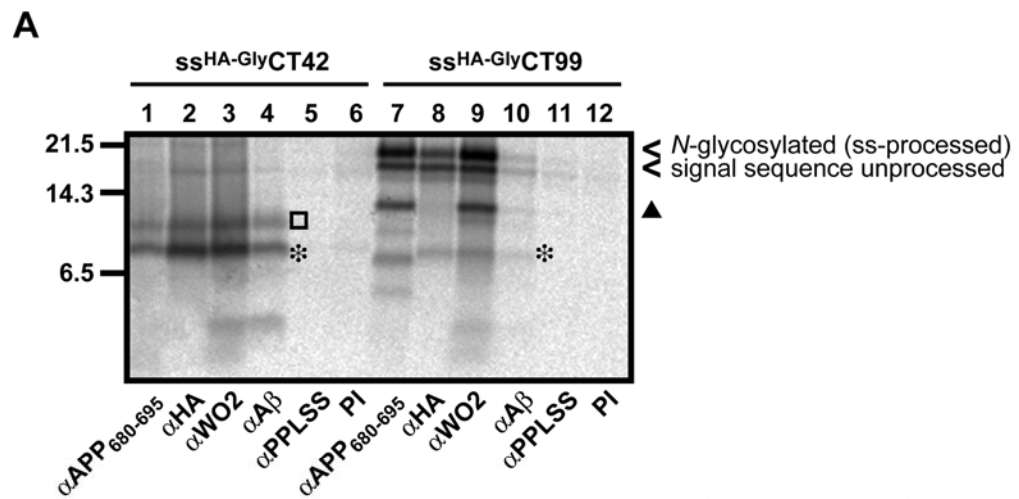
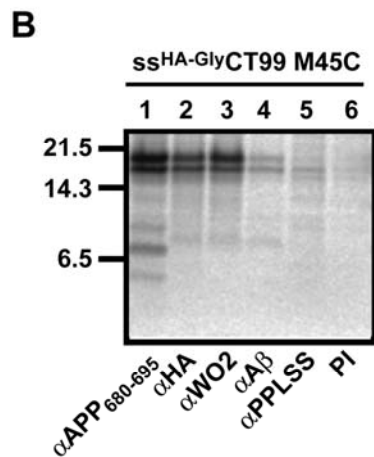


Fig 4.4. Characterisation of lower molecular weight products generated with ss<sup>HA-Gly</sup>CT99.



(A) [<sup>35</sup>S]-labelled ss<sup>HA-Gly</sup>CT99 and ss<sup>HA-Gly</sup>CT42 were synthesised in rabbit reticulocyte lysate in the presence of canine pancreatic microsomes for 30 minutes at 30°C. Products were immunoprecipitated with the antisera indicated (for epitopes, see Fig 4.3; PI refers to a pre-immune serum), and samples were analysed directly by SDS-PAGE. A product proposed to be the result of alternative initiation from Met-45 is shown by a filled triangle. A potential N-terminal product of  $\gamma$ -secretase processing is indicated by an asterisk. The product observed in lane 8 that has a similar mobility to this product is believed to be the result of alternative initiation. A product proposed to be glycosylated ss<sup>HA-Gly</sup>CT42 is indicated by an open square.

(B) ss<sup>HA-Gly</sup>CT99 M45C was synthesised as in (A). Samples were immunoprecipitated with the antisera indicated prior to analysis by SDS-PAGE.

Five major products were observed with ss<sup>HA-Gly</sup>CT99 (Fig 4.4A, cf. lane 7), but when Met-45 was mutated to a cysteine, the product with an apparent molecular

weight of approximately 14kDa was lost (Fig 4.4, compare panel A lane 7 with panel B lane 1, fragment indicated by a black triangle), suggesting that this product was indeed a result of alternative initiation.

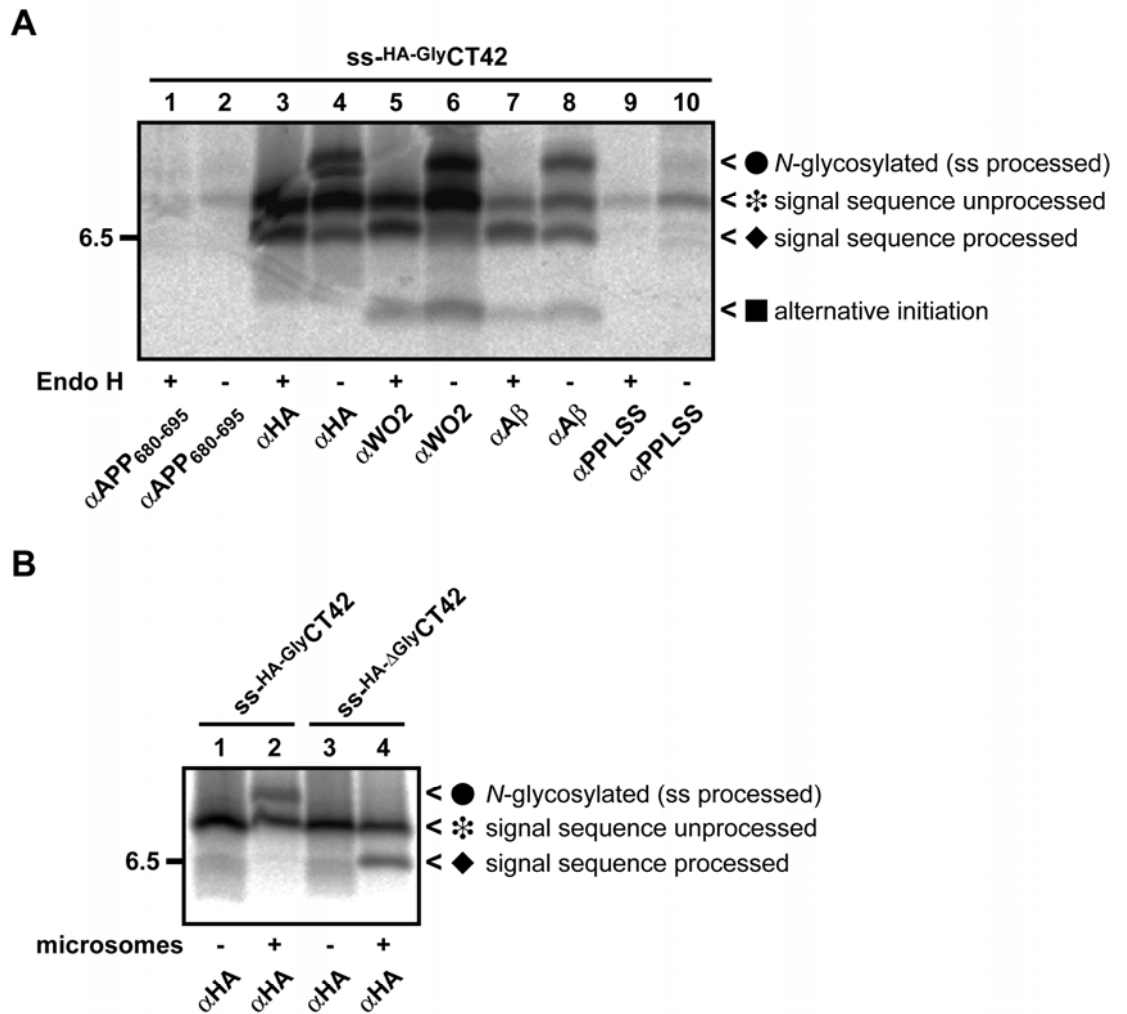


Fig 4.5. Characterisation of ss-HA-GlyCT42.

(A) ss-HA-GlyCT42 was synthesised in rabbit reticulocyte lysate in the presence of canine pancreatic microsomes for 30 minutes at 30°C. Products were immunoprecipitated with the antisera indicated, and samples were either analysed directly by SDS-PAGE (even lanes) or first treated with endoglycosidase H (odd lanes). Black arrowheads indicate the major products generated.

(B) ss-HA-GlyCT42 and ss-HA- $\Delta$ GlyCT42 were synthesised as in (A) in the presence or absence of microsomal membranes. Samples were immunoprecipitated with  $\alpha$ HA antisera prior to analysis by SDS-PAGE. Black arrowheads indicate the major products generated.

In order to further characterise the lower molecular weight products generated with ss-HA-GlyCT42, samples were immunoprecipitated with a number of different antisera and treated with EndoH to assess their glycosylation status (Fig 4.5A). Four major products were observed, depending on the presence of EndoH and the antiserum used. These were identified to correspond, in descending order of size, to the N-glycosylated form (Fig 4.5A, cf. filled circle), the signal sequence un-

processed form (Fig 4.5A, cf. asterisk), signal sequence processed non-glycosylated form (Fig 4.5A, cf. diamond), and a low molecular weight product resulting from alternative initiation at Met-45 (Fig 4.5A, cf. filled square). This assignment was further confirmed by the generation of a glycosylation mutant of  $ss\text{-}^{\text{HA-Gly}}\text{CT42}$ ,  $ss\text{-}^{\text{HA-}\Delta\text{Gly}}\text{CT42}$ , by site directed mutagenesis (see Materials and Methods). Translation of  $ss\text{-}^{\text{HA-}\Delta\text{Gly}}\text{CT42}$  abolished the upper band (Fig 4.5B, cf. filled circle), but had no effect on the presence of the signal sequence unprocessed and signal sequence processed non-glycosylated forms (Fig 4.5B, cf. asterisk and diamond). It appeared from its relative mobility that the signal sequence un-processed, non-glycosylated, form of  $ss\text{-}^{\text{HA-Gly}}\text{CT42}$  (Fig 4.5A and B, cf. asterisk) was most likely to correspond to the  $ss\text{-}^{\text{HA-Gly}}\text{CT42}$ -like product observed with  $ss\text{-}^{\text{HA-Gly}}\text{CT99}$ . One additional method that could have aided identification of the products would have been to use protease protection. This would have determined whether the signal sequenced unprocessed form of  $ss\text{-}^{\text{HA-Gly}}\text{CT42}$  had been imported into the microsomes, and therefore whether it was a potential  $\gamma$ -secretase product.

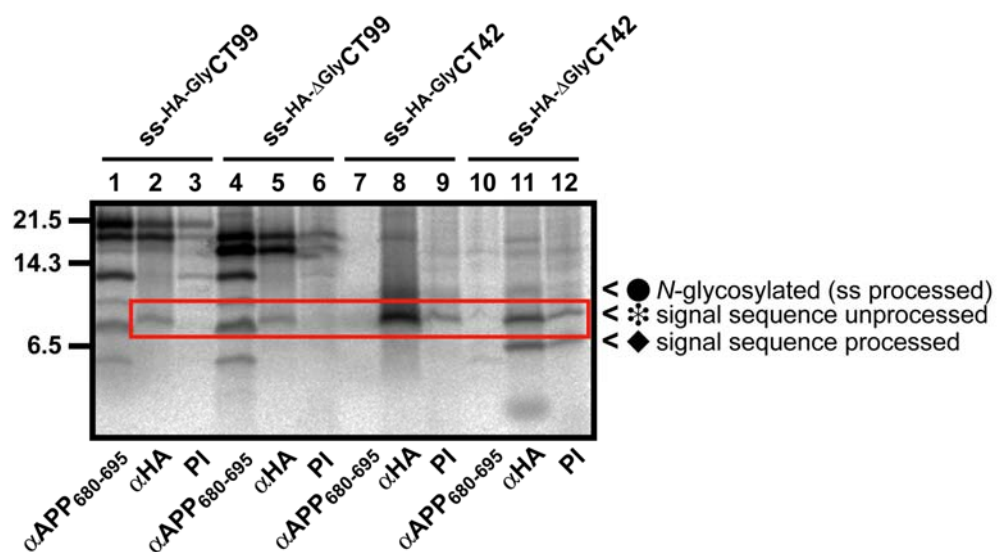


Fig 4.6. **Generation of a  $ss\text{-}^{\text{HA-Gly}}\text{CT42}$ -like product from  $ss\text{-}^{\text{HA-Gly}}\text{CT99}$ .**

$ss\text{-}^{\text{HA-Gly}}\text{CT99}$ ,  $ss\text{-}^{\text{HA-Gly}}\text{CT42}$  and the glycosylation mutants  $ss\text{-}^{\text{HA-}\Delta\text{Gly}}\text{CT99}$  and  $ss\text{-}^{\text{HA-}\Delta\text{Gly}}\text{CT42}$  were synthesised in rabbit reticulocyte lysate in the presence of canine pancreatic microsomes for 30 minutes at 30°C. Products were immunoprecipitated with the antisera indicated, and samples were analysed directly by SDS-PAGE. Products likely to be derivatives of  $ss\text{-}^{\text{HA-Gly}}\text{CT42}$  are indicated by black arrows, and the red box contains products of the correct molecular weight to correspond to signal sequence unprocessed  $ss\text{-}^{\text{HA-Gly}}\text{CT42}$ . The presence of bands in the pre-immune sera lanes is most likely due to spill-over from adjacent lanes.

To further establish the identity of the fragments observed with ss-<sup>HA-Gly</sup>CT99, it was translated alongside ss-<sup>HA-Gly</sup>CT42 and their corresponding glycosylation mutants, ss-<sup>HA-ΔGly</sup>CT99 and ss-<sup>HA-ΔGly</sup>CT42 respectively (Fig 4.6). The ss-<sup>HA-Gly</sup>CT42-like product observed with ss-<sup>HA-Gly</sup>CT99 was unaffected by the mutation in the glycosylation site (Fig 4.6, compare lanes 2 and 5) and had a similar mobility to the signal sequence un-processed form of ss-<sup>HA-Gly</sup>CT42 (Fig 4.6, bands within red box).

### **4.3 Effect of inhibitors on generation of the ss-<sup>HA-Gly</sup>CT42-like product**

Taken together, the data outlined above suggested that the ss-<sup>HA-Gly</sup>CT42-like lower molecular weight product observed with ss-<sup>HA-Gly</sup>CT99 could result from  $\gamma$ -secretase processing. However, since authentic  $\gamma$ -secretase processing is a membrane-dependent process, it was unclear why a product generated as the result of such a cleavage event would not be *N*-glycosylated. However, no evidence of a product analogous to *N*-glycosylated ss-<sup>HA-Gly</sup>CT42 was observed with the ss-<sup>HA-Gly</sup>CT99 polypeptide during any of the work presented in this chapter (cf. Figs 4.2 and 4.4). Therefore, in order to investigate whether the ss-<sup>HA-Gly</sup>CT42-like product observed with ss-<sup>HA-Gly</sup>CT99 was generated by  $\gamma$ -secretase processing, I explored the effect of adding different concentrations of a  $\gamma$ -secretase inhibitor, inhibitor-X (L-685,458) upon its production. L-685,458 has previously been shown efficiently inhibit  $\gamma$ -secretase cleavage (Shearman et al., 2000). An inhibitor of the signal peptidase, N-methylsuccinyl-ala-ala-pro-val-chloromethyl ketone, was also added for comparison (Nilsson and von Heijne, 2000). No significant effect on the levels of the ss-<sup>HA-Gly</sup>CT42-like product was observed with any of the concentrations of  $\gamma$ -secretase inhibitor-X tested, or with the signal peptidase inhibitor (Fig 4.7, cf. asterisk). However, on addition of either the signal peptidase inhibitor or inhibitor-X at 100nM, a previously unobserved product with an apparent molecular weight of ~12kDa (Fig 4.7, cf. lanes 2 and 5, open circle) appeared. Although this product has a similar mobility to the product of alternative initiation from Met-45 (Figs 4.2 and 4.4, cf. filled triangle), it is distinguished from this fragment by the presence of the HA-epitope (Fig 4.4, cf. lanes 7 and 8, filled triangle). This product appears too large to be the result of an inhibition of  $\gamma$ -secretase processing (Fig 4.7, cf. lanes 2, 5 and 6) and its appearance upon

treatment with two different inhibitors suggests it arises from the inhibition of an undefined proteolytic pathway that occurs *in vitro*.

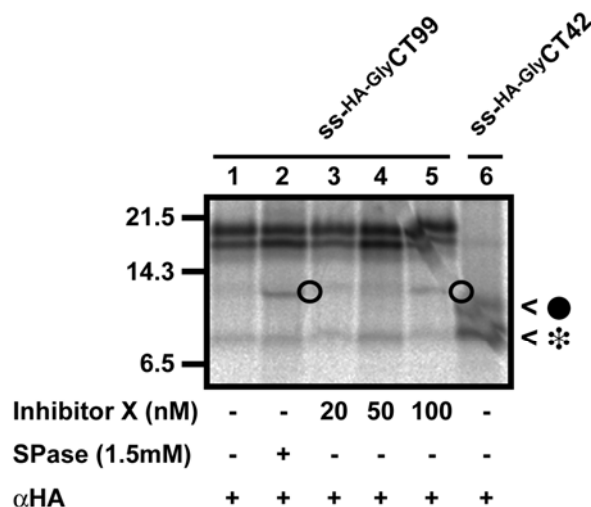


Fig 4.7. Effect of inhibitors on the presence of the ss-HA-GlyCT42-like product generated with ss-HA-GlyCT99.

ss-HA-GlyCT99 and ss-HA-GlyCT42 were synthesised in rabbit reticulocyte lysate in the presence of canine pancreatic microsomes and the appropriate inhibitor (indicated above) for 30 minutes at 30°C. Products were immunoprecipitated with  $\alpha$ HA antisera, and samples were analysed directly by SDS-PAGE. The position of the ss-HA-GlyCT42-like product is indicated by an asterisk (signal sequence unprocessed). N-glycosylated, signal-sequence processed ss-HA-GlyCT42 is indicated by a filled circle. The position of an unknown product is indicated by open circles.

#### 4.4 Summary

The aim of the work presented in this chapter was to explore whether  $\gamma$ -secretase cleavage could be observed in an *in vitro* system by using two N-terminally HA-tagged derivatives of APP, ss-HA-GlyCT99 and ss-HA-GlyCT42. Having established that the ss-HA-GlyCT99 derivative was integrated into the ER membrane, I went on to look for evidence of  $\gamma$ -secretase processing of the polypeptide using an *in vitro* translation system supplemented with canine pancreatic microsomes. Whilst a lower molecular weight product was generated with ss-HA-GlyCT99 that had a similar mobility to one of the fragments observed upon the synthesis of the putative  $\gamma$ -secretase product, ss-HA-GlyCT42, this fragment was not N-glycosylated, nor was its signal peptide cleaved, suggesting that it was produced prior to the

membrane integration of ss-<sup>HA-Gly</sup>CT99. Furthermore, the ss-<sup>HA-Gly</sup>CT42-like product was unaffected by the inclusion of a potent  $\gamma$ -secretase inhibitor, inhibitor-X. Taken together, these data suggest that the lower molecular weight product observed was not a result of *in vitro* cleavage by the  $\gamma$ -secretase.

#### **4.5 Conclusion**

The data presented in this chapter indicate that whilst lower molecular weight fragments derived from model APP-based polypeptides are generated in an *in vitro* system supplemented with canine pancreatic microsomes, these fragments are not a result of  $\gamma$ -secretase processing. This might be because the cellular components required for such processing are located in compartments “downstream” of the ER and are therefore unavailable in the microsome-based system that was used. For this reason, my subsequent analysis of *in vitro*  $\gamma$ -secretase activity focussed upon potential strategies to manipulate my *in vitro* system so as to allow any such factors to come into contact with the model APP-C99 derivatives used during this study.

## CHAPTER 5

---

**Results:**

**Investigating the *in vitro* processing of APP**

## 5 Investigating the *in vitro* processing of APP

In the previous chapters, the potential for the  $\gamma$ -secretase-like processing of APP derivatives was explored using an *in vitro* system supplemented with canine pancreatic microsomes. However, I found no evidence for the processing of a minimal  $\gamma$ -secretase substrate, CT72, or an N-terminally tagged derivative of C99, ss-<sup>HA-Gly</sup>CT99, using this system.

One potential explanation for the lack of  $\gamma$ -secretase cleavage observed in my microsomal system might be that the cellular components required for such processing are located in compartments “downstream” of the ER and are therefore unavailable in a microsome-based system such as that used. I therefore investigated whether it was possible to manipulate the *in vitro* system so as to favour  $\gamma$ -secretase processing.

### 5.1 APP-derived model substrates

In the course of this work, four derivatives of APP that all preserved the transmembrane domain  $\gamma$ -secretase cleavage site, were used to study *in vitro* processing (Fig 5.1). Whilst the cleavage of full-length APP by either the  $\alpha$ - or  $\beta$ -secretase is a prerequisite for  $\gamma$ -secretase processing (see Introduction, section 1.8), the derivatives used here are all based upon the product of the  $\beta$ -secretase cleavage and should therefore be direct substrates for the  $\gamma$ -secretase. CT72 (Chapter 3) and ss-<sup>HA-Gly</sup>CT99 (Chapter 4) are as previously described. In order to facilitate the detection of any  $\gamma$ -secretase cleavage events, the putative N-terminal product of ss-<sup>HA-Gly</sup>CT99 processing, ss-<sup>HA-Gly</sup>CT42 (Chapter 4), was also used as an internal reference. <sup>Met</sup>CT99 (100aa) represents a natural  $\gamma$ -secretase substrate, C99, with an additional methionine residue to allow the initiation of polypeptide synthesis (Fig 5.1B).

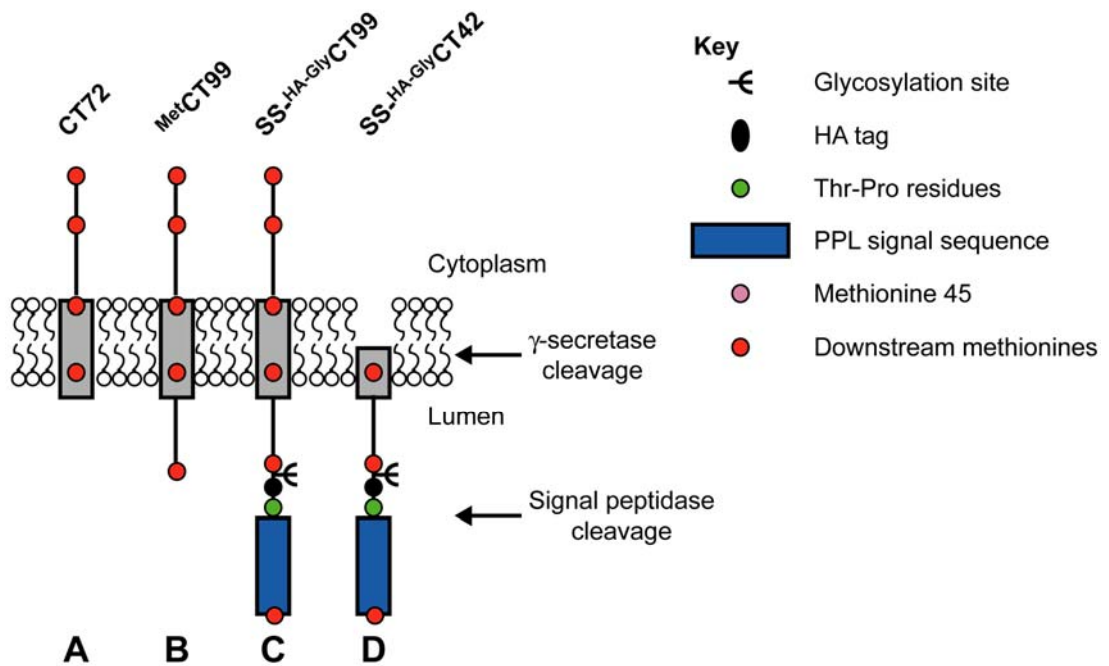


Fig 5.1. **APP-derivative constructs used to investigate *in vitro* processing.**

Pre-prolactin signal sequences are shown as blue rectangles, additional Thr-Pro residues are shown as green circles, *N*-glycosylation sites are shown as  $\Psi$ , transmembrane domains are shown as grey rectangles, approximate positions of methionine residues are indicated by red circles, additional APP-derived sequence are shown as black lines,  $\gamma$ -secretase and signal peptidase cleavage sites are indicated by black arrows.

## 5.2 Membrane-dependent processing *in vitro*

In chapters 3 and 4, canine pancreatic microsomes were used as a source of ER-derived membranes to study APP processing. In order to investigate processing in a system that more closely resembles the *in vivo* situation, I exploited semi-intact mammalian cells (Wilson et al., 1995) during the course of the work presented in this chapter. Since I had found AICD-like fragments can be highly unstable in reticulocyte lysate (see Chapter 3), PNT was included during experiments designed to detect C-terminal polypeptides of APP in order to stabilise these fragments. To further facilitate the detection of potential  $\gamma$ -secretase processing products, I also exploited a ss-<sup>HA-Gly</sup>CT99 derivative that would allow the identification of any N-terminal cleavage products via an HA-epitope tag (see Chapter 4).

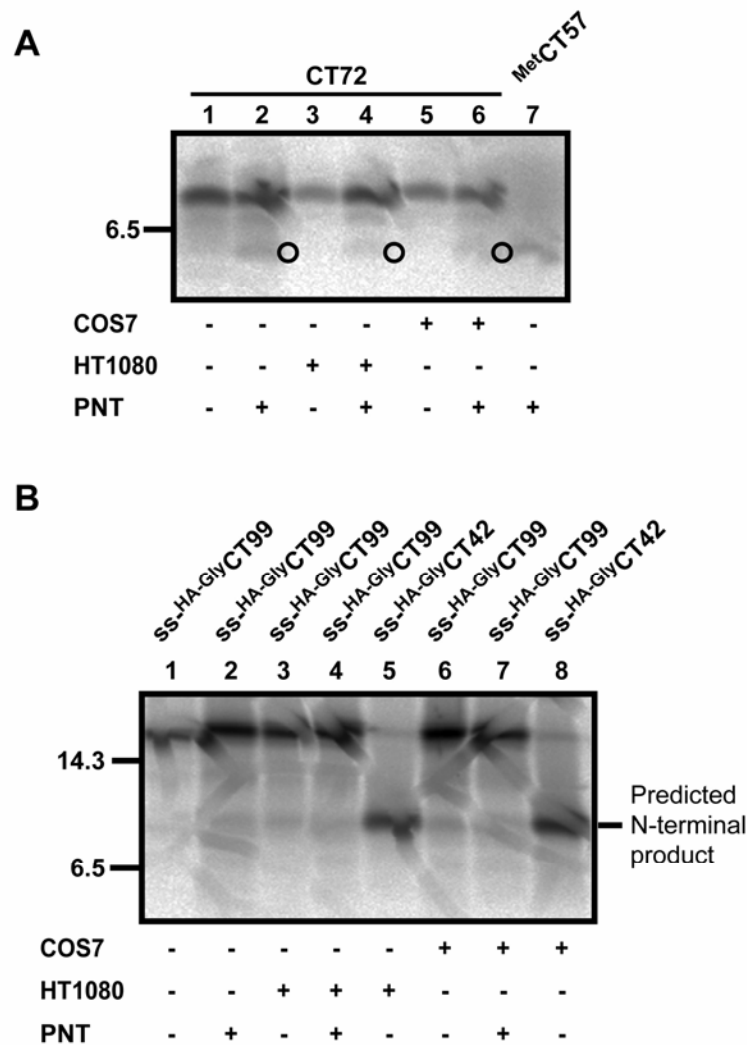


Fig 5.2. Processing of APP-derivatives using semi-intact cells.

CT72 or ss-HA-GlyCT99 were synthesised in the presence of semi-intact COS7 or HT1080 cells, or in the absence of membranes for 15 minutes at 30°C. 5mM PNT was included in the reaction where indicated. Products immunoprecipitated by  $\alpha$ APP (CT72) or  $\alpha$ HA (ss-HA-GlyCT99) were separated by SDS-PAGE and analysed for the presence of lower molecular weight products that might be a result of  $\gamma$ -secretase cleavage.

The results obtained when CT72 was synthesised in the presence of semi-intact mammalian cells were similar to those obtained in microsomes (see Chapter 3); lower molecular weight products were observed in the presence of PNT that had a similar mobility to <sup>Met</sup>CT57 (Fig 5.2A, cf. lanes 4 and 6, open circles), but this product was seen in the absence of membranes (Fig 5.2A, cf. lane 2) and proved to be the result of alternative initiation (data not shown). No evidence for the processing of ss-HA-GlyCT99 was observed in this system (Fig 5.2B, cf. lanes 2, 4

and 7), and I concluded that detectable  $\gamma$ -secretase processing could not be achieved simply by using semi-intact mammalian cells in place of canine pancreatic microsomes.

### **5.3 PEG-mediated membrane fusion**

Several *in vivo* studies using mammalian expression systems have suggested that the  $\gamma$ -secretase-dependent cleavage of APP occurs in a post-ER location within the secretory pathway (Cupers et al., 2001a). However, whilst canine pancreatic microsomes and semi-intact cells are good sources of ER-derived membranes for *in vitro* studies and allow reconstitution of the early secretory pathway, there is no evidence that the inserted proteins have ready access to any post-ER compartments (Plutner et al., 1991; Wilson et al., 1995). It was therefore possible that even in the semi-intact cell system used above, APP-derivatives were unable to gain access to the appropriate membrane system necessary for  $\gamma$ -secretase-mediated cleavage. In order to test this hypothesis further, I first investigated whether the non-specific fusion of different membrane compartments was able to promote processing *in vitro*. Polyethylene glycol (PEG) has previously been shown to facilitate membrane fusion *in vitro* (Lentz and Lee, 1999), and I tested its ability to promote the processing of APP derivatives. Since I was looking for stable N-terminal fragments generated as a result of  $\gamma$ -secretase processing, these experiments were performed in the absence of PNT in case the removal of divalent cations may affect membrane fusion in some way.

The ss-<sup>HA-Gly</sup>CT99 polypeptide was synthesised in the presence of digitonin permeabilised COS7 or HT1080 cells. The membrane fraction was then isolated and incubated with two concentrations of PEG to establish whether this resulted in any additional ss-<sup>HA-Gly</sup>CT99 derived fragments. This analysis showed that the addition of PEG to the two different semi-intact cell lines had no major effect on the products observed (Fig 5.3, cf. lanes 1-3 and 4-6). Evidence of differences between the two systems was seen (Fig 5.3, cf. lanes 1 and 4, product indicated by arrow), but the additional fragment seen in COS7 cells did not require the addition of PEG. I therefore concluded that the use of PEG was not sufficient to enable the  $\gamma$ -secretase-dependent processing of ss-<sup>HA-Gly</sup>CT99.

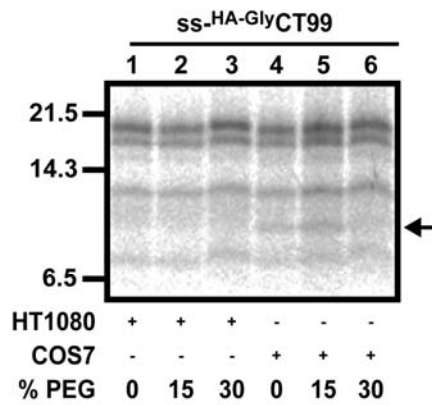


Fig 5.3. Effect of polyethylene glycol treatment of semi-intact cells on processing of APP-derivatives.

ss-HA-GlyCT99 was synthesised in the presence of semi-intact COS7 or HT1080 cells in the absence of PNT for 30 minutes at 30°C. The membrane fraction was isolated by centrifugation through a high salt cushion, as described in section 2.8. The membrane pellets were resuspended in KHM buffer and treated with 0, 15 or 30% PEG (W/V) for 5 minutes at 30°C as indicated. The membrane fraction was re-isolated as before and products were analysed by SDS-PAGE. The black arrow indicates a COS7 specific product.

The lack of any detectable  $\gamma$ -secretase activity upon PEG treatment may simply reflect a lack of membrane fusion under the conditions used. I therefore investigated whether the PEG treatments utilised were capable of fusing Golgi-derived compartments with the ER localised ss-HA-GlyCT99 present in semi-intact cells. It is well documented that *N*-linked glycans are modified in the Golgi such that they alter from being sensitive to digestion with Endo H and become resistant to such treatment (Maley et al., 1989). Thus, the acquisition of EndoH resistant glycans can be used as a measure for the access a glycoprotein has to the cis/medial Golgi where the appropriate glycosyltransferases reside (Maley et al., 1989). I therefore repeated the experiment outlined above, and analysed ss-HA-GlyCT99 for the ability of the *N*-linked glycan to be removed by EndoH. I found that in each case the behaviour of the ss-HA-GlyCT99 polypeptides made in semi-intact cells were essentially identical to that seen in microsomes, and that all of the glycosylated chains were EndoH sensitive (Fig 5.4, lanes 1-8).

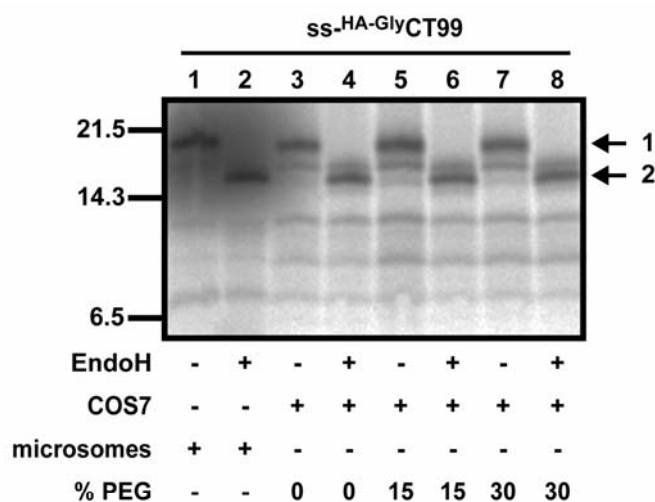


Fig 5.4. **Effect of polyethylene glycol treatment on N-linked glycans.**

ss-HA-GlyCT99 was synthesised in the presence of semi-intact COS7 cells or canine pancreatic microsomes in the absence of PNT for 30 minutes at 30°C. Microsomal samples were left untreated and were analysed directly by SDS-PAGE. The semi-intact cell membrane fraction was isolated by centrifugation through a high salt cushion, resuspended in KHM buffer, and treated with 0, 15 or 30% PEG (W/V) for 15 minutes at 30°C as indicated. The membrane fraction was re-isolated and either treated with EndoH for 2 hours at 37°C or left untreated as indicated. Products were analysed by SDS-PAGE. The black arrows indicate the full length <sup>HA</sup>-GlyCT99 (1) and deglycosylated <sup>HA</sup>-GlyCT99 (2).

Pre-incubation with PEG at two concentrations had no effect on the fraction of EndoH resistant material and almost complete digestion was observed in each case (Fig 5.4, lanes 4, 6 and 8). I therefore concluded that the PEG treatments were unsuccessful in promoting any detectable fusion between the ER and post-ER compartments.

#### 5.4 BFA-mediated compartment fusion

Whilst the use of PEG to promote membrane fusion is a relatively non-specific and poorly defined procedure, the use of the drug brefeldin A (BFA) to promote the mixing of the compartments in the secretory pathway is well established and the molecular basis for this effect is well defined (Fujiwara et al., 1988; Sciaky et al., 1997). Furthermore, in an *in vivo* expression system, the use of BFA allows the  $\gamma$ -secretase dependent cleavage of an ER-retained form of APP-C99 that is otherwise unprocessed (Cupers et al., 2001a). Since the effects of BFA require active vesicular transport between subcellular compartments (Sciaky et al., 1997),

growing cells were treated with BFA prior to being semi-permeabilised with digitonin. The resulting cells and control cells treated in parallel were then used for the membrane integration of ss-<sup>HA-Gly</sup>CT99 and subsequent incubation for potential processing by the  $\gamma$ -secretase. Although I was looking for stable N-terminal fragments of  $\gamma$ -secretase processing, these studies were performed in the presence of PNT to increase the likelihood of detecting any cleavage products. To aid the detection of N-terminal fragments of ss-<sup>HA-Gly</sup>CT99 that would result from such processing, the putative product, ss-<sup>HA-Gly</sup>CT42 was created by the introduction of a premature termination codon. ss-<sup>HA-Gly</sup>CT42 was then run alongside the ss-<sup>HA-Gly</sup>CT99 samples to provide an internal reference.

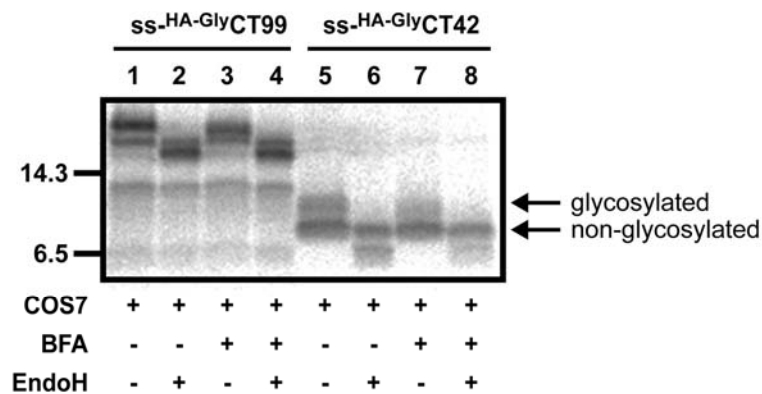


Fig 5.5. **Effect of brefeldin-A treatment of cells on processing of APP-derivatives.**

Prior to production of semi-intact cells, COS7 cells were treated with brefeldin-A or an equivalent volume of methanol (control) for 135 minutes at 37°C. Semi-intact cells were prepared as before, and ss-<sup>HA-Gly</sup>CT99 and ss-<sup>HA-Gly</sup>CT42 were synthesised in the presence of these cells for 30 minutes at 30°C with 5mM PNT included in the reaction. Samples were treated with ATCA before adding puromycin and EDTA. Samples were incubated for 2 hours at 37°C. Cells were pelleted by centrifugation and washed with KHM buffer. The cell pellets were resuspended in KHM buffer and either treated with EndoH for 2 hours at 37°C or left untreated as indicated. Products were analysed by SDS-PAGE.

In neither the presence nor the absence of BFA was an ss-<sup>HA-Gly</sup>CT42-like fragment seen with the ss-<sup>HA-Gly</sup>CT99 (Fig 5.5, lanes 1, 3, 5 and 7 with regards to position of ss-<sup>HA-Gly</sup>CT42/99 product). The effect of BFA treatment upon the EndoH sensitivity was also determined. There was some evidence that mannose trimming had occurred, which is suggestive of the Golgi having merged with the ER, as indicated by the slight decrease in mobility of the glycosylated species

following treatment of cells with BFA (Fig 5.5, compare the uppermost bands in lanes 1 and 3 and lanes 5 and 7). However, as with the PEG treatment, no obvious acquisition of Endo-H resistant glycans was seen upon BFA treatment for either the ss-<sup>HA-Gly</sup>CT99 substrate (Fig 5.5, cf. lanes 2 and 4) or its putative product (Fig 5.5, cf. lanes 6 and 8). Thus, despite its effects *in vivo* with regards to APP-processing (Cupers et al., 2001a), BFA treatment had only a limited effect on the *in vitro* system outlined above.

Given the lack of any detectable effect of BFA treatment upon the processing of *N*-linked glycans (Fig 5.5), it was possible that the BFA treatment had not worked as previously described (Cupers et al., 2001a). For this reason, immunofluorescence microscopy was used in an *in vivo* system to analyse the effects of BFA treatment upon COS7 cells, and in particular its effects upon the distribution of GM130, a marker for the *cis* Golgi. In the untreated cells, the GM130 staining (Fig 5.6, cf. panels B and D) had a juxtannuclear localisation, characteristic of the Golgi apparatus and quite distinct from the reticular ER staining seen for calreticulin (Fig 5.6, cf. panels A and C; see also merged image, panel E).

However, when cells were treated with BFA, the pattern of GM130 staining was altered, becoming more diffuse and reticular in appearance (Fig 5.6, cf. Panels G and I) and showing partial co-localisation with the calreticulin labelling (Fig 5.6, cf. panel J). The gross staining pattern for calreticulin appeared unchanged by BFA treatment (Fig 5.6, cf. panels C and H).

These results suggest that the BFA treatment of COS7 cells used during this study was successful and that proteins from the *cis* and medial Golgi compartments were redistributed to the ER as described previously (Cupers et al., 2001a; Sciaky et al., 1997). The lack of APP processing observed following BFA treatment suggests that the availability of Golgi proteins by BFA treatment is insufficient to allow  $\gamma$ -secretase processing. This implies that the appropriate compartment containing the factors required for  $\gamma$ -secretase activity is not delivered back to the ER following BFA treatment *in vitro* although it is in an *in vivo* system using primary neurones (Cupers et al., 2001a). The reconstitution of BFA-induced Golgi fusion has also previously been observed in semi-intact CHO cells permeabilised using streptolysin O (Kano et al., 2000).

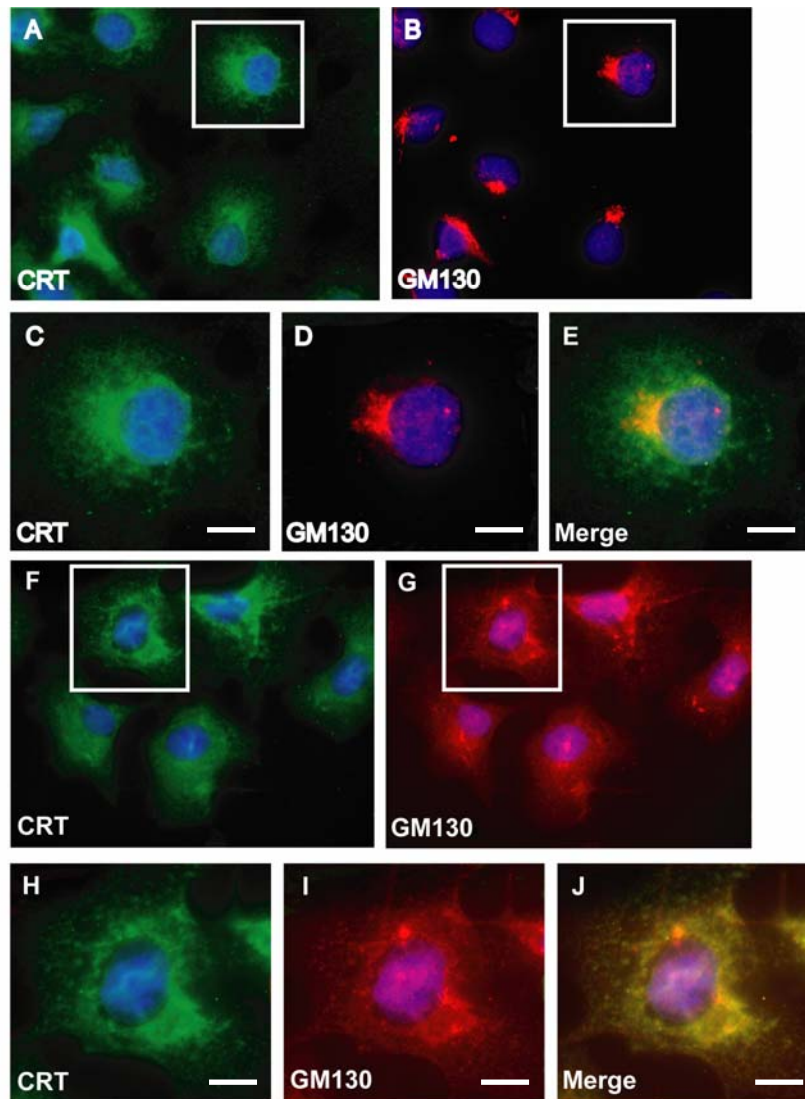


**Fig 5.6. Immunofluorescence microscopy experiments of the BFA-induced redistribution of Golgi proteins.**

Cos7 cells were grown on coverslips in either the absence (panels A-E) or presence (panels F-J) of BFA. Cells were fixed with methanol and incubated with rabbit anti-GM130 and sheep anti-calreticulin (CRT) antibodies as indicated, followed by TRITC-labelled anti-rabbit IgG and FITC-labelled anti-sheep IgG. In panels E and J, images C and D or H and I respectively are superimposed to create a merged image. Bars 10 $\mu$ m.

## **5.5 CHAPSO-solubilised crude membrane extract**

Since neither PEG nor BFA treatments had yielded  $\gamma$ -secretase processing, I tried using a CHAPSO-solubilised membrane preparation that had previously been shown to cleave an APP-derivative via its intrinsic  $\gamma$ -secretase activity (Li et al., 2000a; Weihofen et al., 2003). Since the cleavage of APP by  $\alpha$ - or  $\beta$ -secretase is a prerequisite for  $\gamma$ -secretase processing, I used the CT72 construct in my initial assays as it contains only the transmembrane region and the C-terminus of APP and would not require a prior cleavage event. Given the lability of the AICD fragment of APP on its release into the cytosol (see Chapter 3), these experiments were performed in the presence of PNT, which I have shown to stabilise the AICD (see Chapter 3).

No lower molecular weight products were observed when the CT72 product was incubated with the solubilised membrane extract and both the total products (Fig 5.7, cf. panel A) and C-terminal fragments (Fig 5.7, cf. panel B) were analysed. In case the lack of processing observed was due to the presence of the reticulocyte lysate translation system, the experiment was repeated using stop codon-minus mRNA transcripts of CT72 to generate ribosome-nascent chain complexes. These RNCs were then isolated by centrifugation (cf. section 3.7 and Fig 3.11), the ribosome-trapped polypeptides were released by the addition of puromycin, and the solubilised membrane extract added. Despite this additional purification step, no extract-dependent processing of CT72 was seen (Fig 5.7, cf. panels C and D). In this case a doublet of fragments was seen in all cases (Fig 5.7, cf. panels C and D, arrows), but the smaller product is most likely due to alternative initiation or could potentially be a degradation product of the CT72 protein.

A CHAPSO-solubilised membrane extract has recently been used recently to show the  $\gamma$ -secretase cleavage of a met-C99 construct (Weihofen et al., 2003). I therefore repeated the analysis of my own solubilised membrane extract using an identical <sup>Met</sup>C99 substrate (see Fig 5.1). As with the CT72 studies, <sup>Met</sup>C99 was translated in a rabbit reticulocyte lysate system in the absence of membranes and the resulting products were used in a  $\gamma$ -secretase processing assay containing either solubilised membrane extract or 1% detergent as a control (Fig 5.8). PNT

was included in the reactions in order to stabilise any potential processing products.

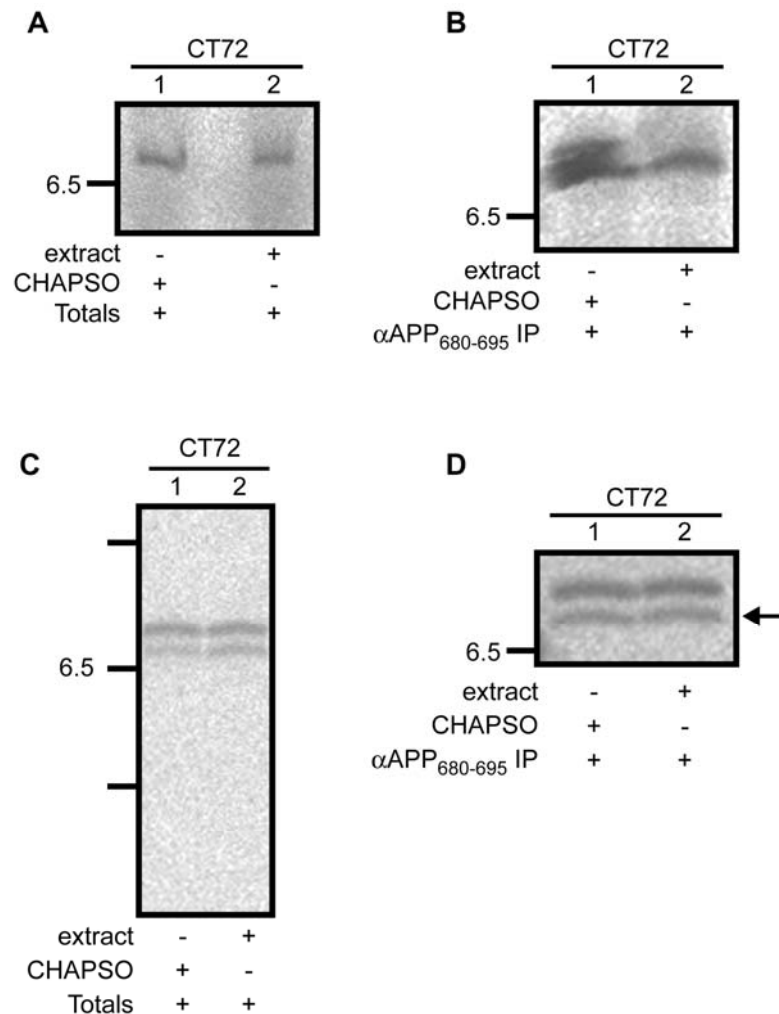
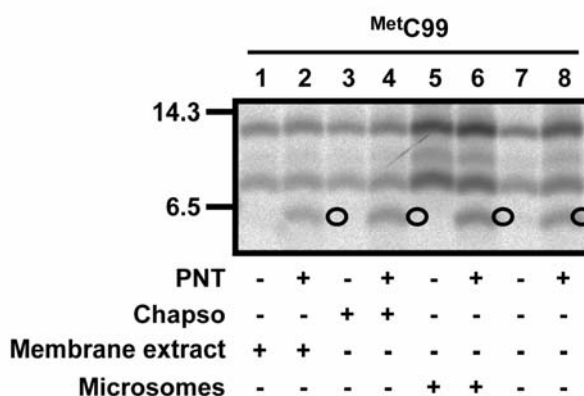


Fig 5.7. *In vitro*  $\gamma$ -secretase assay.

CT72 was synthesised using rabbit reticulocyte lysate in the absence of membranes for 30 minutes at 30°C. Initiation of translation was inhibited by addition of ATCA for 10 minutes at 30°C. Translation products were either used directly in the assay (panels A and B), or ribosome-nascent chain complexes were first isolated by centrifugation prior to setting up the assay (panels C and D). Buffer, PNT and either CHAPSO-solubilised membrane extract (extract) or 1% CHAPSO (as indicated) were added to the CT72 products and the mixture was incubated at 30°C for 1 hour. 20% of the mixture was removed and TCA precipitated (totals; panels A and C). The remaining samples were immunoprecipitated with  $\alpha$ APP<sub>680-695</sub> antisera ( $\alpha$ APP<sub>680-695</sub> IP; panels B and D). Both total products and immunoprecipitated samples were then analysed by SDS-PAGE. A lower molecular weight product observed in panels C and D is indicated (arrows).

As a further control, <sup>Met</sup>C99 was also synthesised in the presence of microsomal membranes to establish that the products observed resulted directly from the translation of its encoding mRNA. In all cases, lower molecular weight products

were observed in the presence of PNT (Fig 5.8, cf. lanes 2 ,4, 6, 8, open circles). These C-terminal fragments were not dependent on the inclusion of solubilised membrane extract, and were still observed even in the absence of any added membranes (Fig 5.8, cf. lanes 7 and 8). This product is most likely the result of alternative initiation from one of the methionine residues downstream of the initiation codon, and not to processing by the  $\gamma$ -secretase (cf. Figs 5.1 and 5.2).



**Fig 5.8. C-terminal fragments generated with MetC99 are not dependent on the presence of the CHAPSO-solubilised membrane extract.**

MetC99 was synthesised using rabbit reticulocyte lysate in the presence (lanes 5 and 6) or absence (lanes 1-5 and 7-8) of microsomes for 30 minutes at 30°C. Initiation of translation was inhibited by addition of ATCA for 10 minutes at 30°C. Samples were either immunoprecipitated with  $\alpha$ APP<sub>680-695</sub> antisera (lanes 5-8) or were used in a solubilised  $\gamma$ -secretase assay. For the assay, buffer, PNT (where indicated) and either CHAPSO-solubilised membrane extract or 1% CHAPSO (as indicated) were added to the synthesised MetC99 and the mixture was incubated at 30°C for 1 hour. The samples were immunoprecipitated with  $\alpha$ APP<sub>680-695</sub> antisera and analysed by SDS-PAGE. A lower molecular weight product is indicated (open circles).

To determine whether the lack of processing observed was due to the inefficient extraction of any  $\gamma$ -secretase present in my membrane preparation, I immunoblotted the extract for presenilin, a component of the  $\gamma$ -secretase for which a good quality serum was available. The solubilised extract was compared with samples from HEK293 cells, COS7 cells and mouse brain microsomes (cf. Fig 5.9). All four samples appeared to contain high levels of the N-terminal fragment of presenilin (Fig 5.9, cf. lanes 1-4), consistent with the endoproteolytic processing of the immature polypeptide (Steiner et al., 1999; Thinakaran et al., 1996), and

hence the potential presence of an active  $\gamma$ -secretase complex (Fraering et al., 2004).

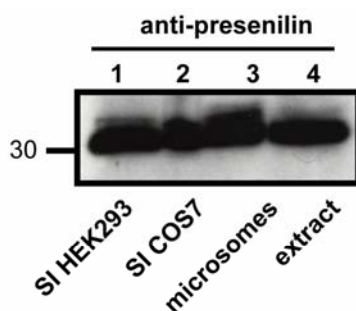


**Fig 5.9. Immunoblot of CHAPSO-solubilised membrane extract for presenilin.**

Samples of semi-intact HEK293 cells (lane 1), semi-intact COS7 cells (lane 2), mouse brain microsomes (lane 3), and a CHAPSO-solubilised HeLa cell extract (lane 4) were resolved by SDS-PAGE and transferred to a nitrocellulose membrane. The membrane was incubated with an antiserum specific for the N-terminus of presenilin. Visualisation was then performed with a secondary antibody coupled to horseradish peroxidase and subsequent addition of the substrate for this enzyme.

## 5.6 Summary

The aim of the experiments presented in this chapter was to attempt to reconstitute  $\gamma$ -secretase processing in an *in vitro* system. Since the data presented in chapter 3 suggested that processing did not occur in an *in vitro*, cell-free, system supplemented with canine pancreatic microsomes, I used semi-intact cells as an alternative source of ER membranes. However, no evidence for  $\gamma$ -secretase cleavage was detected, and I postulated that this may be because factors were required that are present in a “late” compartment of the secretory pathway, and which were therefore unavailable in my system. To resolve this, I attempted to fuse downstream compartments of the secretory pathway with the ER present in semi-intact cells using both polyethylene glycol (PEG) and brefeldin-A (BFA) treatments. Neither PEG nor BFA treatment of cells resulted in detectable  $\gamma$ -secretase processing. Whilst immunofluorescence microscopy suggested that BFA did cause redistribution of Golgi proteins, no acquisition of Endo-H resistant glycans was observed, suggesting compartment mixing was unsuccessful at a “biochemical level”.

Previous studies have used a detergent-solubilised membrane extract to achieve APP processing *in vitro* (Li et al., 2000a; Weihofen et al., 2003). I used a similar extract with both my CT72 peptide, and with a previously studied <sup>Met</sup>C99 fragment (Weihofen et al., 2003). However, in both cases I failed to detect any evidence of  $\gamma$ -secretase processing. This apparent lack of processing was not due to the degradation of C-terminal fragments since PNT was included in the reactions to stabilise AICD-like polypeptides (see chapter 3). The solubilised membrane extract was analysed for components of the  $\gamma$ -secretase and found to contain significant levels of presenilin-1. However, due to a lack of antisera, I was not able to test the extract for the other subunits of the  $\gamma$ -secretase complex.

## **5.7 Conclusion**

Taken together, the results presented in this chapter indicate that establishing an *in vitro* system that can reproducibly reconstitute the  $\gamma$ -secretase processing of APP is technically complex and challenging and will require significant additional refinements. The increased understanding of this processing pathway that can be obtained using *in vivo*-based model systems may assist in the long-term development of an *in vitro* assay.

## CHAPTER 6

---

**Results:**

**Preliminary *in vivo* analysis of APP-derivatives**

## 6 Preliminary *in vivo* analysis of APP-derivatives

In the previous chapters, the potential for the  $\gamma$ -secretase processing of several APP-derivatives was explored using a number of *in vitro* systems. However, none of these systems yielded detectable levels of  $\gamma$ -secretase cleavage. Since the majority of studies of APP processing to date have been performed *in vivo*, I investigated whether my APP-derivatives could be cleaved when transiently expressed in cultured mammalian cells.

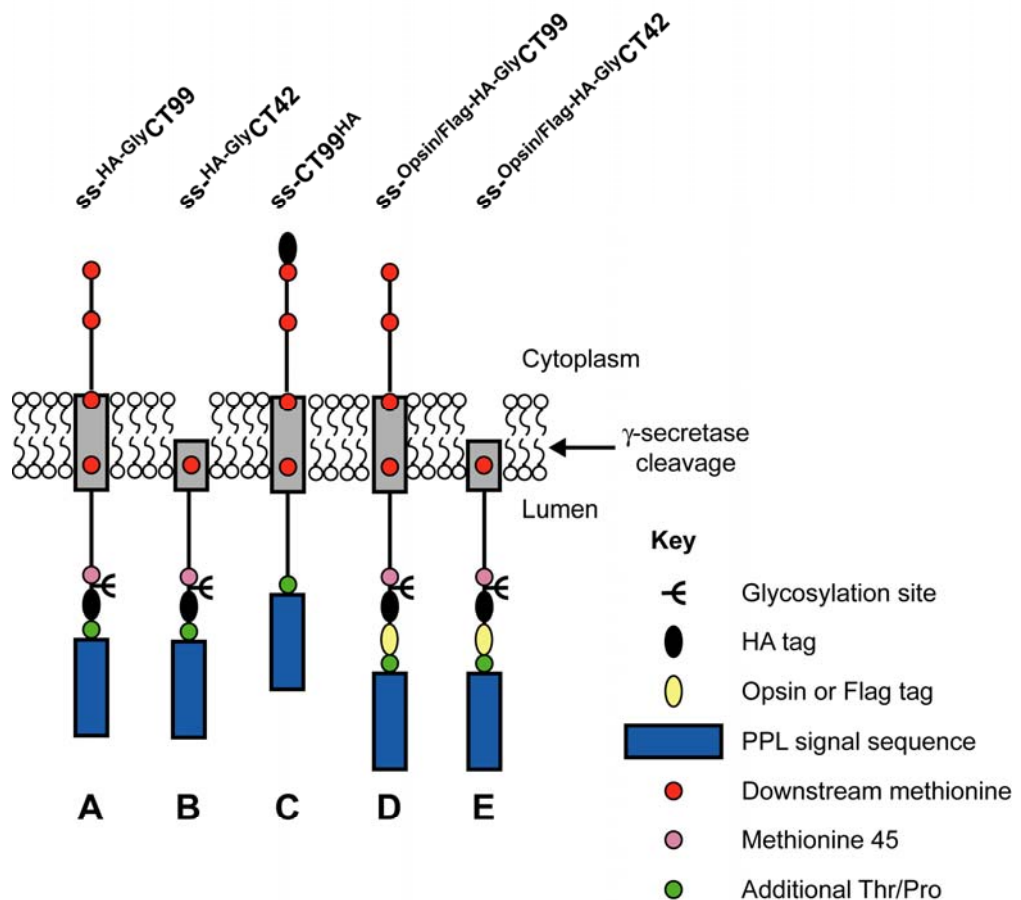


Fig 6.1. APP-derivative constructs used to investigate *in vivo* processing.

Pre-prolactin signal sequences are shown as blue rectangles, *N*-glycosylation sites are shown as  $\Psi$  (2 additional sites present in the opsin tag), transmembrane domains are shown as grey rectangles, approximate positions of methionine residues are indicated by red or pink circles, additional Thr/Pro residues are shown as green circles, the opsin or flag tags are indicated by yellow ovals, the HA tag is indicated by a black oval, additional APP-derived sequence are shown as black lines, the  $\gamma$ -secretase cleavage site is indicated by a black arrow.

Since cultured mammalian cells often express detectable levels of endogenous APP and its fragments (Kraft, 2001), I used epitope-tagged versions of the APP-derivatives previously characterised *in vitro* (see Chapters 3-5). In order to facilitate the detection of all fragments derived from these exogenously expressed APP-derivatives, epitope tags were incorporated at both their N- and C-termini.

### **6.1 Analysis of HA-tagged derivatives**

In the first instance, APP-C99 was tagged with an HA epitope tag at its N- or C-terminus. ss-<sup>HA-Gly</sup>CT99 is as previously described (Chapter 4; Fig 6.1A), whilst ss-CT99<sup>HA</sup> represents ss-CT99 with an HA epitope tag inserted immediately prior to the stop-codon (Fig 6.1C). Both these APP-derivatives were transiently expressed in COS7 cells, and the products analysed by Western blotting (Fig 6.2).

In addition to transfecting cells with the two ss-CT99-derived constructs, empty vector (pcDNA3.1(+)) and an HA-tagged Notch derivative were also used. There was efficient detection of the C-terminally tagged ss-CT99<sup>HA</sup> derived product by the  $\alpha$ HA antiserum (Fig 6.2A, cf. lane 1), but the N-terminally tagged version was poorly recognised (Fig 6.2A, cf. lane 2). Only a faint background signal was seen with the vector control (Fig 6.2A, cf. lane 3), whilst the Notch fragment was highly expressed and easily detected via its HA-tag (Fig 6.2A, cf. lane 4).

In order to further investigate the poor recognition of the N-terminally tagged APP-C99 derivative, the same samples were analysed using an antiserum recognising the authentic C-terminus of APP ( $\alpha$ APP<sub>680-695</sub>). An endogenous APP-derived fragment was detected in all cases, confirming the serum's reactivity with the monkey version of the protein (Fig 6.2B, cf. lanes 1-4, as indicated). Both of the cell lines expressing HA-tagged versions of APP-C99 displayed distinct, higher molecular weight products of a similar intensity and of the appropriate size for the signal-sequence cleaved version of the APP-derived peptides encoded by the plasmids used for transfection (Fig 6.2B, cf. lanes 1 and 2, see cross). Thus, whilst the HA-epitope served as an effective tag at the C-terminus of APP-C99, it was poorly detected when present at the N-terminus, even when good levels of

expression were achieved. I therefore investigated the use of an alternative epitope at the N-terminus of APP-C99.

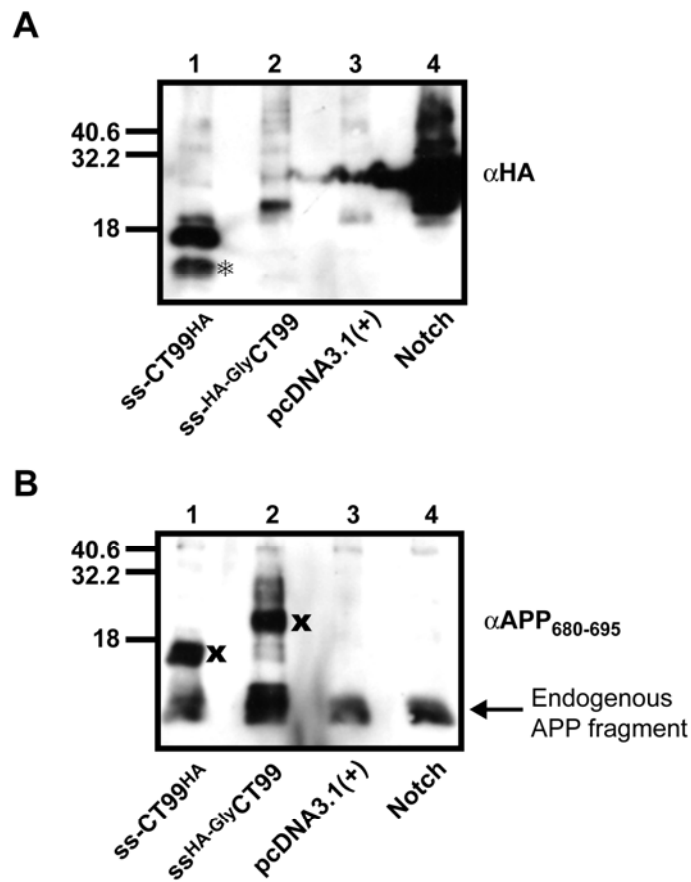


**Fig 6.2. Detection of HA-tagged ss-CT99 derivatives by western blotting.**

COS7 cells were transfected with the constructs indicated using Lipofectamine-2000 according to the manufacturer's instructions. Cells were incubated at 37°C for 48 hours before removing the media. Cells were solubilised by the addition of Triton X-100 immunoprecipitation buffer. SDS-PAGE loading buffer was added, and samples were heated at 70°C for 10 minutes. Samples were resolved by SDS-PAGE on a 19% tris-tricine gel. Samples were transferred to nitrocellulose membrane and immunoblotted with anti-sera specific for either the HA epitope tag (panel A) or the C-terminus of APP (panel B). The identity of the lower molecular weight product in panel A lane 1 (indicated by an asterisk) is unknown.

## 6.2 Use of opsin and flag tags at the N-terminus

Having verified that the HA epitope could be used to efficiently detect C-terminally derived products of my APP-derivatives, I wanted to construct other versions that

could be used to detect potential N-terminal products of  $\gamma$ -secretase processing. To this end, I generated ss-<sup>HA-Gly</sup>CT99 derivatives with either the flag epitope (ss-<sup>flag-HA-Gly</sup>CT99) or an opsin epitope (ss-<sup>opsin-HA-Gly</sup>CT99) inserted immediately after the cleavable N-terminal signal sequence (cf. Fig 6.1D). In addition to the consensus *N*-glycosylation site that was already present in the ss-<sup>HA-Gly</sup>CT99 derivative, two additional *N*-glycosylation sites were incorporated within the opsin epitope tag. To further facilitate the detection of any  $\gamma$ -secretase cleavage products, the putative N-terminal products of ss-<sup>opsin-HA-Gly</sup>CT99 and ss-<sup>flag-HA-Gly</sup>CT99 processing, ss-<sup>opsin-HA-Gly</sup>CT42 and ss-<sup>flag-HA-Gly</sup>CT42 respectively, were also generated to serve as internal references (cf. Fig 6.1E).

To establish whether the opsin or flag tag could be used to detect N-terminal fragments that may result from  $\gamma$ -secretase processing, I first synthesised the ss-<sup>flag-HA-Gly</sup>CT99, ss-<sup>opsin-HA-Gly</sup>CT99, ss-<sup>flag-HA-Gly</sup>CT42 and ss-<sup>opsin-HA-Gly</sup>CT42 derivatives *in vitro* and used  $\alpha$ opsin,  $\alpha$ flag and  $\alpha$ HA antisera to identify N-terminal fragments by immunoprecipitation (cf. Fig 6.3).

Both the  $\alpha$ HA and the  $\alpha$ opsin anti-sera detected fragments of the expected size for ss-<sup>opsin-HA-Gly</sup>CT99 and ss-<sup>opsin-HA-Gly</sup>CT42 (Fig 6.3, cf. lanes 1-4, arrows). Similarly, both the  $\alpha$ HA and  $\alpha$ flag antisera recognised products within the predicted molecular weight range for ss-<sup>flag-HA-Gly</sup>CT99 and ss-<sup>flag-HA-Gly</sup>CT42 (Fig 6.3, cf. lanes 5-8, arrows). Taken together, these data indicate that both epitope tags could potentially be used to detect N-terminally derived fragments generated by  $\gamma$ -secretase processing *in vivo*.

Whilst the data above indicate that ss-<sup>flag-HA-Gly</sup>CT99 can be recognised by  $\alpha$ HA and  $\alpha$ flag antisera during immunoprecipitation, they provide no information regarding its detection by Western blotting using samples from an *in vivo*-expression system. In order to determine whether ss-<sup>flag-HA-Gly</sup>CT99 could also be detected by this approach, COS7 cells were transiently transfected with a ss-<sup>flag-HA-Gly</sup>CT99 expressing plasmid and the products were analysed by Western blotting (Fig 6.4).

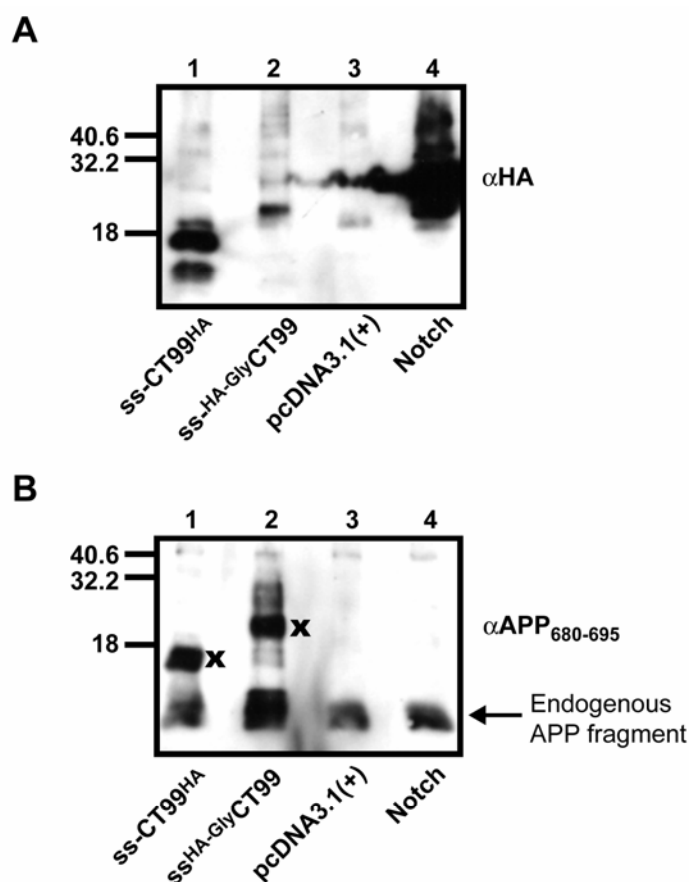


**Fig 6.2. Detection of HA-tagged ss-CT99 derivatives by western blotting.**

COS7 cells were transfected with the constructs indicated using Lipofectamine-2000 according to the manufacturer's instructions. Cells were incubated at 37°C for 48 hours before removing the media. Cells were solubilised by the addition of Triton X-100 immunoprecipitation buffer. SDS-PAGE loading buffer was added, and samples were heated at 70°C for 10 minutes. Samples were resolved by SDS-PAGE on a 19% tris-tricine gel. Samples were transferred to nitrocellulose membrane and immunoblotted with anti-sera specific for either the HA epitope tag (panel A) or the C-terminus of APP (panel B).

Although the ss-<sup>flag-HA-Gly</sup>CT99 product was efficiently immunoprecipitated by the  $\alpha$ HA antisera (cf. Fig 6.3), no ss-<sup>flag-HA-Gly</sup>CT99-derived products were identified by immunoblotting (Fig 6.4, cf. lane 4) despite a strong signal from a positive control (Fig 6.4, cf. lane 2). This was consistent with previous evidence that the N-terminal HA-tag was poorly recognised (cf. Fig 6.2). The ss-<sup>flag-HA-Gly</sup>CT99 products were, however, recognised by the  $\alpha$ flag antisera (Fig 6.4B, cf. lane 3).

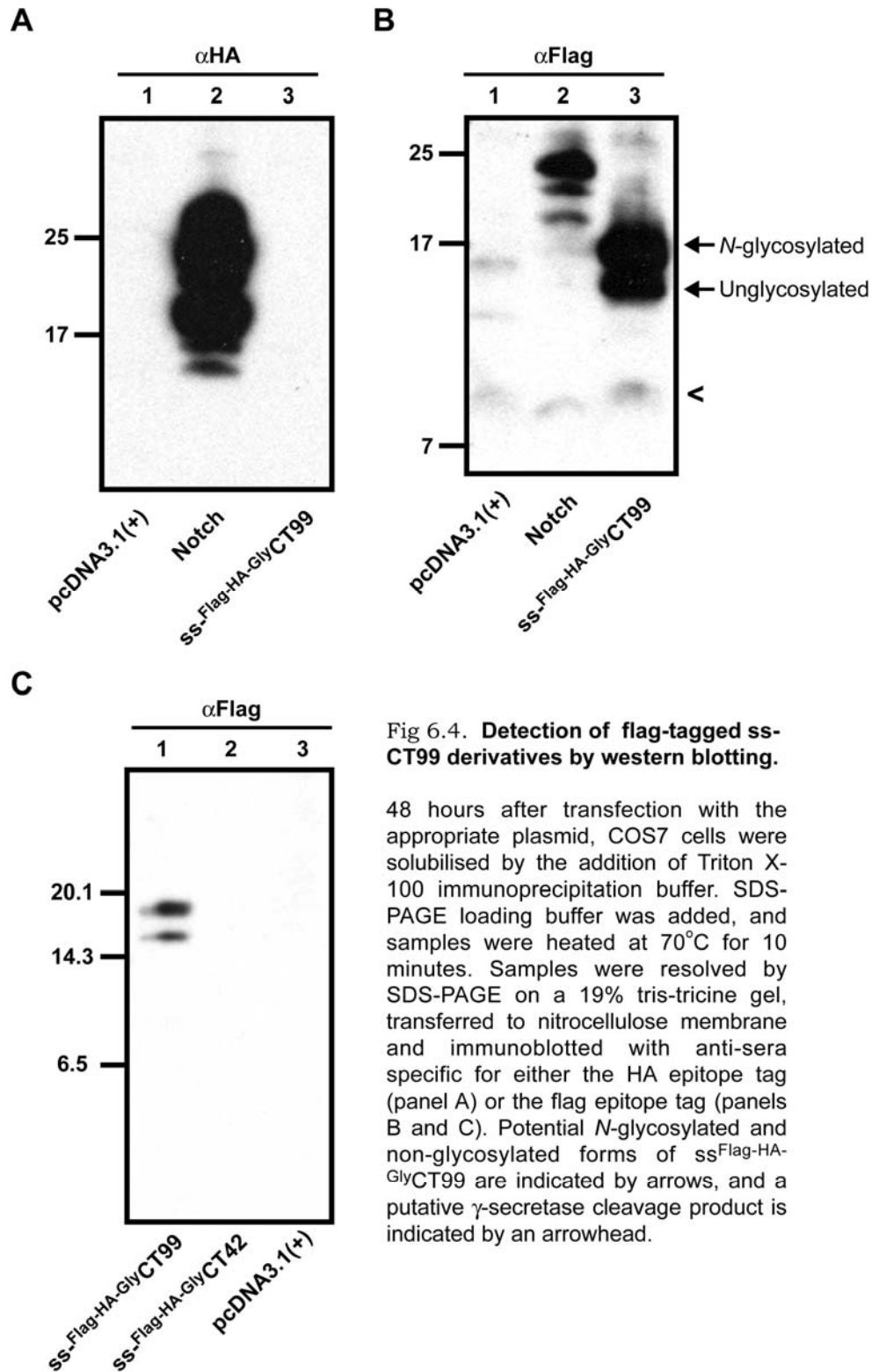


**Fig 6.4. Detection of flag-tagged ss-CT99 derivatives by western blotting.**

48 hours after transfection with the appropriate plasmid, COS7 cells were solubilised by the addition of Triton X-100 immunoprecipitation buffer. SDS-PAGE loading buffer was added, and samples were heated at 70°C for 10 minutes. Samples were resolved by SDS-PAGE on a 19% tris-tricine gel, transferred to nitrocellulose membrane and immunoblotted with anti-sera specific for either the HA epitope tag (panel A) or the flag epitope tag (panels B and C). Potential N-glycosylated and non-glycosylated forms of ss<sup>Flag</sup>-HA-GlyCT99 are indicated by arrows, and a putative  $\gamma$ -secretase cleavage product is indicated by an arrowhead.

In fact, 2 species were observed that most likely correspond to the N-glycosylated and non-glycosylated forms of the ss-<sup>flag</sup>-HA-GlyCT99 after signal sequence cleavage (cf. Fig 6.4B, see arrows). A faint lower molecular weight product was also seen that could potentially correspond to the N-terminal product of  $\gamma$ -secretase

processing (Fig 6.4B, cf. arrowhead). However, when a similar analysis was performed using ss-<sup>flag</sup>-HA-GlyCT42 in addition to ss-<sup>flag</sup>-HA-GlyCT99, no lower molecular weight products were observed (Fig 6.3C, cf. lane 1) and the ss-<sup>flag</sup>-HA-GlyCT42 derivative was not detectable by either the  $\alpha$ flag (Fig 6.4C, cf. lane 2) or  $\alpha$ HA antisera (data not shown).

Since neither the flag nor the HA epitope tags were reproducibly successful in detecting N-terminal APP-C99 fragments, I went on to analyse the ss-<sup>opsin</sup>-HA-GlyCT99 and ss-<sup>opsin</sup>-HA-GlyCT42 derivatives by Western blotting (Fig 6.5).

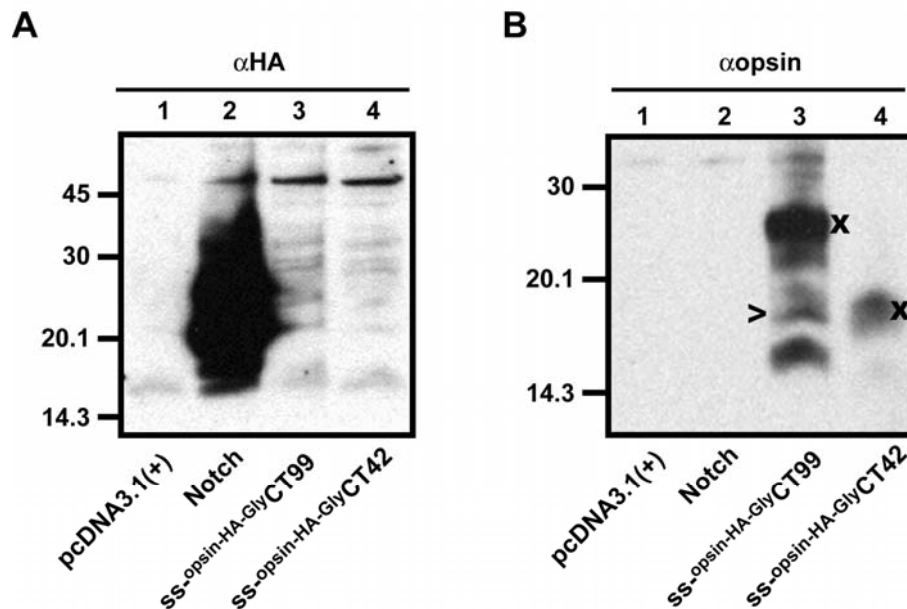


Fig 6.5. **Detection of opsin-tagged ss-CT99 derivatives by immunoblotting.**

Samples were prepared as described in the legend to Fig 6.4. Samples were resolved by SDS-PAGE on a 19% tris-tricine gel. Samples were transferred to nitrocellulose membrane and immunoblotted with anti-sera specific for either the HA epitope tag (panel A) or the opsin epitope tag (panel B). Both ss-<sup>opsin</sup>-HA-GlyCT99 and ss-<sup>opsin</sup>-HA-GlyCT42 products were recognised by  $\alpha$ opsin antisera (indicated by crosses). A putative  $\gamma$ -secretase cleavage product is indicated by an arrowhead.

As with previous experiments (Figs 6.2 and 6.4), neither ss-<sup>opsin</sup>-HA-GlyCT99 nor ss-<sup>opsin</sup>-HA-GlyCT42 were detectable by the  $\alpha$ HA antisera during immunoblotting analysis (Fig 6.5A, cf. lanes 3 and 4), despite the serum's ability to recognise both polypeptides during immunoprecipitation (Fig 6.2). In contrast, both the ss-<sup>opsin</sup>-HA-GlyCT99 and ss-<sup>opsin</sup>-HA-GlyCT42 were recognised by the  $\alpha$ opsin antisera (Fig 6.5B,

cf. lanes 3 and 4, see cross). Interestingly, a lower molecular weight product was observed in the ss-<sup>opsin-HA-Gly</sup>CT99 products that appeared to have a similar mobility to that of the ss-<sup>opsin-HA-Gly</sup>CT42 reference, suggesting that it could correspond to the N-terminal product of  $\gamma$ -secretase processing of the precursor (Fig 6.5B, see arrowhead).

### **6.3 Summary**

The objective of the work presented in this chapter was to establish whether N- and C-terminally tagged ss-CT99 derivatives could be used to study  $\gamma$ -secretase processing *in vivo*. Having determined that an HA-epitope tag could be used to detect C-terminal fragments of ss-CT99, I went on to look for an epitope tag that could be used to study N-terminal fragments. Neither an HA-tag, nor a flag tag could be used to detect both the N-terminally tagged construct and its putative N-terminal  $\gamma$ -secretase cleavage product. Use of an opsin-tag, however, enabled the efficient detection of both the full-length ss-CT99 derivative and its putative product.

### **6.4 Conclusion**

The results presented in this chapter show that ss-CT99 can be tagged with an HA-epitope at its C-terminus and an opsin-epitope at its N-terminus in order to facilitate detection of potential  $\gamma$ -secretase derived-products. The presence of endogenous APP-derived fragments in many mammalian cell lines highlights the need for the use of such epitope tags to detect recombinantly expressed proteins and their fragments. Although I generated ss-CT99 and ss-CT42 derivatives containing both the N- and C-terminal tags together, time constraints meant I was unable to complete the characterisation of these derivatives. The presence of a potential N-terminal  $\gamma$ -secretase cleavage product upon the *in vivo* expression of ss-<sup>opsin-HA-Gly</sup>CT99 suggests that this APP-derivative may be processed by the  $\gamma$ -secretase in COS7 cells. However, further analysis using  $\gamma$ -secretase inhibitors and/or presenilin knock-out cell lines will be required in order to verify this preliminary conclusion.

# **CHAPTER 7**



## **Discussion**

## 7 Discussion

### 7.1 Introduction

Whilst the function of APP is unknown, recent evidence suggests that APP and its family members may function as receptors that, upon ligand binding, are cleaved by a membrane-associated metalloproteinase (see Introduction). This processing event would result in ectodomain shedding and produce C-terminal “stubs” suitable for intramembrane proteolysis by the  $\gamma$ -secretase. Upon cleavage by the  $\gamma$ -secretase, APP would liberate its intracellular domain (AICD) which, by analogy to the Notch processing pathway, might enter the nucleus and regulate gene expression (Kimberly et al., 2001).

The aim of this project was to exploit a homologous cell-free system, to study the generation and stability of the AICD fragment. A number of short C-terminal APP-derivatives were synthesised *in vitro* in either the presence or absence of canine pancreatic microsomes or semi-permeabilised cells. The generation of low molecular weight fragments was then analysed by immunoprecipitation and SDS-PAGE. The effect of adding various protease inhibitors upon the production of these fragments was then investigated.

### 7.2 ***A CT72 APP-derivative is efficiently targeted to and integrated into the ER membrane***

A short 72-residue C-terminal fragment of APP that reflected an artificial “signal-anchor” version of the protein (CT72) was generated as the hypothetical minimal APP-derived substrate that would be cleaved by the  $\gamma$ -secretase whilst still being capable of efficient ER targeting. CT72 behaved as an integral membrane protein, as judged by its resistance to extraction with alkaline sodium carbonate (cf. Fig 3.1A). However, this analysis gave no information regarding the orientation of CT72 within the membrane, and this was established via proteinase protection (cf. Fig 3.1D) and defining the *N*-glycosylation state of the variant CT72-Gly (cf. Fig 3.1C). Taken together, these studies showed that CT72 was efficiently membrane targeted and inserted in an orientation compatible with  $\gamma$ -secretase cleavage (type

I orientation; cf. Fig 3.1B). Thus, the transmembrane domain of APP, present in CT72, is sufficient to permit its membrane integration.

### **7.3 *In vitro* synthesised AICD fragments are rapidly degraded by a metalloproteinase activity, probably IDE**

Radiolabelled CT72 polypeptides were generated in the presence and absence of canine pancreatic microsomes, the products were immunoprecipitated with  $\alpha$ APP<sub>680-695</sub> antisera, and analysed for the presence of membrane-dependent AICD-like fragments (cf. Fig 3.2). Lower molecular weight products with a similar mobility to that expected for the AICD were seen, but these were not dependent on the inclusion of membranes, nor were they generated as a result of membrane contamination of the lysate (cf. Fig 3.2). In order to determine whether the “AICD-like” fragment generated with CT72 was due to proteolytic processing, I set up a “pulse-chase” type experiment to look at the levels of the AICD-like product with time (cf. Fig 3.3). Rather than the levels of this product increasing with time, as might be expected if it was generated as a result of the protease cleavage of a precursor, the levels rapidly decreased, suggesting that it was labile in my *in vitro* system (cf. Fig 3.3). This is similar to the situation observed *in vivo* where a CT49 AICD fragment is highly unstable (Walsh et al., 2003).

Further analysis of the AICD-like fragment indicated that its stability was unaffected by the addition of the proteasome inhibitor, ALLN, a result that is consistent with data obtained by other groups using crude cell extracts (cf. Fig 3.5A) (Edbauer et al., 2002a; Pinnix et al., 2001). These data suggest that the AICD is cleared via a different pathway from the Notch NICD fragment, which is degraded by a ubiquitin-dependent proteasomal pathway (De Strooper et al., 1999). The factor responsible for mediating AICD degradation appeared to be cytosolic, since AICD fragments were rapidly removed in the absence of membranes (cf. Fig 3.3). It was also observed that AICD stability was enhanced by incubation at 0°C (cf. Fig 3.5B) or the inclusion of the metalloproteinase inhibitors EDTA and PNT (cf. Fig 3.6). This observation correlates with results that have been obtained *in vivo* in which EDTA and PNT have been shown to stabilise AICD fragments (Edbauer et al., 2002a; Pinnix et al., 2001). Further studies *in*

*in vivo* have suggested that AICD degradation may be mediated by the so-called insulin degrading enzyme, IDE (see section 1.10.3) (Edbauer et al., 2002a; Farris et al., 2003). Western blotting confirmed the presence of IDE in the reticulocyte lysate used for the “pulse-chase” experiments (cf. Fig 3.13).

To further investigate the potential role of IDE in AICD degradation, I investigated the stability of my AICD-like fragments using reticulocyte lysate that had first been immunoprecipitated with either  $\alpha$ IDE or a preimmune serum (Fig 3.15). Interestingly, use of immunodepleted lysate appeared to stabilise the <sup>Met</sup>CT57 fragment (Fig 3.15, lanes 9-12). However, use of a preimmune serum had a similar effect (Fig 3.15, lanes 13-16), suggesting that the AICD-degrading activity had been non-specifically removed from the lysate during the immunoprecipitation procedure. Another explanation could be that the presence of other proteins (pre-immune antibodies) “protected” the radiolabelled polypeptide by competing as substrates for the proteases(s) in the lysate. Previous studies have shown that immunodepletion of IDE from cytosol led to the stabilisation of AICD fragments (Edbauer et al., 2002a). In this study, a “mock” immunodepletion in the absence of antibody was used as a control rather than the use of an unrelated antiserum. Data obtained *in vivo* has suggested that IDE may selectively regulate the levels of unphosphorylated AICD, but not the phosphorylated form (Farris et al., 2003). However, no analysis of the phosphorylation state of the AICD fragments was performed in my studies.

Taken together, my findings suggest that a metalloproteinase, most probably IDE, is responsible for the degradation of the AICD *in vitro*. Further experiments, for example using cytosol from cells depleted of IDE by RNA interference, and use of SH-alkylating agents to determine whether the degrading activity is thiol dependent, will help to resolve this issue. However, the possibility that other components may contribute to AICD degradation cannot be excluded. If the AICD does function in nuclear signalling, its rapid removal might be expected in order to prevent constitutive, un-regulated, signalling *in vivo*. Thus, its lability *in vitro* may be biologically significant.

#### **7.4 AICD-like products generated with a CT72 APP-derivative are due to alternative initiation**

Given that authentic  $\gamma$ -secretase cleavage would be a membrane-dependent process, it seemed possible that the AICD fragments I observed upon CT72 synthesis may be the result of alternative initiation. The generation of CT72 mutants that lacked downstream methionine residues at positions 8 (CT72-1) and 24 (CT72-2) and the use of alternative derivatives that initiated from Met-8 (CT65) or Met-24 (CT49) indicated that this was indeed the case (cf. Fig 3.4). Alternative initiation from downstream methionine residues present in the coding regions of APP family members has also been observed *in vivo* and when <sup>Met</sup>CT59 of APP-like protein-1 (APLP1) was transiently expressed alternative initiation was observed (Walsh et al., 2003). Since alternative initiation from Met-8 and Met-24 of CT72 generates polypeptides within the expected size range of the product of  $\gamma$ -secretase cleavage, this might prevent attempts to detect authentic AICD-like fragments. In order to establish whether any authentic products of  $\gamma$ -secretase processing were being “masked” by the presence of these alternative initiation products, similar experiments were repeated using a derivative lacking the first two downstream methionines CT72-2, and using <sup>3</sup>H-isoleucine to radiolabel the resulting products (data not shown). However, no evidence of any lower molecular weight fragments was observed, suggesting that no detectable  $\gamma$ -secretase processing had occurred in this system. This lack of processing was not a result of the unusual CT72 substrate used, since similar experiments with a CT99 polypeptide lacking the equivalent methionine residues also failed to yield evidence of  $\gamma$ -secretase cleavage (data not shown).

Taken together, these studies indicate that the only detectable lower molecular weight fragments generated with CT72 in a microsomal system were the result of alternative initiation and that  $\gamma$ -secretase processing did not occur. This suggested that future experiments should use an alternative system to study such cleavage.

## **7.5 Factors present in human brain nuclear extract stabilise the AICD**

Studies *in vivo* have suggested that the AICD is stabilised by the nuclear adaptor protein Fe65 (Kimberly et al., 2001; Walsh et al., 2003). One hypothesis is that Fe65 stabilises the AICD and enables it to translocate to the nucleus where it can then influence gene regulation (Cao and Sudhof, 2001). In order to determine whether Fe65 had a stabilising effect on the AICD in my *in vitro* system, semi-purified <sup>Met</sup>CT57, generated in wheat germ extract, was mixed with reticulocyte lysate that had been pre-incubated with a nuclear extract from human brain or recombinant Fe65 (Zhao and Lee, 2003) (cf. Fig 3.12). Fe65 did not appear to have a stabilising effect on <sup>Met</sup>CT57, and in fact its degradation appeared to be more rapid (cf. Fig 3.12, lanes 7-9). The addition of brain nuclear extract did, however, partially stabilise the AICD (cf. Fig 3.12, lanes 10-12). The reason for the inability of the recombinant Fe65 to stabilise the AICD is unclear, since no “functional” assay to confirm the activity of the protein was available, however, the nuclear extract should contain Fe65, since this protein is expressed in brain (Kesavapany et al., 2002) and localises to the nucleus (Walsh et al., 2003). Unfortunately, no antibodies could be obtained to confirm the presence of Fe65 in the extract used during this study. It is therefore possible that the stabilising effect observed in the presence of the nuclear extract is due to Fe65 binding. Further experiments, for example immunodepleting the extract of Fe65, would be required to verify whether this was indeed the case. An alternative explanation could be that excess protein in the brain extract either inactivated the rabbit reticulocyte lysate proteases or protected the radiolabelled protein from proteolysis.

Alternatively, the lack of stabilisation observed with the Fe65 may be due to the absence of membranes in this experiment. The *in vivo* studies in which a stabilising effect was seen used co-expression of Fe65 with the AICD in cells. Recent studies by Cao and Sudhof have suggested that rather than Fe65 and the AICD forming a complex in which the two proteins are translocated to the nucleus, that membrane-tethered AICD recruits Fe65 and mediates its activation through  $\gamma$ -secretase processing (Cao and Sudhof, 2004). Since my *in vitro* analysis was carried out in the absence of membranes, this may be the reason for the lack of

stabilisation observed. It may be that the presence of membranes in the crude human brain nuclear extract enabled some AICD to become attached to the membrane where it could bind Fe65 and become stabilised.

### **7.6 Only specific lengths of AICD are degraded in vitro**

In order to determine whether the degradation observed with CT49 and <sup>Met</sup>CT57 was specific to these derivatives or was a more general phenomenon, several alternative AICDs of differing lengths were studied. AICDs of 57 (<sup>Met</sup>CT56), 59 (<sup>Met</sup>CT58), 60 (<sup>Met</sup>CT59) and 61 (<sup>Met</sup>CT60) residues were generated by incorporating an in-frame methionine residue in front of the relevant coding region. Whilst CT49 and <sup>Met</sup>CT57 were rapidly degraded in reticulocyte lysate in the absence of the metalloproteinase inhibitor, PNT, all of these other AICD derivatives were stable, regardless of the presence of PNT (cf. Fig 3.9). These data suggest that the degradation observed for CT49 and <sup>Met</sup>CT57 is indeed specific to these AICD lengths. The results obtained for <sup>Met</sup>CT59 are consistent with studies using transient expression following transfection, in which a CT60 (<sup>Met</sup>CT59) fragment was shown to be more stable than a CT49 derivative (Walsh et al., 2003). However, an earlier study suggested that <sup>Met</sup>CT59, whilst more stable than CT49, behaves similarly and is degraded (Kimberly et al., 2001). The analysis carried out by Kimberly and co-workers was performed over a significantly longer time scale than the work presented here, and no significant loss of <sup>Met</sup>CT59 occurred during the relatively short time course used.

The stability of alternative AICD fragments has not been widely analysed, and others have focussed on <sup>Met</sup>CT59, as this is equivalent, except the initiating methionine, to the fragment generated by  $\gamma$ -secretase processing that produces A $\beta$ 40 (generation of A $\beta$ 42 produces CT57). CT49 and CT51 derivatives of APLP1 have been studied, and these lengths were found to be unexpectedly stable compared with ICD fragments generated from APP or APLP2 (Walsh et al., 2003). Because most of these AICD-derived fragments require the inclusion of a non-natural methionine residue at their N-termini to enable synthesis, it is possible that this exogenous initiating methionine might influence the subsequent fate of the polypeptide. Hence, only if the second residue in a polypeptide is a small, uncharged amino acid (Ala, Cys, Gly, Pro, Ser, Thr or Val), is the initiator

methionine likely to be removed by methionine aminopeptidase (MAP) (Lowther and Matthews, 2002). However, there is no obvious pattern to suggest that removal or retention of this methionine affects degradation of the AICD lengths studied. Whilst the initiator methionine of <sup>Met</sup>CT57 would be expected to be cotranslationally removed as the penultimate residue is a Thr, this would also be the case for <sup>Met</sup>CT56, <sup>Met</sup>CT58 and <sup>Met</sup>CT60, whose second residues are Val, Ala and Val respectively. <sup>Met</sup>CT59, however, which has been used by a number of groups, would be unlikely to have its initiator methionine removed as this would reveal an isoleucine residue, which would be destabilizing (Lowther and Matthews, 2002). Since removal of this exogenous methionine would be required to generate authentic CT59 akin to that which would be produced as a result of  $\gamma$ -secretase processing, this could account for its relative stability in my *in vitro* system. Hence, it is possible that the presence of this methionine during studies by other groups may also have influenced its behaviour. Furthermore, MAP is a metalloproteinase that is thought to be dependent on  $\text{Co}^{2+}$ ,  $\text{Mg}^{2+}$  and/or  $\text{Fe}^{2+}$  (Lowther and Matthews, 2002), and the use of divalent cation chelators and the like to inhibit IDE may also influence N-terminal methionine processing.

### **7.7 <sup>Met</sup>CT57 may be N-terminally processed in reticulocyte lysate to generate a CT49-like product**

Since AICD-like fragments were found to be highly labile in a reticulocyte lysate translation system, I wanted to investigate whether an alternative system could be used to generate more stable products. However, when <sup>Met</sup>CT57 and CT49 were synthesised in a wheat germ translation system, rather than having almost indistinguishable mobilities as was seen with reticulocyte lysate, <sup>Met</sup>CT57 appeared distinctly larger than the CT49 product (Fig 3.10). That the mobilities of <sup>Met</sup>CT57 and CT49 appear so similar in reticulocyte lysate is unexpected, since the apparent molecular weights of CT72 and CT65 are clearly different when synthesised in the same system, despite there being only a 7 residue difference between the two polypeptides compared with an 8 residue difference between CT49 and <sup>Met</sup>CT57 (see Fig 3.4). It is possible that the apparent similarity in mobilities is due to processing of <sup>Met</sup>CT57, by an unknown protease, to a size akin

to that of CT49 in reticulocyte lysate, but that this protease is not present in wheat germ extract.

Interestingly, when AICD fragments of 57 or 59 amino acids, that would be predicted from the generation of N-terminal A $\beta$  peptides, have been looked for *in vivo*, only a smaller C-terminal product has been found, apparently generated by proteolysis distal to the known  $\gamma$ -secretase cleavage site between Leu-49 and Val-50 at a point termed the  $\epsilon$ -cleavage site (see introduction section 1.14). It has been proposed that the  $\gamma$ - and  $\epsilon$ - cleavage events are distinct, but the order of these events is uncertain. It is possible that APP is first cleaved at the  $\gamma$ -secretase site to generate CT57 or CT59 and that these fragments are then rapidly processed to shorter CT50 fragments at the  $\epsilon$ -cleavage site. This would generate a 7-residue peptide in addition to the  $\epsilon$ -CTF that would be very difficult to detect due to its small size (cf. Fig 1.6). This hypothesis has been disputed by other groups as when a hypothetical  $\gamma$ -CTF substrate was transfected into cells, no resulting  $\epsilon$ -CTF was detected, however the data for these studies was not shown (Weidemann et al., 2002). The  $\epsilon$ -cleavage of APP has been found to have similar properties to the  $\gamma$ -secretase cleavage, but this could be because  $\gamma$ -secretase processing is a prerequisite for  $\epsilon$ -cleavage.

### **7.8 An A $\beta$ -like fragment generated with ss<sup>HA-Gly</sup>CT99 is not a result of $\gamma$ -secretase cleavage**

Since no evidence for the generation of the AICD fragment of APP was obtained, I decided to look for the potentially more stable, N-terminal product of  $\gamma$ -secretase processing, the A $\beta$  peptide. An alternative APP-derivative, ss<sup>HA-Gly</sup>CT99, was prepared with an HA-epitope tag at its N-terminus to facilitate the identification of cleavage products (cf. Fig 4.1). A lower molecular weight product was observed that had a mobility similar to an *in vitro* synthesised standard for the putative N-terminal fragment (cf. Figs 4.2-4.5). However, the formation of this product was not affected by the presence of the potent  $\gamma$ -secretase inhibitor L-685,458 (inhibitor-X) (cf. Fig 4.6). Since this inhibitor has been widely used to prevent  $\gamma$ -secretase processing (Li et al., 2000a; Li et al., 2000b; Shearman et al., 2000), it

seems unlikely that the ss<sup>-HA-Gly</sup>CT42-like product generated with ss<sup>-HA-Gly</sup>CT99 is a result of  $\gamma$ -secretase processing. However, there is data to suggest the existence of a presenilin-independent  $\gamma$ -secretase activity that is not inhibited by L-685,458 (Wilson et al., 2003). The presence of a second  $\gamma$ -secretase was suggested following observations that A $\beta$ 42 production can occur in cells lacking both PS1 and PS2 (Wilson et al., 2002). This distinct  $\gamma$ -secretase activity is thought to be responsible for the generation of intracellular A $\beta$ 42 in the early secretory pathway (ER and intermediate compartments) (Wilson et al., 2003). It is therefore possible that the ss<sup>-HA-Gly</sup>CT42-like product produced with ss<sup>-HA-Gly</sup>CT99 is the result of a presenilin-independent  $\gamma$ -secretase activity. However, the identity of this second  $\gamma$ -secretase activity is unknown, although it is postulated to be an I-CLiP, and there are currently no available inhibitors for this enzyme (Wilson et al., 2003).

### **7.9 Fusion of different membrane compartments was unable to promote processing *in vitro***

A drawback of microsomal membranes and semi-permeabilised cells is that these systems are restricted to studying events that occur early in the secretory pathway (Wilson et al., 1995). In order to overcome the limitations of these systems, I attempted to manipulate my *in vitro* approach to allow the fusion of downstream membrane compartments with the ER localised APP derivatives.

No evidence for  $\gamma$ -secretase processing of any of the APP polypeptides was observed using semi-permeabilised HT1080 or COS7 cells (cf. Fig 5.2), and in fact this is in line with recent advances in the field. If the presenilin present within the ER was capable of cleaving APP, experiments in which APP-derivatives were restricted to the ER should yield an increase in  $\gamma$ -secretase cleavage (Cupers et al., 2001a; Maltese et al., 2001). However, this was not found to be the case, and in fact a decrease in cellular levels of A $\beta$  was observed. Such observations, that the co-localisation of  $\gamma$ -secretase substrates with the bulk of the presenilins was not sufficient to allow processing and suggested that additional factors most likely located in downstream compartments of the secretory pathway are required.

Consistent with such models, complexes containing presenilins, nicastrin and APP-derivatives have been observed in “late” compartments of the secretory pathway, such as the endosomes and lysosomes (Pasternak et al., 2003a; Siman and Velji, 2003). Thus, whilst my *in vitro* system introduces APP derivatives into an ER-derived membrane system with significant levels of PS1, this most likely does not constitute the active  $\gamma$ -secretase.

No  $\gamma$ -secretase processing was observed when either PEG (cf. Figs 5.3 and 5.4) or Brefeldin-A (cf. Figs 5.5 and 5.6) was used to supplement my semi-intact cell system. This may be a consequence of the method used to prepare semi-intact cells since this process involves permeabilising the plasma membrane with digitonin, releasing the cytosol, and leaving internal membrane systems largely intact (Wilson et al., 1995). Semi-intact cells were not treated with PEG until after they had been produced and it may be that some of the components required for  $\gamma$ -secretase processing are present at the plasma membrane which was perturbed by the permeabilisation procedure. Alternatively, some of the internal compartments may have been damaged during preparation of the cells. A third possibility is that the PEG treatment simply did not cause sufficient mixing of the appropriate membrane compartments, a possibility that was difficult to test for.

Although Brefeldin-A treatment has previously been shown to result in the partial processing of an ER retained APP derivative (Cupers et al., 2001a), BFA treatment did not induce  $\gamma$ -secretase processing in my *in vitro* system (cf. Figs 5.5 and 5.6). The lack of processing observed may be due to differences between the two systems; Cupers and co-workers used a neuronal cell line that was virally infected with an APP-C99 derivative (Cupers et al., 2001a), whilst my studies were performed in semi-permeabilised COS7 cells (see Materials and Methods). A second difference was in the time of treatment with BFA; in the study by Cupers and co-workers, cells expressing an APP-C99 derivative that was retained in the ER were treated with BFA and the effects on APP processing were assessed (Cupers et al., 2001a). In my experiments, COS7 cells were treated with BFA, semi-permeabilised cells were prepared, and radiolabelled APP-CT72 was synthesised. Analysis of COS7 cells treated with BFA indicated that there was

redistribution of Golgi components (cf. Fig 5.6) but, there was no biochemical evidence to support these studies since no acquisition of EndoH resistant glycans was seen (cf. Fig 5.5), although some sugar trimming was apparent. It may be that compartments containing components necessary for  $\gamma$ -secretase processing were lost during the permeabilisation procedure in my studies. Therefore, although more proteins would have become available to the substrate protein, those required for  $\gamma$ -secretase cleavage may have remained inaccessible. Recently there has been evidence to suggest that A $\beta$  is produced in endosomes and lysosomes (Haass et al., 1992; Pasternak et al., 2003b; Sisodia and St George-Hyslop, 2002). Alternatively, the effects of BFA in the studies by Cupers and co-workers may be a result of fusion of “late” secretory pathway compartments such as the trans-Golgi network with endosomes (Klausner et al., 1992; Lippincott-Schwartz et al., 1991), although the presence of an ER-retention motif in the APP-C99 derivative should mean that it remains unaffected by “downstream” events. It is unlikely that the effects of BFA treatment on APP processing observed *in vivo* are due to forward traffic of APP-C99 since BFA has been found to affect traffic out of, but not back to, the ER (Lippincott-Schwartz et al., 1989).

### **7.10 Use of a solubilised membrane extract**

That the use of a solubilised membrane extract resulted in no  $\gamma$ -secretase processing of either CT72 (cf. Fig 5.7) or <sup>Met</sup>C99 (cf. Fig 5.8) was at first somewhat surprising since cleavage using this assay has been observed by another group (Weihofen et al., 2003). Western blots of the solubilised  $\gamma$ -secretase extract showed that it contained the N-terminal fragment of presenilin (cf. Fig 5.9 panel A), indicating that at least one component of the  $\gamma$ -secretase was effectively solubilised. However, the  $\gamma$ -secretase is a multi-subunit enzyme (Edbauer et al., 2003; Kimberly et al., 2003), and I was unable to test the extract for the presence of nicastrin, Aph-1 or Pen-2 due to the lack of available anti-sera. It may be that the  $\gamma$ -secretase activity was not efficiently extracted from the membranes, a potential problem during the preparation of such extracts (B Martoglio, ETH Zurich,

personal communication). An immunoblotting analysis of the insoluble fraction for  $\gamma$ -secretase components would help to resolve this issue.

### **7.11 *In vivo* analysis can be used to study APP processing in future**

The majority of studies of the  $\gamma$ -secretase processing of APP to date have been performed *in vivo* (Mattson, 2004). Therefore, in order to establish whether my APP-derivatives were capable of being cleaved by the  $\gamma$ -secretase, it seemed prudent to test them in an *in vivo* system. Since cells contain endogenous APP, I engineered my APP-derivatives to contain epitope tags so as to allow their detection after transient transfection (cf. Fig 6.1). I found that I could successfully detect C-terminal fragments of APP using an HA-epitope tag (cf. Fig 6.2), however, the same tag was not suitable for the detection of N-terminal fragments (cf. Fig 6.2), and an opsin tag was found to be the most appropriate for this purpose (cf. Fig 6.5). Although time constraints meant that I have been unable to fully exploit these epitope-tagged APP derivatives to look for  $\gamma$ -secretase processing, my preliminary data indicates that such analysis will be possible in the future.

### **7.12 Conclusions**

By analysing AICD production *in vitro* I have been able to establish that CT49 and MetCT57 AICD fragments are highly labile in reticulocyte lysate, and have identified candidates for both the factors responsible for their degradation (IDE) and the components that may stabilise these fragments in the cell (Fe65). From the data presented in this thesis, it would appear that presenilin-dependent  $\gamma$ -secretase processing cannot be achieved in the *in vitro* systems that I have established. However, it appears that some level of presenilin-independent cleavage is occurring.

## References

- Abell, B. M., Pool, M. R., Schlenker, O., Sinning, I., and High, S. (2004). Signal recognition particle mediates post-translational targeting in eukaryotes. *Embo J.* 23, 2755-2764.
- Allinson, T. M., Parkin, E. T., Turner, A. J., and Hooper, N. M. (2003). ADAMs family members as amyloid precursor protein alpha-secretases. *J Neurosci Res* 74, 342-352.
- Alzheimer's Disease Collaborative Group (1995). The structure of the presenilin 1 (S182) gene and identification of six novel mutations in early onset AD families. *Nat Genet* 11, 219-222.
- Armogida, M., Petit, A., Vincent, B., Scarzello, S., da Costa, C. A., and Checler, F. (2001). Endogenous beta-amyloid production in presenilin-deficient embryonic mouse fibroblasts. *Nat Cell Biol* 3, 1030-1033.
- Baek, S. H., Ohgi, K. A., Rose, D. W., Koo, E. H., Glass, C. K., and Rosenfeld, M. G. (2002). Exchange of N-CoR corepressor and Tip60 coactivator complexes links gene expression by NF-kappaB and beta-amyloid precursor protein. *Cell* 110, 55-67.
- Baulac, S., LaVoie, M. J., Kimberly, W. T., Strahle, J., Wolfe, M. S., Selkoe, D. J., and Xia, W. (2003). Functional gamma-secretase complex assembly in Golgi/trans-Golgi network: interactions among presenilin, nicastrin, Aph1, Pen-2, and gamma-secretase substrates. *Neurobiol Dis* 14, 194-204.
- Bergman, A., Religa, D., Karlstrom, H., Laudon, H., Winblad, B., Lannfelt, L., Lundkvist, J., and Naslund, J. (2003). APP intracellular domain formation and unaltered signaling in the presence of familial Alzheimer's disease mutations. *Exp Cell Res* 287, 1-9.
- Blobel, G., and Dobberstein, B. (1975). Transfer of proteins across membranes. I. Presence of proteolytically processed and unprocessed nascent immunoglobulin light chains on membrane-bound ribosomes of murine myeloma. *J Cell Biol* 67, 835-851.
- Bonifacino, J. S., and Glick, B. S. (2004). The mechanisms of vesicle budding and fusion. *Cell* 116, 153-166.
- Brown, M. S., and Goldstein, J. L. (1997). The SREBP pathway: regulation of cholesterol metabolism by proteolysis of a membrane-bound transcription factor. *Cell* 89, 331-340.
- Brown, M. S., Ye, J., Rawson, R. B., and Goldstein, J. L. (2000). Regulated intramembrane proteolysis: a control mechanism conserved from bacteria to humans. *Cell* 100, 391-398.

- Buxbaum, J. D., Liu, K. N., Luo, Y., Slack, J. L., Stocking, K. L., Peschon, J. J., Johnson, R. S., Castner, B. J., Cerretti, D. P., and Black, R. A. (1998). Evidence that tumor necrosis factor alpha converting enzyme is involved in regulated alpha-secretase cleavage of the Alzheimer amyloid protein precursor. *J Biol Chem* 273, 27765-27767.
- Cai, H., Wang, Y., McCarthy, D., Wen, H., Borchelt, D. R., Price, D. L., and Wong, P. C. (2001). BACE1 is the major beta-secretase for generation of Abeta peptides by neurons. *Nat Neurosci* 4, 233-234.
- Cao, X., and Sudhof, T. C. (2001). A transcriptionally [correction of transcriptively] active complex of APP with Fe65 and histone acetyltransferase Tip60. *Science* 293, 115-120.
- Cao, X., and Sudhof, T. C. (2004). Dissection of amyloid-beta precursor protein-dependent transcriptional transactivation. *J Biol Chem* 279, 24601-24611.
- Chapman, P. F., Falinska, A. M., Knevet, S. G., and Ramsay, M. F. (2001). Genes, models and Alzheimer's disease. *Trends Genet* 17, 254-261.
- Chung, H. M., and Struhl, G. (2001). Nicastrin is required for Presenilin-mediated transmembrane cleavage in *Drosophila*. *Nat Cell Biol* 3, 1129-1132.
- Citron, M., Westaway, D., Xia, W., Carlson, G., Diehl, T., Levesque, G., Johnson-Wood, K., Lee, M., Seubert, P., Davis, A., *et al.* (1997). Mutant presenilins of Alzheimer's disease increase production of 42-residue amyloid beta-protein in both transfected cells and transgenic mice. *Nat Med* 3, 67-72.
- Crowley, K. S., Liao, S., Worrell, V. E., Reinhart, G. D., and Johnson, A. E. (1994). Secretory proteins move through the endoplasmic reticulum membrane via an aqueous, gated pore. *Cell* 78, 461-471.
- Crystal, A. S., Morais, V. A., Pierson, T. C., Pijak, D. S., Carlin, D., Lee, V. M., and Doms, R. W. (2003). Membrane topology of gamma-secretase component PEN-2. *J Biol Chem* 278, 20117-20123.
- Cupers, P., Bentahir, M., Craessaerts, K., Orlans, I., Vanderstichele, H., Saftig, P., De Strooper, B., and Annaert, W. (2001a). The discrepancy between presenilin subcellular localization and gamma-secretase processing of amyloid precursor protein. *J Cell Biol* 154, 731-740.
- Cupers, P., Orlans, I., Craessaerts, K., Annaert, W., and De Strooper, B. (2001b). The amyloid precursor protein (APP)-cytoplasmic fragment generated by gamma-secretase is rapidly degraded but distributes partially in a nuclear fraction of neurones in culture. *J Neurochem* 78, 1168-1178.
- Davis, J. A., Naruse, S., Chen, H., Eckman, C., Younkin, S., Price, D. L., Borchelt, D. R., Sisodia, S. S., and Wong, P. C. (1998). An Alzheimer's disease-linked PS1 variant rescues the developmental abnormalities of PS1-deficient embryos. *Neuron* 20, 603-609.

De Strooper, B. (2003). Aph-1, Pen-2, and Nicastrin with Presenilin Generate an Active gamma-Secretase Complex. *Neuron* 38, 9-12.

De Strooper, B., and Annaert, W. (2000). Proteolytic processing and cell biological functions of the amyloid precursor protein. *J Cell Sci* 113 ( Pt 11), 1857-1870.

De Strooper, B., Annaert, W., Cupers, P., Saftig, P., Craessaerts, K., Mumm, J. S., Schroeter, E. H., Schrijvers, V., Wolfe, M. S., Ray, W. J., *et al.* (1999). A presenilin-1-dependent gamma-secretase-like protease mediates release of Notch intracellular domain. *Nature* 398, 518-522.

De Strooper, B., Beullens, M., Contreras, B., Levesque, L., Craessaerts, K., Cordell, B., Moechars, D., Bollen, M., Fraser, P., George-Hyslop, P. S., and Van Leuven, F. (1997). Phosphorylation, subcellular localization, and membrane orientation of the Alzheimer's disease-associated presenilins. *J Biol Chem* 272, 3590-3598.

De Strooper, B., Saftig, P., Craessaerts, K., Vanderstichele, H., Guhde, G., Annaert, W., Von Figura, K., and Van Leuven, F. (1998). Deficiency of presenilin-1 inhibits the normal cleavage of amyloid precursor protein. *Nature* 391, 387-390.

Doan, A., Thinakaran, G., Borchelt, D. R., Slunt, H. H., Ratovitsky, T., Podlisny, M., Selkoe, D. J., Seeger, M., Gandy, S. E., Price, D. L., and Sisodia, S. S. (1996). Protein topology of presenilin 1. *Neuron* 17, 1023-1030.

Ebinu, J. O., and Yankner, B. A. (2002). A RIP tide in neuronal signal transduction. *Neuron* 34, 499-502.

Edbauer, D., Willem, M., Lammich, S., Steiner, H., and Haass, C. (2002a). Insulin-degrading enzyme rapidly removes the beta-amyloid precursor protein intracellular domain (AICD). *J Biol Chem* 277, 13389-13393.

Edbauer, D., Winkler, E., Haass, C., and Steiner, H. (2002b). Presenilin and nicastrin regulate each other and determine amyloid beta-peptide production via complex formation. *Proc Natl Acad Sci U S A* 99, 8666-8671.

Edbauer, D., Winkler, E., Regula, J. T., Pesold, B., Steiner, H., and Haass, C. (2003). Reconstitution of gamma-secretase activity. *Nat Cell Biol* 5, 486-488.

Ermekova, K. S., Zambrano, N., Linn, H., Minopoli, G., Gertler, F., Russo, T., and Sudol, M. (1997). The WW domain of neural protein FE65 interacts with proline-rich motifs in Mena, the mammalian homolog of *Drosophila* enabled. *J Biol Chem* 272, 32869-32877.

Farris, W., Mansourian, S., Chang, Y., Lindsley, L., Eckman, E. A., Frosch, M. P., Eckman, C. B., Tanzi, R. E., Selkoe, D. J., and Guenette, S. (2003). Insulin-degrading enzyme regulates the levels of insulin, amyloid beta-protein, and the beta-amyloid precursor protein intracellular domain in vivo. *Proc Natl Acad Sci U S A* 100, 4162-4167.

- Fortna, R. R., Crystal, A. S., Morais, V. A., Pijak, D. S., Lee, V. M., and Doms, R. W. (2004). Membrane topology and nicastrin-enhanced endoproteolysis of APH-1, a component of the gamma-secretase complex. *J Biol Chem* 279, 3685-3693.
- Fraering, P. C., LaVoie, M. J., Ye, W., Ostaszewski, B. L., Kimberly, W. T., Selkoe, D. J., and Wolfe, M. S. (2004). Detergent-dependent dissociation of active gamma-secretase reveals an interaction between Pen-2 and PS1-NTF and offers a model for subunit organization within the complex. *Biochemistry* 43, 323-333.
- Francis, R., McGrath, G., Zhang, J., Ruddy, D. A., Sym, M., Apfeld, J., Nicoll, M., Maxwell, M., Hai, B., Ellis, M. C., *et al.* (2002). *aph-1* and *pen-2* are required for Notch pathway signaling, gamma-secretase cleavage of betaAPP, and presenilin protein accumulation. *Dev Cell* 3, 85-97.
- Fraser, P. E., Yang, D. S., Yu, G., Levesque, L., Nishimura, M., Arawaka, S., Serpell, L. C., Rogaeva, E., and St George-Hyslop, P. (2000). Presenilin structure, function and role in Alzheimer disease. *Biochim Biophys Acta* 1502, 1-15.
- Fujiki, Y., Hubbard, A. L., Fowler, S., and Lazarow, P. B. (1982). Isolation of intracellular membranes by means of sodium carbonate treatment: application to endoplasmic reticulum. *J Cell Biol* 93, 97-102.
- Fujiwara, T., Oda, K., Yokota, S., Takatsuki, A., and Ikehara, Y. (1988). Brefeldin A causes disassembly of the Golgi complex and accumulation of secretory proteins in the endoplasmic reticulum. *J Biol Chem* 263, 18545-18552.
- Gao, Y., and Pimplikar, S. W. (2001). The gamma -secretase-cleaved C-terminal fragment of amyloid precursor protein mediates signaling to the nucleus. *Proc Natl Acad Sci U S A* 98, 14979-14984.
- Gillespie, S. L., Golde, T. E., and Younkin, S. G. (1992). Secretory processing of the Alzheimer amyloid beta/A4 protein precursor is increased by protein phosphorylation. *Biochem Biophys Res Commun* 187, 1285-1290.
- Golde, T. E., Eckman, C. B., and Younkin, S. G. (2000). Biochemical detection of Abeta isoforms: implications for pathogenesis, diagnosis, and treatment of Alzheimer's disease. *Biochim Biophys Acta* 1502, 172-187.
- Gorelick, F. S., and Shugrue, C. (2001). Exiting the endoplasmic reticulum. *Mol Cell Endocrinol* 177, 13-18.
- Gorlich, D., and Rapoport, T. A. (1993). Protein translocation into proteoliposomes reconstituted from purified components of the endoplasmic reticulum membrane. *Cell* 75, 615-630.
- Goutte, C., Tsunozaki, M., Hale, V. A., and Priess, J. R. (2002). APH-1 is a multipass membrane protein essential for the Notch signaling pathway in *Caenorhabditis elegans* embryos. *Proc Natl Acad Sci U S A* 99, 775-779.

Gu, Y., Chen, F., Sanjo, N., Kawarai, T., Hasegawa, H., Duthie, M., Li, W., Ruan, X., Luthra, A., Mount, H. T., *et al.* (2003). APH-1 interacts with mature and immature forms of presenilins and nicastrin and may play a role in maturation of presenilin.nicastrin complexes. *J Biol Chem* 278, 7374-7380.

Gu, Y., Misonou, H., Sato, T., Dohmae, N., Takio, K., and Ihara, Y. (2001). Distinct intramembrane cleavage of the beta-amyloid precursor protein family resembling gamma-secretase-like cleavage of Notch. *J Biol Chem* 276, 35235-35238.

Gupta-Rossi, N., Six, E., LeBail, O., Logeat, F., Chastagner, P., Olry, A., Israel, A., and Brou, C. (2004). Monoubiquitination and endocytosis direct gamma-secretase cleavage of activated Notch receptor. *J Cell Biol* 166, 73-83.

Haass, C., Schlossmacher, M. G., Hung, A. Y., Vigo-Pelfrey, C., Mellon, A., Ostaszewski, B. L., Lieberburg, I., Koo, E. H., Schenk, D., Teplow, D. B., and *et al.* (1992). Amyloid beta-peptide is produced by cultured cells during normal metabolism. *Nature* 359, 322-325.

Hamman, B. D., Hendershot, L. M., and Johnson, A. E. (1998). BiP maintains the permeability barrier of the ER membrane by sealing the luminal end of the translocon pore before and early in translocation. *Cell* 92, 747-758.

Hanein, D., Matlack, K. E., Jungnickel, B., Plath, K., Kalies, K. U., Miller, K. R., Rapoport, T. A., and Akey, C. W. (1996). Oligomeric rings of the Sec61p complex induced by ligands required for protein translocation. *Cell* 87, 721-732.

Haniu, M., Denis, P., Young, Y., Mendiaz, E. A., Fuller, J., Hui, J. O., Bennett, B. D., Kahn, S., Ross, S., Burgess, T., *et al.* (2000). Characterization of Alzheimer's beta -secretase protein BACE. A pepsin family member with unusual properties. *J Biol Chem* 275, 21099-21106.

Hardy, J. (1997). Amyloid, the presenilins and Alzheimer's disease. *Trends Neurosci* 20, 154-159.

Hartmann, D., de Strooper, B., Serneels, L., Craessaerts, K., Herreman, A., Annaert, W., Umans, L., Lubke, T., Lena Illert, A., von Figura, K., and Saftig, P. (2002). The disintegrin/metalloprotease ADAM 10 is essential for Notch signalling but not for alpha-secretase activity in fibroblasts. *Hum Mol Genet* 11, 2615-2624.

Hegde, R. S., Voigt, S., Rapoport, T. A., and Lingappa, V. R. (1998). TRAM regulates the exposure of nascent secretory proteins to the cytosol during translocation into the endoplasmic reticulum. *Cell* 92, 621-631.

Herreman, A., Hartmann, D., Annaert, W., Saftig, P., Craessaerts, K., Serneels, L., Umans, L., Schrijvers, V., Checler, F., Vanderstichele, H., *et al.* (1999). Presenilin 2 deficiency causes a mild pulmonary phenotype and no changes in amyloid precursor protein processing but enhances the embryonic

lethal phenotype of presenilin 1 deficiency. *Proc Natl Acad Sci U S A* 96, 11872-11877.

Herreman, A., Van Gassen, G., Bentahir, M., Nyabi, O., Craessaerts, K., Mueller, U., Annaert, W., and De Strooper, B. (2003). gamma-Secretase activity requires the presenilin-dependent trafficking of nicastrin through the Golgi apparatus but not its complex glycosylation. *J Cell Sci* 116, 1127-1136.

High, S. (1995). Protein translocation at the membrane of the endoplasmic reticulum. *Prog Biophys Mol Biol* 63, 233-250.

High, S., and Dobberstein, B. (1992). Mechanisms that determine the transmembrane disposition of proteins. *Curr Opin Cell Biol* 4, 581-586.

Hu, Y., and Fortini, M. E. (2003). Different cofactor activities in gamma-secretase assembly: evidence for a nicastrin-Aph-1 subcomplex. *J Cell Biol* 161, 685-690.

Hu, Y., Ye, Y., and Fortini, M. E. (2002). Nicastrin is required for gamma-secretase cleavage of the Drosophila Notch receptor. *Dev Cell* 2, 69-78.

Hua, X., Wu, J., Goldstein, J. L., Brown, M. S., and Hobbs, H. H. (1995). Structure of the human gene encoding sterol regulatory element binding protein-1 (SREBF1) and localization of SREBF1 and SREBF2 to chromosomes 17p11.2 and 22q13. *Genomics* 25, 667-673.

Huse, J. T., and Doms, R. W. (2001). Neurotoxic traffic: uncovering the mechanics of amyloid production in Alzheimer's disease. *Traffic* 2, 75-81.

Hussain, I., Powell, D., Howlett, D. R., Tew, D. G., Meek, T. D., Chapman, C., Gloger, I. S., Murphy, K. E., Southan, C. D., Ryan, D. M., *et al.* (1999). Identification of a novel aspartic protease (Asp 2) as beta-secretase. *Mol Cell Neurosci* 14, 419-427.

Iwatsubo, T. (2004). The gamma-secretase complex: machinery for intramembrane proteolysis. *Curr Opin Neurobiol* 14, 379-383.

Johnson, A. E. (2003). Maintaining the permeability barrier during protein trafficking at the endoplasmic reticulum membrane. *Biochem Soc Trans* 31, 1227-1231.

Johnson, A. E., and van Waes, M. A. (1999). The translocon: a dynamic gateway at the ER membrane. *Annu Rev Cell Dev Biol* 15, 799-842.

Kano, F., Sako, Y., Tagaya, M., Yanagida, T., and Murata, M. (2000). Reconstitution of brefeldin A-induced golgi tubulation and fusion with the endoplasmic reticulum in semi-intact chinese hamster ovary cells. *Mol Biol Cell* 11, 3073-3087.

Keenan, R. J., Freymann, D. M., Stroud, R. M., and Walter, P. (2001). The signal recognition particle. *Annu Rev Biochem* 70, 755-775.

- Kehoe, P., Wavrant-De Vrieze, F., Crook, R., Wu, W. S., Holmans, P., Fenton, I., Spurlock, G., Norton, N., Williams, H., Williams, N., *et al.* (1999). A full genome scan for late onset Alzheimer's disease. *Hum Mol Genet* 8, 237-245.
- Kesavapany, S., Banner, S. J., Lau, K. F., Shaw, C. E., Miller, C. C., Cooper, J. D., and McLoughlin, D. M. (2002). Expression of the Fe65 adapter protein in adult and developing mouse brain. *Neuroscience* 115, 951-960.
- Khvotchev, M., and Sudhof, T. C. (2004). Proteolytic processing of APP by secretases does not require cell-surface transport. *J Biol Chem* 279, 15037-15043.
- Kimberly, W. T., LaVoie, M. J., Ostaszewski, B. L., Ye, W., Wolfe, M. S., and Selkoe, D. J. (2002). Complex N-linked glycosylated nicastrin associates with active gamma-secretase and undergoes tight cellular regulation. *J Biol Chem* 277, 35113-35117.
- Kimberly, W. T., LaVoie, M. J., Ostaszewski, B. L., Ye, W., Wolfe, M. S., and Selkoe, D. J. (2003). Gamma-secretase is a membrane protein complex comprised of presenilin, nicastrin, Aph-1, and Pen-2. *Proc Natl Acad Sci U S A* 100, 6382-6387.
- Kimberly, W. T., Zheng, J. B., Guenette, S. Y., and Selkoe, D. J. (2001). The intracellular domain of the beta-amyloid precursor protein is stabilized by Fe65 and translocates to the nucleus in a notch-like manner. *J Biol Chem* 276, 40288-40292.
- Kinoshita, A., Whelan, C. M., Berezovska, O., and Hyman, B. T. (2002). The gamma secretase-generated carboxyl-terminal domain of the amyloid precursor protein induces apoptosis via Tip60 in H4 cells. *J Biol Chem* 277, 28530-28536.
- Kitazume, S., Tachida, Y., Oka, R., Shirotani, K., Saido, T. C., and Hashimoto, Y. (2001). Alzheimer's beta-secretase, beta-site amyloid precursor protein-cleaving enzyme, is responsible for cleavage secretion of a Golgi-resident sialyltransferase. *Proc Natl Acad Sci U S A* 98, 13554-13559.
- Klappa, P., Freedman, R. B., and Zimmermann, R. (1995). Protein disulphide isomerase and a luminal cyclophilin-type peptidyl prolyl cis-trans isomerase are in transient contact with secretory proteins during late stages of translocation. *Eur J Biochem* 232, 755-764.
- Klausner, R. D., Donaldson, J. G., and Lippincott-Schwartz, J. (1992). Brefeldin A: insights into the control of membrane traffic and organelle structure. *J Cell Biol* 116, 1071-1080.
- Knauer, R., and Lehle, L. (1999). The oligosaccharyltransferase complex from yeast. *Biochim Biophys Acta* 1426, 259-273.
- Koike, H., Tomioka, S., Sorimachi, H., Saido, T. C., Maruyama, K., Okuyama, A., Fujisawa-Sehara, A., Ohno, S., Suzuki, K., and Ishiura, S. (1999).

Membrane-anchored metalloprotease MDC9 has an alpha-secretase activity responsible for processing the amyloid precursor protein. *Biochem J* 343 Pt 2, 371-375.

Komano, H., Seeger, M., Gandy, S., Wang, G. T., Krafft, G. A., and Fuller, R. S. (1998). Involvement of cell surface glycosyl-phosphatidylinositol-linked aspartyl proteases in alpha-secretase-type cleavage and ectodomain solubilization of human Alzheimer beta-amyloid precursor protein in yeast. *J Biol Chem* 273, 31648-31651.

Kraft, C. (2001) A molecular analysis of the ER components associated with a membrane-inserted fragment of the amyloid precursor protein. Diploma Thesis., University of Basel.

Lai, A., Sisodia, S. S., and Trowbridge, I. S. (1995). Characterization of sorting signals in the beta-amyloid precursor protein cytoplasmic domain. *J Biol Chem* 270, 3565-3573.

Lammich, S., Kojro, E., Postina, R., Gilbert, S., Pfeiffer, R., Jasionowski, M., Haass, C., and Fahrenholz, F. (1999). Constitutive and regulated alpha-secretase cleavage of Alzheimer's amyloid precursor protein by a disintegrin metalloprotease. *Proc Natl Acad Sci U S A* 96, 3922-3927.

Lansbury, P. T., Jr. (1997). Structural neurology: are seeds at the root of neuronal degeneration? *Neuron* 19, 1151-1154.

LaVoie, M. J., Fraering, P. C., Ostaszewski, B. L., Ye, W., Kimberly, W. T., Wolfe, M. S., and Selkoe, D. J. (2003). Assembly of the gamma-secretase complex involves early formation of an intermediate subcomplex of Aph-1 and nicastrin. *J Biol Chem* 278, 37213-37222.

Le Gall, S., Neuhof, A., and Rapoport, T. (2004). The endoplasmic reticulum membrane is permeable to small molecules. *Mol Biol Cell* 15, 447-455.

Lentz, B. R., and Lee, J. K. (1999). Poly(ethylene glycol) (PEG)-mediated fusion between pure lipid bilayers: a mechanism in common with viral fusion and secretory vesicle release? *Mol Membr Biol* 16, 279-296.

Li, X., and Greenwald, I. (1998). Additional evidence for an eight-transmembrane-domain topology for *Caenorhabditis elegans* and human presenilins. *Proc Natl Acad Sci U S A* 95, 7109-7114.

Li, Y. M., Lai, M. T., Xu, M., Huang, Q., DiMuzio-Mower, J., Sardana, M. K., Shi, X. P., Yin, K. C., Shafer, J. A., and Gardell, S. J. (2000a). Presenilin 1 is linked with gamma-secretase activity in the detergent solubilized state. *Proc Natl Acad Sci U S A* 97, 6138-6143.

Li, Y. M., Xu, M., Lai, M. T., Huang, Q., Castro, J. L., DiMuzio-Mower, J., Harrison, T., Lellis, C., Nadin, A., Neduelil, J. G., *et al.* (2000b). Photoactivated gamma-secretase inhibitors directed to the active site covalently label presenilin 1. *Nature* 405, 689-694.

Lichtenthaler, S. F., Dominguez, D. I., Westmeyer, G. G., Reiss, K., Haass, C., Saftig, P., De Strooper, B., and Seed, B. (2003). The cell adhesion protein P-selectin glycoprotein ligand-1 is a substrate for the aspartyl protease BACE1. *J Biol Chem* 278, 48713-48719.

Lippincott-Schwartz, J., Yuan, L., Tipper, C., Amherdt, M., Orci, L., and Klausner, R. D. (1991). Brefeldin A's effects on endosomes, lysosomes, and the TGN suggest a general mechanism for regulating organelle structure and membrane traffic. *Cell* 67, 601-616.

Lippincott-Schwartz, J., Yuan, L. C., Bonifacino, J. S., and Klausner, R. D. (1989). Rapid redistribution of Golgi proteins into the ER in cells treated with brefeldin A: evidence for membrane cycling from Golgi to ER. *Cell* 56, 801-813.

Longin, A., Souchier C., Ffrench M. and Byron P. A. (1993). Comparison of anti-fading agents used in fluorescence microscopy: image analysis and laser confocal microscopy study. *J Histochem Cytochem* 41, 1833-1840.

Lopez-Schier, H., and St Johnston, D. (2002). Drosophila nicastrin is essential for the intramembranous cleavage of notch. *Dev Cell* 2, 79-89.

Lowther, W. T., and Matthews, B. W. (2002). Metalloaminopeptidases: common functional themes in disparate structural surroundings. *Chem Rev* 102, 4581-4608.

Maley, F., Trimble, R. B., Tarentino, A. L., and Plummer, T. H., Jr. (1989). Characterization of glycoproteins and their associated oligosaccharides through the use of endoglycosidases. *Anal Biochem* 180, 195-204.

Maltese, W. A., Wilson, S., Tan, Y., Suomensaari, S., Sinha, S., Barbour, R., and McConlogue, L. (2001). Retention of the Alzheimer's amyloid precursor fragment C99 in the endoplasmic reticulum prevents formation of amyloid beta-peptide. *J Biol Chem* 276, 20267-20279.

Martoglio, B. (2003). Intramembrane proteolysis and post-targeting functions of signal peptides. *Biochem Soc Trans* 31, 1243-1247.

Martoglio, B., and Dobberstein, B. (1998). Signal sequences: more than just greasy peptides. *Trends Cell Biol* 8, 410-415.

Mattson, M. P. (2004). Pathways towards and away from Alzheimer's disease. *Nature* 430, 631-639.

Meacock, S. L., Greenfield, J. J., and High, S. (2000). Protein targeting and translocation at the endoplasmic reticulum membrane--through the eye of a needle? *Essays Biochem* 36, 1-13.

Minopoli, G., de Candia, P., Bonetti, A., Faraonio, R., Zambrano, N., and Russo, T. (2001). The beta-amyloid precursor protein functions as a cytosolic anchoring site that prevents Fe65 nuclear translocation. *J Biol Chem* 276, 6545-6550.

- Nakai, T., Yamasaki, A., Sakaguchi, M., Kosaka, K., Mihara, K., Amaya, Y., and Miura, S. (1999). Membrane topology of Alzheimer's disease-related presenilin 1. Evidence for the existence of a molecular species with a seven membrane-spanning and one membrane-embedded structure. *J Biol Chem* 274, 23647-23658.
- Nilsson, I., and von Heijne, G. (2000). Glycosylation efficiency of Asn-Xaa-Thr sequons depends both on the distance from the C terminus and on the presence of a downstream transmembrane segment. *J Biol Chem* 275, 17338-17343.
- Palade, G. (1975). Intracellular aspects of the process of protein synthesis. *Science* 189, 347-358.
- Pasternak, S. H., Bagshaw, R. D., Guiral, M., Zhang, S., Ackerley, C. A., Pak, B. J., Callahan, J. W., and Mahuran, D. J. (2003a). Presenilin-1, nicastrin, APP and gamma-secretase activity are co-localized in the lysosomal membrane. *J Biol Chem*.
- Pasternak, S. H., Bagshaw, R. D., Guiral, M., Zhang, S., Ackerley, C. A., Pak, B. J., Callahan, J. W., and Mahuran, D. J. (2003b). Presenilin, Nicastrin and Beta-Amyloid Production in the Endosomal/ Lysosomal System: Toward a Unifying Model of Alzheimer's Disease. *J Biol Chem*.
- Petit, A., Bihel, F., Alves da Costa, C., Pourquoi, O., Checler, F., and Kraus, J. L. (2001). New protease inhibitors prevent gamma-secretase-mediated production of Abeta40/42 without affecting Notch cleavage. *Nat Cell Biol* 3, 507-511.
- Pinnix, I., Musunuru, U., Tun, H., Sridharan, A., Golde, T., Eckman, C., Ziani-Cherif, C., Onstead, L., and Sambamurti, K. (2001). A novel gamma -secretase assay based on detection of the putative C-terminal fragment-gamma of amyloid beta protein precursor. *J Biol Chem* 276, 481-487.
- Plutner, H., Cox, A. D., Pind, S., Khosravi-Far, R., Bourne, J. R., Schwaninger, R., Der, C. J., and Balch, W. E. (1991). Rab1b regulates vesicular transport between the endoplasmic reticulum and successive Golgi compartments. *J Cell Biol* 115, 31-43.
- Ponting, C. P., Hutton, M., Nyborg, A., Baker, M., Jansen, K., and Golde, T. E. (2002). Identification of a novel family of presenilin homologues. *Hum Mol Genet* 11, 1037-1044.
- Rapoport, T. A., Jungnickel, B., and Kutay, U. (1996a). Protein transport across the eukaryotic endoplasmic reticulum and bacterial inner membranes. *Annu Rev Biochem* 65, 271-303.
- Rapoport, T. A., Matlack, K. E., Plath, K., Misselwitz, B., and Staeck, O. (1999). Posttranslational protein translocation across the membrane of the endoplasmic reticulum. *Biol Chem* 380, 1143-1150.

Rapoport, T. A., Rolls, M. M., and Jungnickel, B. (1996b). Approaching the mechanism of protein transport across the ER membrane. *Curr Opin Cell Biol* 8, 499-504.

Rawson, R. B. (2002). Regulated intramembrane proteolysis: from the endoplasmic reticulum to the nucleus. *Essays Biochem* 38, 155-168.

Ray, W. J., Yao, M., Mumm, J., Schroeter, E. H., Saftig, P., Wolfe, M., Selkoe, D. J., Kopan, R., and Goate, A. M. (1999). Cell surface presenilin-1 participates in the gamma-secretase-like proteolysis of Notch. *J Biol Chem* 274, 36801-36807.

Sabo, S. L., Ikin, A. F., Buxbaum, J. D., and Greengard, P. (2001). The Alzheimer amyloid precursor protein (APP) and FE65, an APP-binding protein, regulate cell movement. *J Cell Biol* 153, 1403-1414.

Sabo, S. L., Ikin, A. F., Buxbaum, J. D., and Greengard, P. (2003). The amyloid precursor protein and its regulatory protein, FE65, in growth cones and synapses in vitro and in vivo. *J Neurosci* 23, 5407-5415.

Sastre, M., Steiner, H., Fuchs, K., Capell, A., Multhaup, G., Condron, M. M., Teplow, D. B., and Haass, C. (2001). Presenilin-dependent gamma-secretase processing of beta-amyloid precursor protein at a site corresponding to the S3 cleavage of Notch. *EMBO Rep* 2, 835-841.

Sato, T., Dohmae, N., Qi, Y., Kakuda, N., Misonou, H., Mitsumori, R., Maruyama, H., Koo, E. H., Haass, C., Takio, K., *et al.* (2003). Potential link between amyloid beta -protein 42 and C-terminal fragment gamma 49-99 of beta -amyloid precursor protein. *J Biol Chem* 278, 24294-24301.

Schlondorff, J., and Blobel, C. P. (1999). Metalloprotease-disintegrins: modular proteins capable of promoting cell-cell interactions and triggering signals by protein-ectodomain shedding. *J Cell Sci* 112 ( Pt 21), 3603-3617.

Schroeter, E. H., Kisslinger, J. A., and Kopan, R. (1998). Notch-1 signalling requires ligand-induced proteolytic release of intracellular domain. *Nature* 393, 382-386.

Sciaky, N., Presley, J., Smith, C., Zaal, K. J., Cole, N., Moreira, J. E., Terasaki, M., Siggia, E., and Lippincott-Schwartz, J. (1997). Golgi tubule traffic and the effects of brefeldin A visualized in living cells. *J Cell Biol* 139, 1137-1155.

Selkoe, D., and Kopan, R. (2003). Notch and Presenilin: Regulated Intramembrane Proteolysis Links Development and Degeneration. *Annu Rev Neurosci* 26, 565-597.

Selkoe, D. J. (1996). Amyloid beta-protein and the genetics of Alzheimer's disease. *J Biol Chem* 271, 18295-18298.

Selkoe, D. J. (1999). Translating cell biology into therapeutic advances in Alzheimer's disease. *Nature* 399, A23-31.

Shearman, M. S., Beher, D., Clarke, E. E., Lewis, H. D., Harrison, T., Hunt, P., Nadin, A., Smith, A. L., Stevenson, G., and Castro, J. L. (2000). L-685,458, an aspartyl protease transition state mimic, is a potent inhibitor of amyloid beta-protein precursor gamma-secretase activity. *Biochemistry* 39, 8698-8704.

Sherrington, R., Rogaev, E. I., Liang, Y., Rogaeva, E. A., Levesque, G., Ikeda, M., Chi, H., Lin, C., Li, G., Holman, K., and et al. (1995). Cloning of a gene bearing missense mutations in early-onset familial Alzheimer's disease. *Nature* 375, 754-760.

Siman, R., and Velji, J. (2003). Localization of presenilin-nicastrin complexes and gamma-secretase activity to the trans-Golgi network. *J Neurochem* 84, 1143-1153.

Sinha, S., Anderson, J. P., Barbour, R., Basi, G. S., Caccavello, R., Davis, D., Doan, M., Dovey, H. F., Frigon, N., Hong, J., et al. (1999). Purification and cloning of amyloid precursor protein beta-secretase from human brain. *Nature* 402, 537-540.

Sisodia, S. S., and St George-Hyslop, P. H. (2002). gamma-Secretase, Notch, Abeta and Alzheimer's disease: where do the presenilins fit in? *Nat Rev Neurosci* 3, 281-290.

Sorbi, S., Forleo, P., Tedde, A., Cellini, E., Ciantelli, M., Bagnoli, S., and Nacmias, B. (2001). Genetic risk factors in familial Alzheimer's disease. *Mech Ageing Dev* 122, 1951-1960.

Steiner, H., Kostka, M., Romig, H., Basset, G., Pesold, B., Hardy, J., Capell, A., Meyn, L., Grim, M. L., Baumeister, R., et al. (2000). Glycine 384 is required for presenilin-1 function and is conserved in bacterial polytopic aspartyl proteases. *Nat Cell Biol* 2, 848-851.

Steiner, H., Romig, H., Pesold, B., Philipp, U., Baader, M., Citron, M., Loetscher, H., Jacobsen, H., and Haass, C. (1999). Amyloidogenic function of the Alzheimer's disease-associated presenilin 1 in the absence of endoproteolysis. *Biochemistry* 38, 14600-14605.

Takasugi, N., Tomita, T., Hayashi, I., Tsuruoka, M., Niimura, M., Takahashi, Y., Thinakaran, G., and Iwatsubo, T. (2003). The role of presenilin cofactors in the gamma-secretase complex. *Nature* 422, 438-441.

Thinakaran, G., Borchelt, D. R., Lee, M. K., Slunt, H. H., Spitzer, L., Kim, G., Ratovitsky, T., Davenport, F., Nordstedt, C., Seeger, M., et al. (1996). Endoproteolysis of presenilin 1 and accumulation of processed derivatives in vivo. *Neuron* 17, 181-190.

Thinakaran, G., Harris, C. L., Ratovitski, T., Davenport, F., Slunt, H. H., Price, D. L., Borchelt, D. R., and Sisodia, S. S. (1997). Evidence that levels of presenilins (PS1 and PS2) are coordinately regulated by competition for limiting cellular factors. *J Biol Chem* 272, 28415-28422.

Thinakaran, G., Regard, J. B., Bouton, C. M., Harris, C. L., Price, D. L., Borchelt, D. R., and Sisodia, S. S. (1998). Stable association of presenilin derivatives and absence of presenilin interactions with APP. *Neurobiol Dis* 4, 438-453.

Van den Berg, B., Clemons, W. M., Jr., Collinson, I., Modis, Y., Hartmann, E., Harrison, S. C., and Rapoport, T. A. (2004). X-ray structure of a protein-conducting channel. *Nature* 427, 36-44.

Vassar, R., Bennett, B. D., Babu-Khan, S., Kahn, S., Mendiaz, E. A., Denis, P., Teplow, D. B., Ross, S., Amarante, P., Loeloff, R., *et al.* (1999). Beta-secretase cleavage of Alzheimer's amyloid precursor protein by the transmembrane aspartic protease BACE. *Science* 286, 735-741.

von Heijne, G. (1995). Protein sorting signals: simple peptides with complex functions. *EXS* 73, 67-76.

Walsh, D. M., Fadeeva, J. V., LaVoie, M. J., Paliga, K., Eggert, S., Kimberly, W. T., Wasco, W., and Selkoe, D. J. (2003). gamma-Secretase Cleavage and Binding to FE65 Regulate the Nuclear Translocation of the Intracellular C-Terminal Domain (ICD) of the APP Family of Proteins. *Biochemistry* 42, 6664-6673.

Wang, L., and Dobberstein, B. (1999). Oligomeric complexes involved in translocation of proteins across the membrane of the endoplasmic reticulum. *FEBS Lett* 457, 316-322.

Wang, X., Sato, R., Brown, M. S., Hua, X., and Goldstein, J. L. (1994). SREBP-1, a membrane-bound transcription factor released by sterol-regulated proteolysis. *Cell* 77, 53-62.

Weidemann, A., Eggert, S., Reinhard, F. B., Vogel, M., Paliga, K., Baier, G., Masters, C. L., Beyreuther, K., and Evin, G. (2002). A novel epsilon-cleavage within the transmembrane domain of the Alzheimer amyloid precursor protein demonstrates homology with Notch processing. *Biochemistry* 41, 2825-2835.

Weihofen, A., Binns, K., Lemberg, M. K., Ashman, K., and Martoglio, B. (2002). Identification of signal peptide peptidase, a presenilin-type aspartic protease. *Science* 296, 2215-2218.

Weihofen, A., Lemberg, M. K., Friedmann, E., Rueeger, H., Schmitz, A., Paganetti, P., Rovelli, G., and Martoglio, B. (2003). Targeting Presenilin-type Aspartic Protease Signal Peptide Peptidase with gamma -Secretase Inhibitors. *J Biol Chem* 278, 16528-16533.

Weihofen, A., and Martoglio, B. (2003). Intramembrane-cleaving proteases: controlled liberation of proteins and bioactive peptides. *Trends Cell Biol* 13, 71-78.

Weskamp, G., Cai, H., Brodie, T. A., Higashyama, S., Manova, K., Ludwig, T., and Blobel, C. P. (2002). Mice lacking the metalloprotease-disintegrin MDC9

(ADAM9) have no evident major abnormalities during development or adult life. *Mol Cell Biol* 22, 1537-1544.

Wilson, C. A., Doms, R. W., and Lee, V. M. (2003). Distinct presenilin-dependent and presenilin-independent gamma-secretases are responsible for total cellular Abeta production. *J Neurosci Res* 74, 361-369.

Wilson, C. A., Doms, R. W., Zheng, H., and Lee, V. M. (2002). Presenilins are not required for A beta 42 production in the early secretory pathway. *Nat Neurosci* 5, 849-855.

Wilson, R., Allen, A. J., Oliver, J., Brookman, J. L., High, S., and Bulleid, N. J. (1995). The translocation, folding, assembly and redox-dependent degradation of secretory and membrane proteins in semi-permeabilized mammalian cells. *Biochem J* 307 ( Pt 3), 679-687.

Wolfe, M. S., and Selkoe, D. J. (2002). Biochemistry. Intramembrane proteases--mixing oil and water. *Science* 296, 2156-2157.

Wolfe, M. S., Xia, W., Ostaszewski, B. L., Diehl, T. S., Kimberly, W. T., and Selkoe, D. J. (1999). Two transmembrane aspartates in presenilin-1 required for presenilin endoproteolysis and gamma-secretase activity. *Nature* 398, 513-517.

Yan, R., Bienkowski, M. J., Shuck, M. E., Miao, H., Tory, M. C., Pauley, A. M., Brashier, J. R., Stratman, N. C., Mathews, W. R., Buhl, A. E., *et al.* (1999). Membrane-anchored aspartyl protease with Alzheimer's disease beta-secretase activity. *Nature* 402, 533-537.

Yu, C., Kim, S. H., Ikeuchi, T., Xu, H., Gasparini, L., Wang, R., and Sisodia, S. S. (2001). Characterization of a presenilin-mediated amyloid precursor protein carboxyl-terminal fragment gamma. Evidence for distinct mechanisms involved in gamma-secretase processing of the APP and Notch1 transmembrane domains. *J Biol Chem* 276, 43756-43760.

Yu, G., Nishimura, M., Arawaka, S., Levitan, D., Zhang, L., Tandon, A., Song, Y. Q., Rogaeva, E., Chen, F., Kawarai, T., *et al.* (2000). Nicastrin modulates presenilin-mediated notch/glp-1 signal transduction and betaAPP processing. *Nature* 407, 48-54.

Zambrano, N., Minopoli, G., de Candia, P., and Russo, T. (1998). The Fe65 adaptor protein interacts through its PID1 domain with the transcription factor CP2/LSF/LBP1. *J Biol Chem* 273, 20128-20133.

Zhang, Z., Nadeau, P., Song, W., Donoviel, D., Yuan, M., Bernstein, A., and Yankner, B. A. (2000). Presenilins are required for gamma-secretase cleavage of beta-APP and transmembrane cleavage of Notch-1. *Nat Cell Biol* 2, 463-465.

Zhao, Q., and Lee, F. S. (2003). The transcriptional activity of the APP intracellular domain-Fe65 complex is inhibited by activation of the NF-kappaB pathway. *Biochemistry* 42, 3627-3634.

## Appendix 1.1

**Table 1.1: Primers used to generate *HindIII*-ss-CT99-*EcoRV* and CT72**

Primer	Sequence 5'-3'
pSputK <i>HindIII</i> for	CAC TAT AGA ATA CAA GCT TCG
pSputK <i>EcoRV</i> rev	GAT CTG ATA TCG CGA TTC TTA
CT72 for	*GGT GCA ATC ATT GGA CTC ATG GTG GGC
CT72 rev	CTA GTT CTG CAT CTG CTC AAA C

\* indicates 5' phosphorylation

**Table 1.2: Primers used to generate substitution mutations**

Primer	Sequence 5'-3'
CT72 M1I for	AGC CCG GGG GAT CCG CCC ATC GGT GCA ATC ATT GGA CTC
CT72 M1I rev	GAG TCC AAT GAT TGC ACC GAT GGG CGG ATC CCC CGG GCT
CT72 M8I for	GGG TGC AAT CAT TGG ACT CAT CGT GGG CGG TGT TGT CAT AG
CT72 M8I rev	CTA TGA CAA CAC CGC CCA CGA TGA GTC CAA TGA TTG CAC CC
CT72 M24I for	GAT CGT CAT CAC CTT GGT GAT CCT GAA GAA GAA ACA GTA C
CT72 M24I rev	GTA CTG TTT CTT CTT CAG GAT CAC CAA GGT GAT GAC GAT C
CT72 T16M for	GGT GTT GTC ATA GCG ATG GTG ATC GTC ATC ACC
CT72 T16M rev	GGT GAT GAC GAT CAC CAT CGC TAT GAC AAC ACC
CT72 A15M for	GGC GGT GTT GTC ATA ATG ACA GTG ATC GTC ATC
CT72 A15M rev	GAT GAC GAT CTC TGT CAT TAT CAG AAC ACC GCC
CT72 I14M for	ATC GTG GGC GGT GTT GTC ATG GCG ACA GTG ATC GTC ATC
CT72 I14M rev	GAT GAC GAT CAC TGT CGC CAT GAC AAC ACC GCC CAG GAT
CT72 V13M for	CAT CGT GGG CGG TGT TAT GAT AGC GAC AGT GAT CG
CT72 V13M rev	CGA TCA CTG TCG CTA TCA TAA CAC CGC CCA CGA TG
CT72 V12M for	GGA CTC ATC GTG GGC GGT ATG GTC ATA GCG ACA GTG ATC
CT72 V12M rev	GAT CAC TGT CGC TAT GAC CAT ACC GCC CAC GAT GAG TCC
CT72 P62Q for	GCA GAA CGG CTA CGA AAA TCA AAC CTA CAA GTT CTT TG
CT72 P62Q rev	CAA AGA ACT TGT AGG TTT GAT TTT CGT AGC CGT TCT GC
ss- <sup>HA-Gly</sup> CT99 M1I for	CCC AGT TTA AAC TTA ATA GAC AGC AAA GGT TCG
ss- <sup>HA-Gly</sup> CT99 M1I rev	CGA ACC TTT GCT GTC TAT TAA GTT TAA ACT GGG

**Table 1.3: Primers used to generate tagged APP derivatives**

Primer	Sequence 5'-3'
HA-Gly for	GTG GTG TCG ACC CCC TAC CCA TAC GAC GTC CCA GAC TAC GCT AAT TCA ACA ATG GAT GCA GAA TTC CGA C
HA-Gly rev	GTC GGA ATT CTG CAT CCA TTG TTG AAT TAG CGT AGT CTG GGA CGT CGT ATG GGT AGG GGG TCG ACA CCA C
HA for	CAG ATG CAG AAC ATG TAC CCA TAC GAC GTC CCA GAC TAC GCT TAG ACC CCC GCC
HA rev	GGC GG GGT CTA AGC GTA GTC TGG GAC GTC GTA TGG GTA CAT GTT CTG CAT CTG
Ospin1 for	GTG TCG ACC CCC AAC GGG ACC GAG GGC CCA AAC TTC TACT AC CCA TAC GAC
Opsin1 rev	GTC GTA TGG GTA GTA GAA GTT TGG GCC CTC GGT CCC GTT GGG GGT CGA CAC
Opsin2 for	GGC CCA AAC TTC TAC GTG CCT TTC TCC ACC AAG ACG TAC CCA TAC GAC GTC
Opsin2 rev	GAC GTC GTA TGG GTA CGT CTT GTT GGA GAA AGG CAC GTA GAA GTT TGG GCC
Flag for	GGT GTC GAC CCC CGA CTA CAA GGA CGA CGA CGA CAA GTA CCC ATA CGA CG
Flag rev	CGT CGT ATG GGT ACT TGT CGT CGT CGT CCT TGT AGT CGG GGG TCG ACA CC
T88/96/104STOP for	GGC GGT GTT GTC ATA GCG TAG GTGATC GTC ATC ACC TTG
T88/96/104STOP rev	CAA GGT GAT GAC GAT CAC CTA CGC TAT GAC AAC ACC GCC

**Table 1.4: Primers used for template production**

Primer	Sequence
-150 T7 PCRscript	CG TCC CAT TCG CCA TTC AGG
-150 T7 pcDNA3.1(+)	GTT TTG GCA CCA AAA TCA ACG
C99 rev	CTA GTT CTG CAT CTG CTC AAA G
C99 CT-HA rev	CTA AGC GTA GTC TGG GAC GTC G
C99 $\gamma$ -sec NT rev	CTA CGC TAT GAC AAC ACC GCC

**Table 1.5: Primers used for truncation**

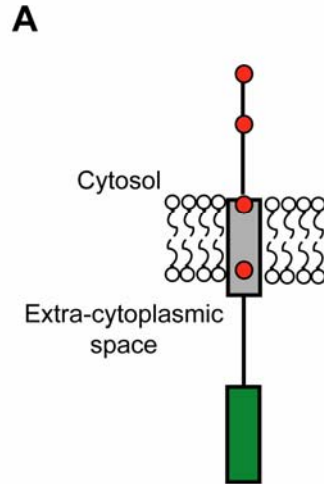
Primer	Sequence 5'-3'
APP-trunc	CTA GTT CTG CAT CTG CTC AAA C

## Appendix 2.1

### ss-CT99 derivative.

**A.** Diagrammatic representation of ss-CT99. Approximate positions of methionine residues shown as red circles, transmembrane domain indicated by grey rectangle, additional APP sequence indicated by black line, pre-prolactin signal sequence shown as green rectangle.

**B.** DNA and amino acid sequence of construct in vector pcDNA3.1(+).



### B

#### pre-prolactin signal sequence

ATG GAC AGC AAA GGT TCG TCG CAG AAA GGG TCC CGC CTG CTC CTG CTG CTG  
 1 Met Asp Ser Lys Gly Ser Ser Gln Lys Gly Ser Arg Leu Leu Leu Leu Leu

#### APP seq

GTG GTG TCA AAT CTA CTC TTG TGC CAG GGT GTG GTG TCG ACC CCC GAT GCA  
 18 Val Val Ser Asn Leu Leu Leu Cys Gln Gly Val Val Ser Thr Pro Asp Ala

GAA TTC CGA CAT GAC TCA GGA TAT GAA GTT CAT CAT CAA AAA TTG GTG TTC  
 35 Glu Phe Arg His Asp Ser Gly Tyr Glu Val His His Gln Lys Leu Val Phe

TTT GCA GAA GAT GTG GGT TCA AAC AAA GGT GCA ATC ATT GGA CTC ATG GTG  
 52 Phe Ala Glu Asp Val Gly Ser Asn Lys Gly Ala Ile Ile Gly Leu Met Val

#### $\gamma$ -cleavage

GGC GGT GTT GTC ATA GCG ACA GTG ATC GTC ATC ACC TTG GTG ATG CTG AAG  
 69 Gly Gly Val Val Ile Ala Thr Val Ile Val Ile Thr Leu Val Met Leu Lys

AAG AAA CAG TAC ACA TCC ATT CAT CAT GGT GTG GTG GAG GTT GAC GCC GCT  
 86 Lys Lys Gln Tyr Thr Ser Ile His His Gly Val Val Glu Val Asp Ala Ala

GTC ACC CCA GAG GAG CGC CAC CTG TCC AAG ATG CAG CAG AAC GGC TAC GAA  
 103 Val Thr Pro Glu Glu Arg His Leu Ser Lys Met Gln Gln Asn Gly Tyr Glu

AAT CCA ACC TAC AAG TTC TTT GAG CAG ATG CAG AAC TAG  
 120 Asn Pro Thr Tyr Lys Phe Phe Glu Gln Met Gln Asn  $\Psi\Psi\Psi$

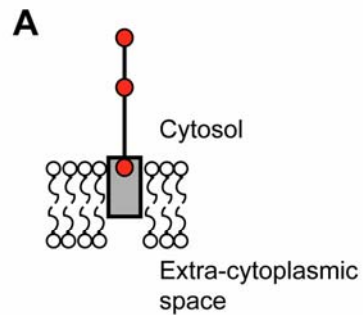


## Appendix 2.3

### Met<sup>CT57</sup> APP-derivative.

**A.** Diagrammatic representation of Met<sup>CT57</sup>. Approximate positions of methionine residues shown as red circles, transmembrane domain indicated by grey rectangle.

**B.** DNA and amino acid sequences of construct (in PCR-Script vector).



### B

#### APP sequence

```

atg aca gtg atc gtc atc acc ttg gtg atg ctg aag aag aaa cag tac aca
1 Met Thr Val Ile Val Ile Thr Leu Val Met Leu Lys Lys Lys Gln Tyr Thr

tcc att cat cat ggt gtg gtg gag gtt gac gcc gct gtc acc cca gag gag
18 Ser Ile His His Gly Val Val Glu Val Asp Ala Ala Val Thr Pro Glu Glu

cgc cac ctg tcc aag atg cag cag aac ggc tac gaa aat cca acc tac aag
35 Arg His Leu Ser Lys Met Gln Gln Asn Gly Tyr Glu Asn Pro Thr Tyr Lys

ttc ttt gag cag atg cag aac tag
52 Phe Phe Glu Gln Met Gln Asn ¥¥¥
  
```

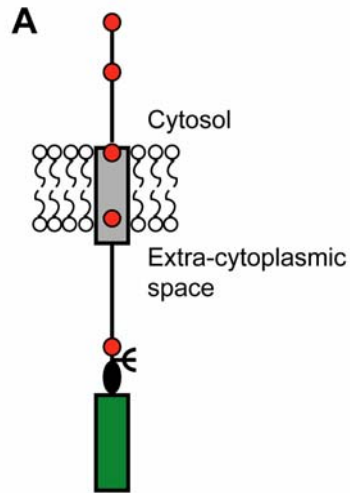


## Appendix 2.5

### ss-HA-GlyCT99 derivative.

**A.** Diagrammatic representation of ss-HA-GlyCT99. Approximate positions of methionine residues shown as red circles, transmembrane domain indicated by grey rectangle, pre-prolactin signal sequence shown as green rectangle, HA tag indicated by black oval, glycosylation site shown as  $\leftarrow$ .

**B.** DNA and amino acid sequences of construct (in pcDNA3.1(+) vector).



### B

#### pre-prolactin signal sequence

ATG GAC AGC AAA GGT TCG TCG CAG AAA GGG TCC CGC CTG CTC CTG CTG CTG  
1 Met Asp Ser Lys Gly Ser Ser Gln Lys Gly Ser Arg Leu Leu Leu Leu Leu

#### HA tag

GTG GTG TCA AAT CTA CTC TTG TGC CAG GGT GTG GTG TCG ACC CCC TAC CCA  
18 Val Val Ser Asn Leu Leu Leu Cys Gln Gly Val Val Ser Thr Pro Tyr Pro

#### Gly site

#### APP sequence

TAC GAC GTC CCA GAC TAC GCT AAT TCA ACA ATG GAT GCA GAA TTC CGA CAT  
35 Tyr Asp Val Pro Asp Tyr Ala Asn Ser Thr Met Asp Ala Glu Phe Arg His

GAC TCA GGA TAT GAA GTT CAT CAT CAA AAA TTG GTG TTC TTT GCA GAA GAT  
52 Asp Ser Gly Tyr Glu Val His His Gln Lys Leu Val Phe Phe Ala Glu Asp

GTG GGT TCA AAC AAA GGT GCA ATC ATT GGA CTC ATG GTG GGC GGT GTT GTC  
69 Val Gly Ser Asn Lys Gly Ala Ile Ile Gly Leu Met Val Gly Gly Val Val

#### $\gamma$ -cleavage

ATA GCG ACA GTG ATC GTC ATC ACC TTG GTG ATG CTG AAG AAG AAA CAG TAC  
86 Ile Ala Thr Val Ile Val Ile Thr Leu Val Met Leu Lys Lys Lys Gln Tyr

ACA TCC ATT CAT CAT GGT GTG GTG GAG GTT GAC GCC GCT GTC ACC CCA GAG  
103 Thr Ser Ile His His Gly Val Val Glu Val Asp Ala Ala Val Thr Pro Glu

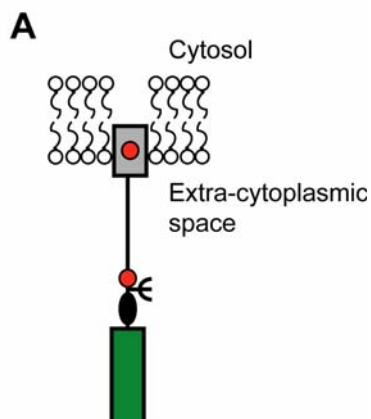
GAG CGC CAC CTG TCC AAG ATG CAG CAG AAC GGC TAC GAA AAT CCA ACC TAC  
120 Glu Arg His Leu Ser Lys Met Gln Gln Asn Gly Tyr Glu Asn Pro Thr Tyr

AAG TTC TTT GAG CAG ATG CAG AAC TAG  
137 Lys Phe Phe Glu Gln Met Gln Asn ¥¥¥

## Appendix 2.6

### ss-HA-GlyCT42 derivative.

**A.** Diagrammatic representation of ss-HA-GlyCT42. Approximate positions of methionine residues shown as red circles, transmembrane domain indicated by grey rectangle, pre-prolactin signal sequence shown as green rectangle, HA tag indicated by black oval, glycosylation site shown as  $\epsilon$ .



**B.** DNA and amino acid sequences of construct (in pcDNA3.1(+) vector).

### B

#### pre-prolactin signal sequence

ATG GAC AGC AAA GGT TCG TCG CAG AAA GGG TCC CGC CTG CTC CTG CTG CTG  
1 Met Asp Ser Lys Gly Ser Ser Gln Lys Gly Ser Arg Leu Leu Leu Leu Leu

GTG GTG TCA AAT CTA CTC TTG TGC CAG GGT GTG GTG TCG ACC CCC TAC CCA  
18 Val Val Ser Asn Leu Leu Leu Cys Gln Gly Val Val Ser Thr Pro Tyr Pro

Gly site                      APP sequence

TAC GAC GTC CCA GAC TAC GCT AAT TCA ACA ATG GAT GCA GAA TTC CGA CAT  
35 Tyr Asp Val Pro Asp Tyr Ala Asn Ser Thr Met Asp Ala Glu Phe Arg His

GAC TCA GGA TAT GAA GTT CAT CAT CAA AAA TTG GTG TTC TTT GCA GAA GAT  
52 Asp Ser Gly Tyr Glu Val His His Gln Lys Leu Val Phe Phe Ala Glu Asp

GTG GGT TCA AAC AAA GGT GCA ATC ATT GGA CTC ATG GTG GGC GGT GTT GTC  
69 Val Gly Ser Asn Lys Gly Ala Ile Ile Gly Leu Met Val Gly Gly Val Val

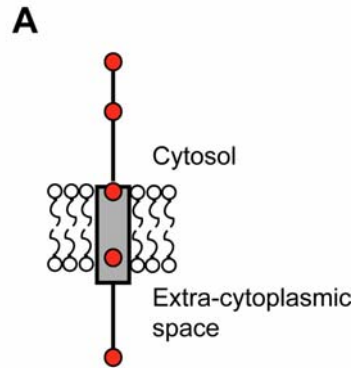
ATA GCG TAG  
86 Ile Ala ¥¥¥

## Appendix 2.7

### MetCT99 APP-derivative.

**A.** Diagrammatic representation of MetCT99. Approximate positions of methionine residues shown as red circles, transmembrane domain indicated by grey rectangle.

**B.** DNA and amino acid sequences of construct (in pcDNA3.1(+) vector).



### B

#### APP sequence

```

1  Met Asp Ala Glu Phe Arg His Asp Ser Gly Tyr Glu Val His His Gln Lys
   ATG GAT GCA GAA TTC CGA CAT GAC TCA GGA TAT GAA GTT CAT CAT CAA AAA
18 Leu Val Phe Phe Ala Glu Asp Val Gly Ser Asn Lys Gly Ala Ile Ile Gly
   TTG GTG TTC TTT GCA GAA GAT GTG GGT TCA AAC AAA GGT GCA ATC ATT GGA
35 Leu Met Val Gly Gly Val Val Ile Ala Thr Val Ile Val Ile Thr Leu Val
   CTC ATG GTG GGC GGT GTT GTC ATA GCG ACA GTG ATC GTC ATC ACC TTG GTG
52 Met Leu Lys Lys Lys Gln Tyr Thr Ser Ile His His Gly Val Val Glu Val
   ATG CTG AAG AAG AAA CAG TAC ACA TCC ATT CAT CAT GGT GTG GTG GAG GTT
69 Asp Ala Ala Val Thr Pro Glu Glu Arg His Leu Ser Lys Met Gln Gln Asn
   GAC GCC GCT GTC ACC CCA GAG GAG CGC CAC CTG TCC AAG ATG CAG CAG AAC
86 Gly Tyr Glu Asn Pro Thr Tyr Lys Phe Phe Glu Gln Met Gln Asn •••
   GGC TAC GAA AAT CCA ACC TAC AAG TTC TTT GAG CAG ATG CAG AAC TAG

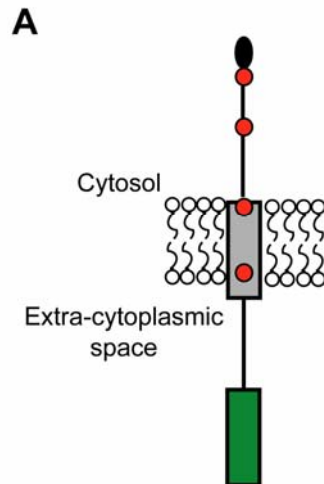
```

## Appendix 2.8

### ss-CT99<sup>HA</sup> derivative.

**A.** Diagrammatic representation of ss-CT99<sup>HA</sup>. Approximate positions of methionine residues shown as red circles, transmembrane domain indicated by grey rectangle, HA tag shown as black oval, additional APP sequence indicated by black line, pre-prolactin signal sequence shown as green rectangle.

**B.** DNA and amino acid sequence of construct in vector pcDNA3.1(+).



### B

#### pre-prolactin signal sequence

ATG GAC AGC AAA GGT TCG TCG CAG AAA GGG TCC CGC CTG CTC CTG CTG CTG  
 1 Met Asp Ser Lys Gly Ser Ser Gln Lys Gly Ser Arg Leu Leu Leu Leu Leu

#### APP seq

GTG GTG TCA AAT CTA CTC TTG TGC CAG GGT GTG GTG TCG ACC CCC GAT GCA  
 18 Val Val Ser Asn Leu Leu Leu Cys Gln Gly Val Val Ser Thr Pro Asp Ala

GAA TTC CGA CAT GAC TCA GGA TAT GAA GTT CAT CAT CAA AAA TTG GTG TTC  
 35 Glu Phe Arg His Asp Ser Gly Tyr Glu Val His His Gln Lys Leu Val Phe

TTT GCA GAA GAT GTG GGT TCA AAC AAA GGT GCA ATC ATT GGA CTC ATG GTG  
 52 Phe Ala Glu Asp Val Gly Ser Asn Lys Gly Ala Ile Ile Gly Leu Met Val

#### γ-cleavage

GGC GGT GTT GTC ATA GCG ACA GTG ATC GTC ATC ACC TTG GTG ATG CTG AAG  
 69 Gly Gly Val Val Ile Ala Thr Val Ile Val Ile Thr Leu Val Met Leu Lys

AAG AAA CAG TAC ACA TCC ATT CAT CAT GGT GTG GTG GAG GTT GAC GCC GCT  
 86 Lys Lys Gln Tyr Thr Ser Ile His His Gly Val Val Glu Val Asp Ala Ala

GTC ACC CCA GAG GAG CGC CAC CTG TCC AAG ATG CAG CAG AAC GGC TAC GAA  
 103 Val Thr Pro Glu Glu Arg His Leu Ser Lys Met Gln Gln Asn Gly Tyr Glu

#### HA tag

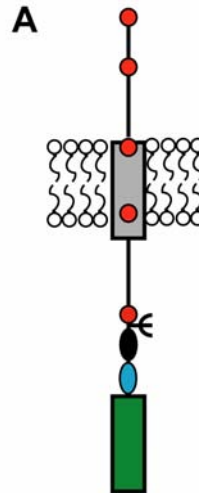
AAT CCA ACC TAC AAG TTC TTT GAG CAG ATG CAG AAC ATG TAC CCA TAC GAC  
 120 Asn Pro Thr Tyr Lys Phe Phe Glu Gln Met Gln Asn Met Tyr Pro Tyr Asp

GTC CCA GAC TAC GCT TAG  
 137 Val Pro Asp Tyr Ala ¥¥¥

## Appendix 2.9

### ss\_opsin-HA-GlyCT99 and ss\_flag-HA-GlyCT99 derivatives.

**A.** Diagrammatic representation of ss\_opsinCT99 or ss\_flagCT99. Approximate positions of methionine residues shown as red circles, transmembrane domain indicated by grey rectangle, pre-prolactin signal sequence shown as green rectangle, HA tag indicated by black oval, opsin (or flag) tag indicated by pale blue oval, glycosylation site shown as  $\Psi$ .



**B.** DNA and amino acid sequences of ss\_opsin-HA-GlyCT99 construct (in pcDNA3.1(+) vector). For ss\_flag-HA-GlyCT99 the opsin sequence (shown in pale blue) was replaced with:

GAC TAC AAG GAC GAC GAC GAC AAG  
Asp Tyr Lys Asp Asp Asp Asp Lys

### B

pre-prolactin signal sequence

ATG GAC AGC AAA GGT TCG TCG CAG AAA GGG TCC CGC CTG CTC CTG CTG CTG  
1 Met Asp Ser Lys Gly Ser Ser Gln Lys Gly Ser Arg Leu Leu Leu Leu Leu

GTG GTG TCA AAT CTA CTC TTG TGC CAG GGT GTG GTG TCG ACC CCC AAC GGG  
18 Val Val Ser Asn Leu Leu Leu Cys Gln Gly Val Val Ser Thr Pro Asn Gly

ACC GAG GGC CCA AAC TTC TAC GTG CCT TTC TCC AAC AAG ACG TAC CCA TAC  
35 Thr Glu Gly Pro Asn Phe Tyr Val Pro Phe Ser Asn Lys Thr Tyr Pro Tyr

Gly site APP sequence  
GAC GTC CCA GAC TAC GCT AAT TCA ACA ATG GAT GCA GAA TTC CGA CAT GAC  
52 Asp Val Pro Asp Tyr Ala Asn Ser Thr Met Asp Ala Glu Phe Arg His Asp

TCA GGA TAT GAA GTT CAT CAT CAA AAA TTG GTG TTC TTT GCA GAA GAT GTG  
69 Ser Gly Tyr Glu Val His His Gln Lys Leu Val Phe Phe Ala Glu Asp Val

GGT TCA AAC AAA GGT GCA ATC ATT GGA CTC ATG GTG GGC GGT GTT GTC ATA  
86 Gly Ser Asn Lys Gly Ala Ile Ile Gly Leu Met Val Gly Gly Val Val Ile

GCG ACA GTG ATC GTC ATC ACC TTG GTG ATG CTG AAG AAG AAA CAG TAC ACA  
103 Ala Thr Val Ile Val Ile Thr Leu Val Met Leu Lys Lys Lys Gln Tyr Thr

TCC ATT CAT CAT GGT GTG GTG GAG GTT GAC GCC GCT GTC ACC CCA GAG GAG  
120 Ser Ile His His Gly Val Val Glu Val Asp Ala Ala Val Thr Pro Glu Glu

CGC CAC CTG TCC AAG ATG CAG CAG AAC GGC TAC GAA AAT CCA ACC TAC AAG  
137 Arg His Leu Ser Lys Met Gln Asn Gly Tyr Glu Asn Pro Thr Tyr Lys

TTC TTT GAG CAG ATG CAG AAC TAG  
154 Phe Phe Glu Gln Met Gln Asn •••